

ISTANBUL BRIDGE CONFERENCE 2020

"THE ENDURING LINK"

PROCEEDINGS

EDITORS

POLAT GULKAN & ALP

CANER

ISBN: 979-8-9856133-0-8

Bridge Analysis & Design & Construction

The Replacement of the Kosciuszko Bridge – Phase 2

K.L. Tam

New Iconic Crossing Across The Scioto River, Dublin – Ohio Connectivity And Inclusivity

M. Hamdi & A. Tognetti

Heavy Transportation Via YSS (Yavuz Sultan Selim Köprüsü) Between Both Side of Bosphorus in Istanbul

S. Gormezoglu

Application of ETAG 032 As A New Level Of Expansion Joint Assessment

K.H. Geyik & S. Hoffmann

Bridge Maintenance

Qualifying Commercial Rapid Repair Media for Partial Depth Bridge Decks Repairs

A.B. Pour, R.J. Thomas, M. Maguire, A.D. Sorensen & Md.A. Al Sarfin

Major Upgrade of Istanbul Iconic Suspension Bridges

D. Khazem & H. Kopkalli

Operation reliability index for maintenance decision making in bridges

S. Lajevardi, H. Sousa, P.B. Lourenço, J.C. Matos & D.V. Oliveira

Gpr And Aerial Photogrammetry Applied To Masonry Arch Bridge Assessment

S. Neves, S. Fontul & M. Solla

Long-Term Anti-Corrosion Protection of Al-Mg Plasma Arc Thermal Spray Applied to Bridge Bearings in Harsh Environments

T. Onal, J.L. Gimenez & T. Himeno

Seismic Analysis of Bridges

Structural Analysis of Seismically Isolated Curved Bridge According to Turkish Earthquake Code

E. Yıldırım & E. Güngör

Historical Bridges

Damage Detection of a Historic Bridge by Operational Modal Analysis

D. Okuyucu & A.Y. Kanbur

Artificial Intelligence

AI On The Management Of Existing Bridges

J. Matos, C. Santos & M. Coelho

Review and Assessment of Technical and Legal Challenges in Drone-Driven Structural Health Monitoring of Bridges

A. Adibfar, M. Razkenari & A. Costin

Bridge Inspection and AI

M.C. Yucel

Bridge Analysis & Design & Construction



The Replacement of the Kosciuszko Bridge – Phase 2

Kwok-Leung Tam

WSP USA
New York, NY

ABSTRACT

The new Kosciuszko Bridge replaces a 1.1-mile segment of the Brooklyn-Queens Expressway over Newtown Creek with two parallel, modern and innovative structures each with a single-tower cable-stayed main span. The signature structures carry an estimated 180,000 vehicles per day and provide a gateway between Brooklyn and Queens and reshape the skyline of these two New York City boroughs. Phase 1 comprised the construction of a new five-lane Queens-bound structure, and demolition of the existing bridge under a Design-Build Contract. Phase 2, a Design-Bid-Build contract, involves the construction of a new four-lane Brooklyn-bound structure with a 20-foot wide shared-use path with views of Manhattan. The bridge deck width is 99'-4" on Phase 1 main span bridge and 93'-4" on Phase 2 main span bridge. The Phase 2 Brooklyn-bound cable-stayed front span is 609-feet long with a 343-feet long back span. The single tower support extends almost 200-feet above the roadway deck for a total height of 287-feet above grade which is similar to Phase 1 bridge.

Keywords: Cable Stayed Bridge, Single-tower cable-stayed structure.

1 INTRODUCTION

The new Kosciuszko Bridge is now opened to motorists, cyclists and pedestrians four years ahead of schedule and on budget. The bridge replaces a 1.1-mile segment of the Brooklyn-Queens Expressway over Newtown Creek with two parallel, modern and innovative structures each with a single-tower cable-stayed main span and prestressed girder approach spans. The signature structures provide a gateway between Brooklyn and Queens and reshape the skyline of these two New York City boroughs (Figure 1).

The Kosciuszko Bridge project replaces the existing 77-year-old highly deteriorated bridge, first opened in 1939 under President Roosevelt's administration, with two new state-of-the-art, cable-stayed bridges: one carrying Queens-bound traffic and one carrying Brooklyn-bound traffic. An estimated 180,000 vehicles per day use this segment of the Brooklyn-Queens Expressway. As one of New York City's few north-south interstates, the original Kosciuszko Bridge could not efficiently handle the present volume of traffic due to its narrow lanes, steep grades, lack of shoulders, and short merge/weave distances near



Figure 1 – Both Phases I and 2 Bridges Open

ramps and interchanges, which did not meet current highway design standards. Shoulders have been added to both bridges, where none previously existed. The roadway incline has also been lowered by approximately 35 feet. This makes it easier for trucks and other large vehicles to maintain consistent speeds on the bridge, helping reduce traffic congestion. The Phase 2 project also includes new open space plazas and new parks in both Brooklyn and Queens.

1.1 CABLE STAYED BRIDGE - SUBSTRUCTURE CONFIGURATION (PHASE 2)

The Phase 2 Brooklyn-bound cable-stayed front span is 609-feet long with a 343-feet long back span. The span lengths and column locations were determined after much study in order to avoid impacting Newtown Creek which is a Superfund site (polluted area and requiring a long-term response to clean up hazardous material contamination), the Class-2 Inactive Hazardous Waste Site at the former Phelps Dodge Refining Site, the Long Island Rail Road tracks and the local street network below. Please see Figure 4 for the elevation view of the Phase 2 bridge.

The single tower support is located on the Queens side of Newtown Creek and extends almost 200-feet above the roadway deck for a total height of 287-feet above grade. This is just below the maximum height allowed due to the bridge's proximity to LaGuardia Airport. The pylon legs are designed without a cross beam to tie the two columns together and they are behaving as independent cantilever beam/column. The single tower is comprised of two reinforced concrete tapered pylon legs that are designed

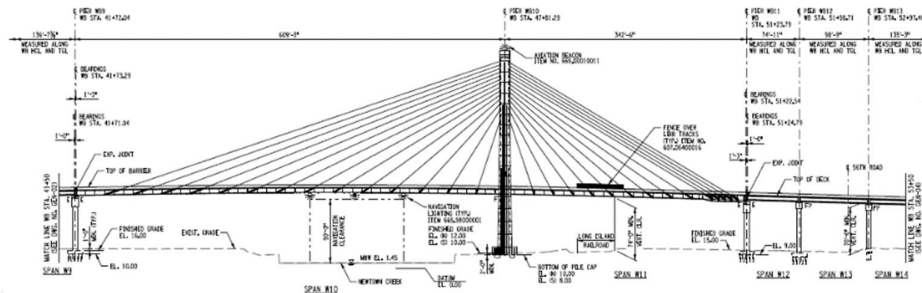


Figure 4 – Phase 2 - Main Span

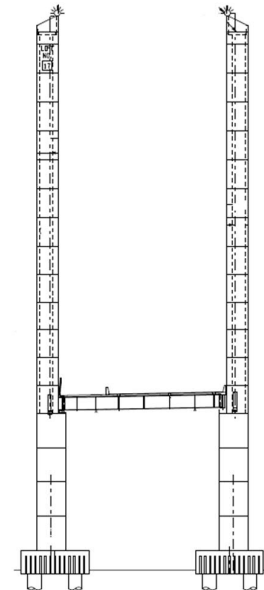


Figure 2 – Pylon

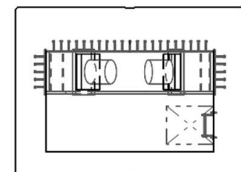


Figure 3
Upper Pylon

as hollow sections. However, the lower portions of the pylon below the bridge deck are filled with concrete to reduce pylon area/surface that would require future inspection and maintenance (See Figures 2 & 3). Internal access platforms and ladders are installed at the upper pylon for access to the cable anchorages and the pylon roof. External access platforms are also installed at the pylon and both anchor piers for inspection and maintenance access. Steel cable anchor boxes (Figure 3) are formed by welded steel plates to house the upper stayed cable anchorages. Three sides of the cable anchor box surfaces are used as formwork and poured with the concrete pylon legs. Each pylon pile cap is supported by four 7-foot diameter drilled shafts that extend approximately 180' deep and are socketed into rock. Each ends of the main spans are supported by anchor piers with two 7 feet diameter columns. The 18 inches diameter cast-in-place driven piles are used to support the anchor pier pile caps.

1.2 CABLE STAYED BRIDGE - SUPERSTRUCTURE CONFIGURATION (PHASE 2)

The precast concrete deck is supported by steel floorbeams and edge girders. Deck post-tensioning tendons were designed and included in the deck region near both anchor piers to eliminate

the deck tension. The floorbeam and edge girders are grades 50 or 70 steel welded plate I beams and bolted connected to form steel framed segments (Figure 5). The floorbeams are spaced at 13'-6" on the main span and 14'-0" on the back span. The concrete bridge deck is 93'-2" in width.

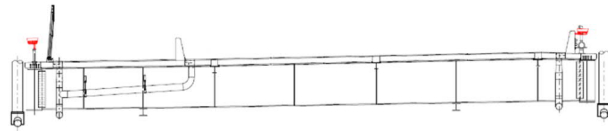


Figure 5 – Phase 2 Main Span Deck Cross Section

The two stayed cable planes use a modified fan layout system. The 56 multistrand stay cables that are placed at various angles to connect the edge girder to the two vertical legs of the pylon tower are made up of approximately one million linear feet of steel strands. The number of strands in each cable range from 21 to 88 strands. The strands are 0.62 inch diameter uncoated seven wire strand conforming to the requirements of ASTM A416, grade 270, weldless grade, low-relaxation strand. The strands are waxed and sheathed. The bundle of strands is contained in a HDPE co-extruded outer pipe. The cable system allows each strand to be installed, tensioned and replaced individually. The cable anchors at each end of the cable are protected by a wax filled cap. The protection caps can be removed for inspection and maintenance of the strands. The cables are tensioned at the active adjustable anchorages where they are located at the deck level. All cable anchorages in the upper pylon are fixed passive anchorages.



Figure 6 – Phase 2 Main Span Lower Cable Connection

The edge girders are designed to run continuously between the two pylon legs. To accommodate the cable and edge girder geometry, the cable connections are offset and located to the outside fascia of the edge girders. Outrigger cable connections (Figure 6) are bolted to the edge girders. Also, on a cable-stayed structure, high wind or rain events can result in high amplitude vibrations of the cables. Internal hydraulic dampers are installed at each cable to absorb this energy and dampen the vibration effects which minimizes the motion of the cable, reduces the fatigue effects and ensures the stability of the structure. The typical cable spacings are 40'-6" at the main span and 28'-0" at the back span. A closer cable spacing is used at the counterweight region at the end of the back span to support the heavy counterweight.

Single-tower cable-stayed structures like this one are extremely rare and the required span arrangement due to environmental and local roadway constraints presented certain design challenges

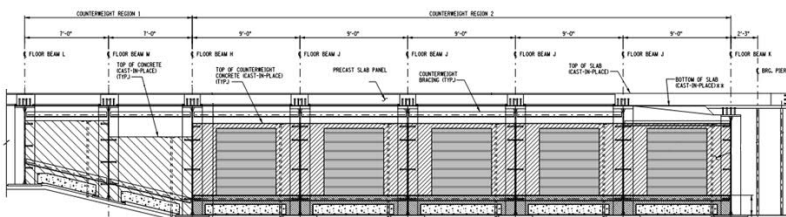


Figure 7 – Phase 2 Main bridge - Back Span Counterweight Layout

such as the unbalanced front and back span lengths, 609-feet and 343 feet, respectively. A concrete and steel counterweight (Figure 7) was designed and constructed at the end of the back span to balance the large weight differential between the main and back spans due to the differing lengths. The total

counterweight weights about 4,600 tons. Concrete precast panels are designed to support the steel ingots and the encasing concrete.

Multi-rotational disc bearings are utilized for longer service life. The superstructure boundary condition (Figure 8) at the pylon is a pinned condition and the superstructure is designed to allow longitudinal movement at the anchor piers.

All main span superstructure longitudinal forces and some of the lateral forces like wind loads, braking forces and seismic forces are transferred from the superstructure to the pylon. In order to reduce the bearing size at the pylon, longitudinal restrainers (Figure 9) and lateral restrainers (Figure 10) are designed and used to transfer the lateral forces directly from the superstructure to the pylon. Concrete lateral restrainer blocks are used to guide the superstructure and transfer transverse forces from the superstructure to the anchor piers.

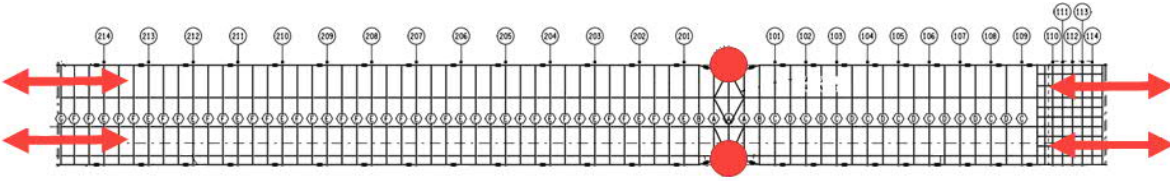


Figure 8 – Bearing Boundary Conditions



Figure 9 – Long. Restrainer

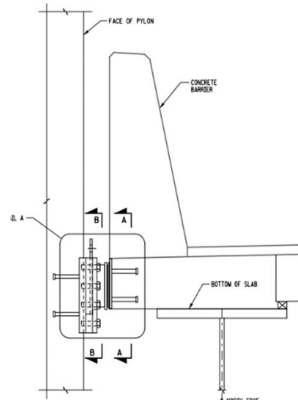


Figure 10 – Lat. Restrainer

One self-propelled maintenance inspection traveler (Figure 11) was installed under the main span bridge deck and provides access to the under deck and stay cable anchorages. A manlift is attached to each end of the traveler apron and the aprons can be extended to allow the manlift to move beyond the fascia region of the edge girders. The manlifts can rise from

under deck level to reach to the deck level and provide hands-on access to the fascia region and provide emergency exit.

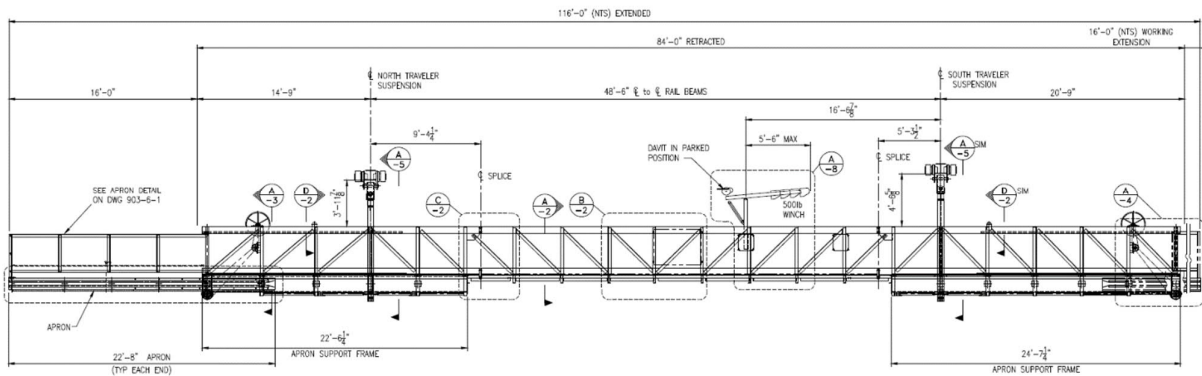


Figure 11 - Traveler

1.3 - APPROACH SPAN CONFIGURATION (PHASE 2)

The sixteen approach spans utilize 79-inch deep prestressed concrete girders to support the cast-in-place concrete decks with spans lengths of up to 136-feet. Each pier bent is comprised of two six-foot diameter reinforced concrete columns with eight-foot deep concrete cap beams. The typical foundations utilize 18-inch diameter concrete filled steel pipe piles.

2.1 - CABLE STAYED BRIDGE DESIGN - 3D FINITE ELEMENT MODEL

In order to accurately capture the behavior of the cable stayed bridge spans under various type of loadings, a highly detailed 3D finite element model was created (Figures 12 & 13). The main span pylon, anchor piers, approach piers, edge girders and floorbeams were modelled by linear elastic beam elements. The concrete decks and cables were modelled with shell elements and the truss elements respectively. The approach superstructure spans were modeled by a series of linear elastic beam elements at the centers of mass of the deck section. A fiber beam was adopted for the plastic hinge zones at the base of the pylon and at the top and bottom pier columns in order to more accurately capture non-linear cyclic moment-curvature behavior. The pile group and pile cap were modeled in a separate model and they were simulated by 6x6 spring element (p-y elements) interactions between the foundations and the foundation soil. All dead loads and superimposed dead loads (barriers, wearing surface and utilities) were accounted for and accurately represented in the model as mass density or added lump mass. The 3D models were used to assess the loading effects that are required by AASHTO LRFD and the project requirements.

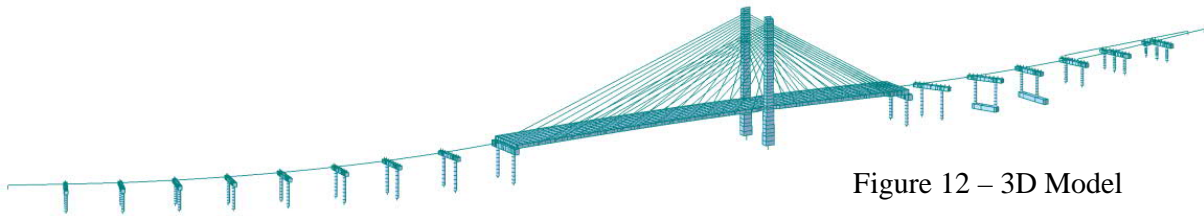


Figure 12 – 3D Model

The loadings that were analyzed account for dead loads, live loads, wind loads, temperature, deck post-tensioning, seismic loads and AASHTO load combinations.

2.2 SEISMIC ANALYSIS

The bridges are classified as Critical for seismic events and classified as Seismic Performance Zone 2. Seismic design was performed for lower level (functional evaluation) event having 1000-year return period and an upper level (safety evaluation) event having 2500-year return period in accordance with the NYSDOT LRFD Blue Pages.

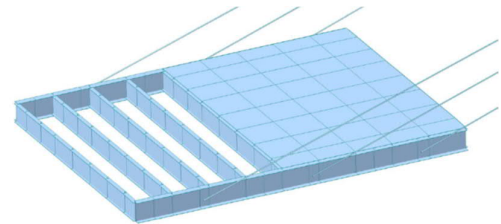


Figure 13 – 3D Model

2.2.1 SEISMIC ANALYSIS - MAIN SPAN – NON-LINEAR TIME-HISTORY ANALYSIS

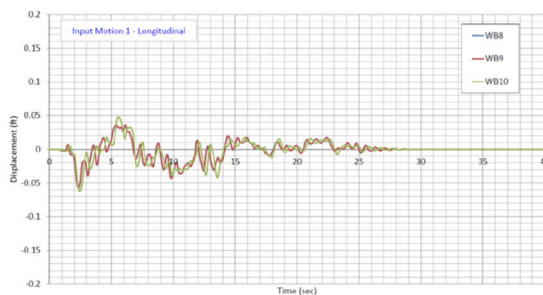


Figure 14 – TH Motion 1 – Long. Dir.
(1000 yrs Return Period)

A non-linear time history analysis computer model for the main span unit and full length of approach spans on either side of the main span was created as mentioned above. Nonlinear time history analysis was performed to evaluate the pylon and anchor piers. The time histories were developed for lower and upper level events. The structure was fully

modelled to include mass, stiffness and both elastic and inelastic material properties. Site specific time history records was developed for this bridge (Figure 14). The smallest time step used in the time history analysis was 0.005-sec. The main span

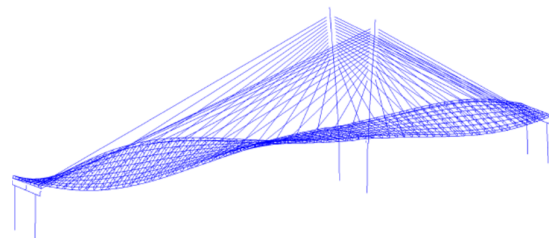


Figure 15 – First Torsional Mode

structure's performance was assessed and the structure adjusted as necessary to meet the proposed seismic performance standards; to ensure potential damage to the structure is above the ground line in repairable components. Displacement values were used in the time history records to allow the inclusion of spatial variation. Rayleigh damping was used with the anchor points defined at the first fundamental mode and the first mode in which 90% of the mass is participating. A damping ratio of 5% was assigned to both anchor points. 50% of the design HL-93 live load was included in Extreme Event I (seismic load combination). However, inertia effects of live load have been considered and were not included in the time history analysis. 50% HL-93 live Load was considered a static load case for Extreme Event I, and live load effects were ignored and when doing so produce a conservative result. Effective (cracked) section properties were used for reinforced concrete components in the global analytical model as appropriate.

2.2.2 SEISMIC ANALYSIS – MAIN SPAN AND APPROACH SPANS – RESPONSE SPECTRUM ANALYSIS

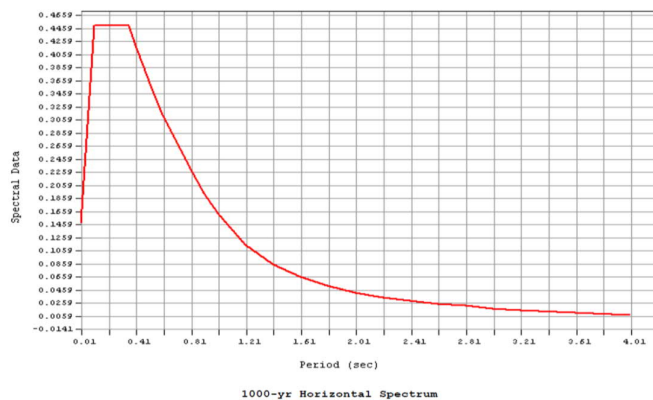


Figure 16 – RSA – Long. Dir.. (1000 yrs Return Period)

The approach spans were designed, and the main spans were checked based on the traditional force-based “R-Factor” method. For FEE, the structure remains elastic and R (response modification factor) was taken as 1.0. For SEE, R factors were established based on the results of an inelastic pushover analysis of individual piers and the material strain limits specified in the AASHTO Guide Specifications for LRFD Seismic Bridge Design. Linear shake analysis was performed and response spectrum for lower and upper level events was developed. The response spectrum (Figure 16) was developed in accordance

with FHWA publication FHWA-NHI-11-032 for each geologic setting. Effective (cracked) section properties were used for reinforced concrete components in the global analytical model as appropriate. The stiffness of the foundations is included through a geotechnical evaluation where the soil-structure interaction is considered; the evaluated foundations are represented numerically in the finite element models applying the foundation stiffness in six degrees-of-freedom.

An elastic multi-modal response spectrum analysis was performed on the 3D finite element models for the approach spans combined with an inelastic pushover analysis. For the SEE, the inelastic pushover analysis was used to determine the response modification factors for each of the structural elements where damage is allowed. The allowable displacements were based on the strain limits set forth in these criteria for the SEE event. Once the response modification factors have been determined, they were applied to the results of the response spectrum analysis to compute the design forces for each supporting member. 50% of the design HL-93 live load was included in Extreme Event I (seismic load combination). However, inertia effects of live load were considered and was not included as part of the response spectrum analysis. 50% HL-93 live load was considered as static load case for Extreme Event I, and live load effects were ignored when neglecting them produces a conservative result.

2.3 ADDITIONAL DETAILED 2D FINITE ELEMENT MODEL

TANGO 2D model was created for the construction stage analyses check and for as an independent check of the 3D main span finite element model.

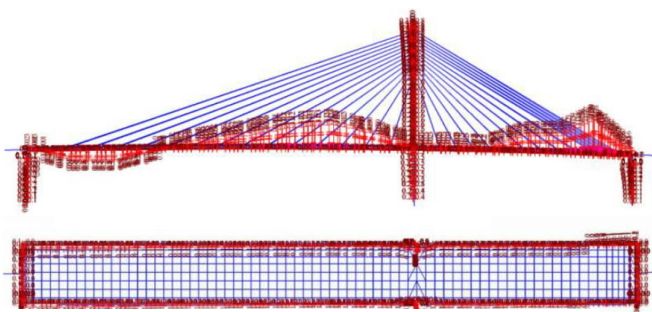


Figure 17 – Sample Static Wind Load

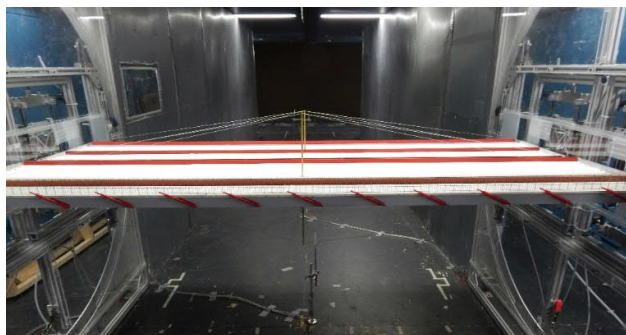


Figure 18 – Sectional Model Wind Tunnel Testing

flutter coefficients, and vortex-induced aerodynamic motions have been obtained from wind tunnel tests using a detailed sectional model of the bridge using an appropriate scale determined by an aerodynamicist. Static aerodynamic coefficients have been determined for a ± 10 degree angle of attack. Dynamic response has been determined for a ± 5 degree angle of attack. The results of the full aeroelastic model testing of the bridge based on the wind tunnel tests findings were used to determine wind design forces.

The main span is designed for minimum of 1) Design wind speed shall be 100-year mean-hourly speed at the deck level, with a corresponding 10-minute mean value; 2) Design flutter speed shall be 10,000- year 10-minute mean speed; 3) Design wind speed for the construction phase shall be mean-hourly and 10-minute mean values for a 20-year return period; and 4) Design flutter speed for the construction phase shall be for 1,000-year return 10-minute speed.

2.5 OTHER DESIGN CONSIDERATIONS

The main span bridge was also designed for cable loss and cable replacement conditions as described in PTI DC45.1. and the structure is capable of withstanding the loss of any one cable without the occurrence of structural instability.

The edge girders (their splices), longitudinal restrainers at the pylon, floorbeams and uplift bearings are considered fracture critical members.

3.1 MAIN SPAN BRIDGE CONSTRUCTION

Drilled shaft foundation are formed by soil excavating using a typical modern drilled shaft rig. Four 7-feet diameter drilled shafts that extend approximately 180' deep and are socketed into rock.

The anchor piers and the pylon concrete are cast in place. The pylon is cast in segments. Traditional formworks were used on the lower pylon. To accelerate the construction, the upper pylon

2.4 WIND LOAD ANALYSIS

Site-specific wind loads were developed for use in the design of the bridge and a total of 68 load cases (Figure 17) were generated and applied to the 3D finite element model.

2.4.1 WIND TUNNEL TESTING

Sectional (Figure 18) and full aeroelastic model testing of the main span, including 400 feet of the approach spans adjacent to each end of the main spans in the bridge's completed form and throughout all critical stages of construction have been performed. The tests have been carried out prior to completion of the final design and the results have been verified to the satisfactory aeroelastic performance of the main span. All wind tunnel studies were fully represented in the aerodynamic and aeroelastic interactions of the eastbound and westbound bridge structures, both in their final completed state as well as critical construction stages. Static aerodynamic coefficients (lift, drag, and moment), aeroelastic

segments were constructed using jump forms and the construction was concurrent with the construction of the superstructure segments of the pier table and the superstructure segments adjacent to the pylon. A tower crane near the pylon was installed to assist the erection of the pylon and the superstructure segments in the pylon region. The main span superstructure was erected using the “balanced cantilever” method (Figure 19). The erection sequence attempts to minimize the dead load imbalanced condition between the back span and the main span.



Figure 19 – Phase 2 Main Span Construction

limit the pylon demands during the erection of the superstructure. Ballast was placed on the back span deck to limit the uplift forces in the temporary bent and to limit the pylon bending moments once the temporary bent was removed following the side span closure. Once the composite deck was completed, the deck ballast was removed and post-tensioning, utilities, drains, stayed cable dampers, expansion joints, barriers and the wearing surface were installed on the bridge per the erection sequence.

As the back span deck segments are typically shorter than the main span deck segments, several erection stages required the construction of the two back span segments for a single main span segment. After back span closure, permanent counterweight at the deck segment near the back span anchor pier was placed progressively along with main span deck segment erection to minimize the dead load imbalance condition in the pylon. A temporary support bent near the middle of the back span was installed to brace the partially erected bridge to

4 Conclusion

The design of a complex structure such as this one is highly demanding and requires intricate analysis, however the result is a project that meets NYSDOT and the public’s need for a structurally sound bridge that can safely and efficiently serve the 180,000 daily motorists and adds pedestrian and cyclist access across the bridge which was not provided on the old structure. This project goes the extra step by delivering a truly signature bridge that redefines the city sky-line. It is the city’s first major cable-stayed structure and the first major crossing in New York City since the Verrazano Bridge in 1964.

REFERENCES

- [1] AASHTO LRFD Bridge Design Specifications, Seventh Edition, 2014, U.S. Customary Units Including Interim Revisions through 2016
- [2] AASHTO Guide Specifications for LRFD Seismic Bridge Design, Second Edition, 2011, Including 2012, 2014 and 2015 Interim Revisions 2014
- [3] AASHTO LRFD Bridge Construction Specifications, Third Edition, 2010, Including Interim Revisions through 2014
- [4] NYSDOT Bridge Manual, LRFD, 1st Edition 2008, with Addendum #3 last updated May 2014.
- [5] NYSDOT Steel Construction Manual, Third Edition March 2008 with Addendum No. 2, October 7, 2013.
- [6] NYSDOT Standard Specifications for Construction and Materials
- [7] MCEER, “Seismic Retrofitting Manual for Highway Structures: Part 1-Bridges”, 2006
- [8] Post-Tensioning Institute, Recommendations for Stay Cable Design, Testing and Installation, PTI DC45.1-12, Sixth Edition, May 2012



NEW ICONIC CROSSING ACROSS THE SCIOTO RIVER, DUBLIN - OHIO CONNECTIVITY AND INCLUSIVITY

Mahtab Hamdi

Redaelli Tecna Spa
Milan, Italy

Andrea Tognetti

Redaelli Tecna Spa
Milan, Italy

ABSTRACT

The Scioto River Pedestrian Bridge is located in Dublin, Ohio. The team involved in the realization of this iconic structure included the City of Dublin Ohio, Paul Endres of Enderstudio, TY Lin, Kokosing Construction, Genesis Structures, Michael Baker, SBP and Redaelli. This pedestrian and bicycle bridge provides a new connection between the Riverside Crossing Park on the east side with Dublin's beloved historic district over the Scioto River. This crucial new link brings together two communities and "serves as landmark for the City of Dublin representing connectivity and inclusivity" the words of Dublin's Deputy City Manager. 232 metres long, 4.3 metres wide, the bridge has a 153-metre-long suspension span in a reverse curve. The bridge is characterized by the needle shape concrete mast, the "S" shape deck and the cable hangers that connect to only one side of the deck. The large diameter main catenary cables are split and connected at the mast top with a neat connection avoiding the need for a traditional large saddle casting that was deemed to have been visually obtrusive. Redaelli designed, manufactured, supplied and installed the two main catenary cables, the tie down cable, and the hanger cable system including clamps and specifically designed spherical pins and washers to accommodate any rotations between the cable sockets and the anchor plates under live load events.

Keywords: FLC Cables, Iconic structures, Conceptual design and realization, Suspension cables bridge, Installation, Tensioning.

1 INTRODUCTION

This \$22 million pedestrian bridge is part of over \$350 million worth of public and private investments in a project labeled as Bridge Street District. The project development has a strong focus on a walkable, mixed-use core settled on the area around old Dublin and in particular on the Scioto River corridor. After Dublin's city approval of the BSD vision, the city began with initial implementation along the Scioto river in the BSD area and envisaged the construction of a roundabout, relocation of a roadway, to create a new river park along both sides of the river as well as an iconic footbridge that links the historic core on the west side with the brand-new urban core on the east side.

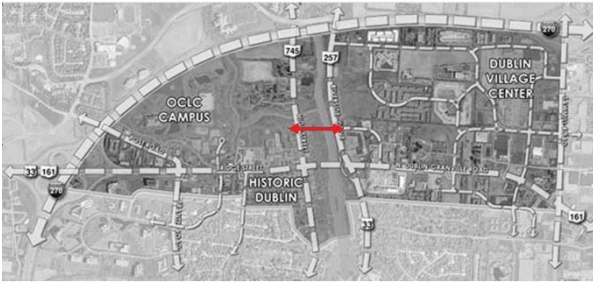


Fig. 1.1. The Bridge Street District

It has been funded by City of Dublin and realized by Paul Endres of Enderstudio, TY Lin, Kokosing Construction, Genesis Structures, Michael Baker, SBP and Redaelli. The sinuous curve of the bridge is suspended on one side only, with the hangers which are connected to the main catenary cables made by Full Locked Coil steel cables.

To verify the long-term durability and quality of cables a series of challenging bespoke fatigue tests were commissioned using some of the largest and most specialized laboratories in the world.

2 CONNECTIVITY AND INCLUSIVITY

The bridge over the river stitches the two sides of the river together connecting Dublin's historic district with the new Bridge Park development and nearby commercial, residential and retail on the river's east side. It engages residents with the river and preserves the scenic Scioto River. It provides views and direct access to water's edge for fishing, canoeing, kayaking, exploring and immersion in nature within the park as well as connections to the community and trail systems. The new pedestrian and cycling bridge over the Scioto river has been named as "The Dublin Link". This name has been given by suggestion of hundreds of Dublin's residents for the critical connectivity which this bridge provides and fosters.

3 DESCRIPTION OF STRUCTURE

The meandering flow shape of the bridge recalls the meandering path of Scioto river. It spans across the river with a vertical needle-shape concrete pylon which is well suited to support two harp-shaped cable systems on its left and right hand including the cable hangers that are distributed along the deck and connected only to one side.

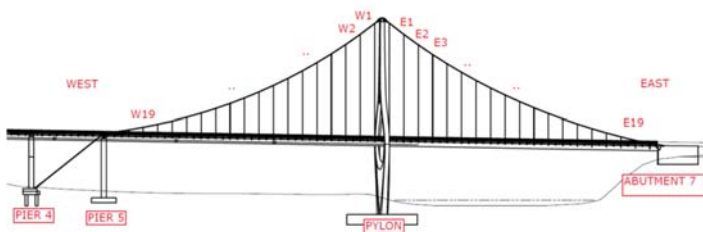


Fig. 3.1. Elevation of the bridge



Fig. 3.2. General view of bridge

The free span of Scioto Bridge is around 153-meters with a total bridge length of 232 meters and a width of 4.3 meters. The cable systems use FLC120 for the main cables and tie down cable, FLC21 & FLC32 for the hangers and FLC50 for the restrainer cables which are connect the pylon and the deck to provide lateral stability.

4 REDAELLI SCOPE OF SUPPLY

For this project Redaelli company provided the complete cable systems including clamps, spherical pins and washers. The following table summarizes the scope of supply, the individual components, cable diameters, quantity of cables and socket types.

Table 4.1 Supply of Cable Systems

Item Description	Cable Type	MBL(kN)	Socket1	Socket2
Main Cable	FLC120	14585	TTF120	TTF120
Tie Down Cable	FLC120	14585	TTF120	CYW116
Restrainer Cable	FLC50	2510	TTF048	TBF048
Hanger Type 1,2	FLC21	435	TTF020	TBF020
Hanger Type 3	FLC32	950	TTF028	TBF028

All the supplied cables are full locked coil cables, produced with a central core made of multiple layers of helically twisted hot dip galvanized steel round wires, spun largely in opposite directions and with external layers of interlocking Z-shaped aluminium-zinc alloy wires with a smooth easily protected exterior surface. The Prefabricated Cable assemblies are indicated in the following pictures.

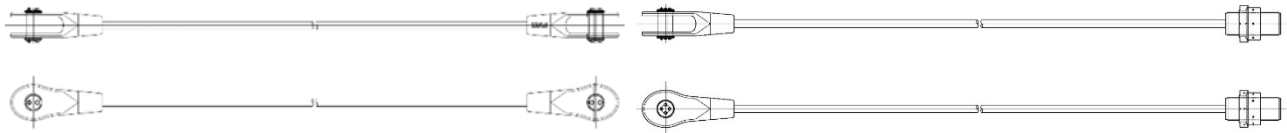


Fig. 4.1. FLC with TTF Sockets

Fig. 4.2. FLC with TTF and CYW sockets

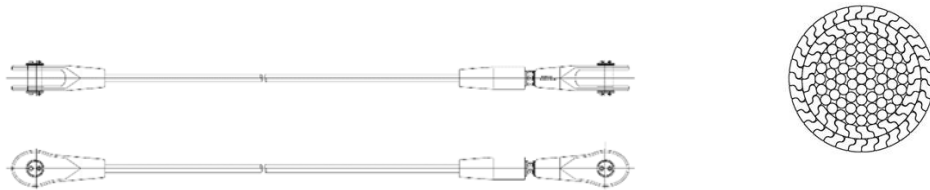
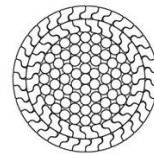
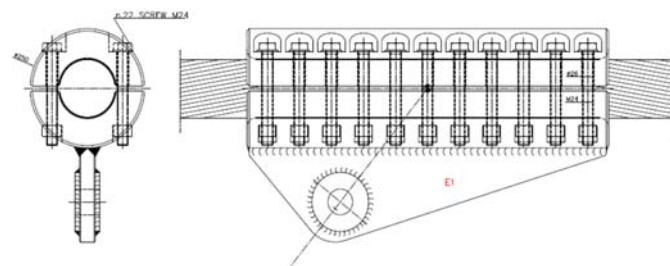


Fig. 4.3. FLC with TTF and TBF sockets

Fig. 4.4. Typical section of a FLC Cables



In addition to the cable systems indicated above, clamps for hanger cables and spherical pins & washers for the lower anchorages of hanger were also designed and supplied. No. 38 hanger clamps positioned on the main cables numbered from the pylon E1 to E19 (east nodes) and W1 to W19 (west nodes) as per the sketches below:



4.5. Hanger clamp 01&02, top of the pylon

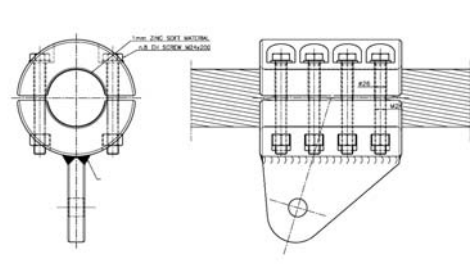


Fig. 4.6. Hanger clamp 7-19, at bottom anchorages.

The spherical washer for the CYW socket of the Tie Down cable was been provided with welded slots, so that they can be fixed to the structures.

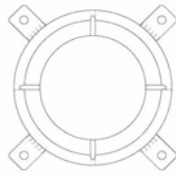


Fig. 4.7. Spherical washer with welded slot



Fig. 4.8. Photo of Spherical washer installed

5 CABLE AXIAL AND BENDING FATIGUE TESTS

In addition to the standard tensile breaking strength and modulus testing the project also specified that, axial and bending fatigue testing should be carried out, in order to try and simulate the loading the cables could be expected to experience during their service life and to better understand how the cables might behave in these high and eccentric fatigue loading circumstances. There were no established international standards for this type of testing yet so Redaelli worked closely with the design engineer, the contractor and test laboratories to devise a testing setup which combined, standard axial fatigue cycles and active bending fatigue cycles. Despite these severe test conditions, the performed tests gave successful results to give all concerned additional peace of mind.

Only few laboratories worldwide have the capability and equipment to do this testing, monitoring and processing all the required data. The laboratories that performed the tests were both in Germany. No.3 axial and bending fatigue tests were performed on FLC032 cable in Kibkon laboratory in Bochum and No.2 axial and bending fatigue tests on FLC120 were done in MPA laboratory in Braunschweig.

During the tests, data such as number of cycles, cycle frequency, temperature, axial and lateral piston forces, and number of broken wires was monitored and recorded.

Redaelli helped design the connections for the pulling machines and, in particular a “saddle” arrangement to apply the lateral active bending cycles to the cables which were imposed by a hydraulic piston placed around middle of the cable sample length. The test on FLC032 required 2×10^6 fatigue cycles imposing axial delta force of 78kN and bending cycles to create a $\pm 0.6^\circ$ angle at each cycle. The test on FLC120 required 1×10^6 fatigue cycles imposing axial delta force of 500kN and bending cycles to create a $\pm 0.6^\circ$ angle at each cycle.

Table 5.1 Fatigue load cycles for FLC032

Cable Type	Cross-Sec mm ²	MBL kN	Nmin kN	Nmax kN	N Avg kN	ΔN kN	Bending Angle °deg	Bending Amptitude mm	No. Of Cycles	Freq. Hz
FLC032	708	950	332	410	371	78	$\pm 0.6^\circ$	± 28.8	2×10^6	≤ 2

Table 5.2 Fatigue load cycles for FLC120

Cable Type	Cross-Sec mm ²	MBL kN	Nmin kN	Nmax kN	N Avg kN	ΔN kN	Bending Angle °deg	Bending Amptitude mm	No. Of Cycles	Freq. Hz
FLC120	9854	14585	6006	6506	6256	500	$\approx \pm 0.6^\circ$	$\approx \pm 17.08/23.7$	1×10^6	≤ 2

Hereafter some photos of the testing setup for FLC120.



Fig. 5.1. Lateral piston for bending cycles



Fig. 5.2. thermocouple & strain gauge



Fig. 5.3. Piston with a "saddle"

6 SPHERICAL PINS AND WASHERS

A critical issue related to the behaviour of the structure under live loads. In order to accommodate the deck movements experienced under live loads and limit bending of the hangers, Redaelli designed a spherical joint. Unfortunately this was rejected because of visual and architectural concerns and major modifications would have been needed to the already fabricated anchor plates.



Fig. 6.1. Spherical pin after test

Subsequently Redaelli designed and manufactured a set of pins with spherical shape in high strength stainless steel material which bore against a spherical washer. This solution was accepted with minor modifications in the structure. In order to test the durability and performance of this component under load, it was also included in the axial and bending fatigue tests. The test result was successful and the elements were free of any signs of damage after the test.

7 REDAELLI SITE ACTIVITIES

Before the cable installation could begin, the pylon was constructed and self-sustained and the main part of the deck was installed and supported by temporary towers as per engineer's construction procedures. The first cable to be installed was the FLC120 Tie Down cable and after a first tensioning in order to give stability to the structure, the two main cables were uncoiled and installed to the mast and to the lower anchor points, using pulling machineries and devices. Since the height of the cranes was not enough to lift completely each main cable, the final part of uncoiling was performed with the assistance of an excavator machine.



Fig. 7.1. Tie Down cable installation



Fig. 7.2. Uncoiling Main cable

Before starting to lift and install the main cables, all the hanger clamps were installed while the cables were lying on wooden supports provided by the client. The clamps were secured to the main cables following the longitudinal and transversal marks made on the cables in the factory which ensured the correct position and alignment. The clamps were installed following a Redaelli procedure to tighten the bolts to 100% of the desired torque. Once all clamps were installed on the main cables, the cable was lifted and connected to the mast.



Fig. 7.3. Marking for clamps positioning



Fig. 7.4. Clamps installed on Main cable



Fig. 7.5. Main cable installation to the mast



Fig. 7.6. Hangers connected loosely

After uncoiling and installation of hangers, all hanger cables and Tie down cables tensioned several times by Redaelli personnel according to the engineer's tensioning procedure. The Tie Down cable was stressed using a tensioning system composed of one "stool" and No.3 jacks with capacity of 2000kN each, resulting in a total pulling capacity of 6000kN. The tensioning system for the hangers and the restrainer cables were composed of temporary rods and a beam pushed by No.2 jacks with capacity of 180kN each, for a total pulling force of 360kN on each hanger.



Fig. 7.7. Tie Down cable tensioning



Fig. 7.8. Hangers tensioning

Another challenge was related to tensioning system of the hanger cables. Since the anchor plates have no room to connect the tensioning system in the usual ways, Redaelli designed a specific tensioning system which did not required any of the steelwork to be modified. The tensioning system was connected to the permanent pins of TBF sockets that were slightly longer than the standard pins without any visual or architectural issues. For the cable tensioning, one system was supplied for the Tie Down cable and four systems were supplied for the hanger cables. In addition, two tensioning systems were used to tension the restrainer cables inside the deck.

8 UNEXPECTED ISSUES; FLOOD

Weather conditions always play an important role in the site activities and the people involved are used to dealing with the non-standard weather conditions that can slow site activities. During the cable installation, strong rains to the North of Dublin significantly raised water levels in the Scioto river and caused the site area to flood which stopped site activities for several days. Unfortunately this occurred during a critical phase when the main cables were uncoiled and placed on the ground before installation and fixing of the hanger clamps. Thanks to the quick thinking and immediate action by personnel on site, suitable wooden support was prepared before the flood hit which kept the cable above out of the flood water and avoided possible damage.



Fig. 8.1. Main cable temporarily lifted



Fig. 8.2. Working site completely covered with water

9 CONCLUSIONS AND REMARKS

The new Scioto river pedestrian bridge characterizes a transformational vision for the Bridge Street Corridor which seeks to foster a compact and sustainable growth by creating a vibrant link between the historic Dublin and the new mixed-use development on the east side of the river. It transforms part of the town into an urbanized, walkable neighborhood and creates a more unified city with connections to green space, to be an iconic symbol for a city's long-term vision.

The detailed engineering of all elements including installation method and accurate design of cable system accessories minimized the supply cost and installation time and resulted in a structure with great efficiency and high quality build standard whilst ensuring safety for everybody involved in the site activities.

Despite all challenges related to component design, manufacturing process and site activities, the bridge construction and cable installation & tensioning were performed successfully with a satisfactory result. This was testament to the close cooperation of engineers, contractors, suppliers and the project owner.

The completion of the Dublin Pedestrian Bridge has been a remarkable achievement for all the parties involved in the project and another valuable experience in Redaelli records.



Fig. 9.1. Bridge at end of tensioning



Fig. 9.2. Finished Bridge

REFERENCES

- [1] BESKE J., DIXON D., Feb 2018, "Suburban Remix", pp. 189-201, Island Press, Washington



Title of Your Paper for the Istanbul Bridge Conference (IBridge 2020)

Selcuk GORMEZOGLU

Association of Heavy Transporters of Turkey
Istanbul, Turkey

ABSTRACT

- 1) Expanding of a Toll Gate of YYS (Yavuz Sultan Selim) Bridge at Asia and Europe Side (Fener Tepe & Mecidiye) to allow passage of OOG Heavy Haulage and increase of Weight Limit from 54 tons to 150 tons.
- 2) Obtaining Road Permits of Turkish Heavy Transporters in Europe same as European Heavy Haulage Companies instead of using quota of Standart TIR Transportation provided by EU Countries.
- 3) Increasing of Speed Limits from 50 Kms to 80 kms for Heavy Transportation.
- 4) Cancel restriction to use Highways in Turkey for Heavy Transportation.
- 5) Driving permit during nighttime instead of daytime for Heavy Transportation.

Passage of YYS Bridge and North Marmara Highway System

- 1-1) 3rd and last one, YYS Bridge opened to Traffic on 26.08.2016 especially for TIR and Bus Passages at Bosphorus, not allowed since 2016. Unfortunately 3rd bridge and its Highway connection not sufficient for Heavy Haulage at all.
- 1-2) Width of Tolls are 4.50 meters and allow upto 4.35 meters Overwidth Passage. In fact allowed upto 6.90 meters overwidth passage at Turkish Road system.
- 1-3) At least 1 toll at Fenertepe and Mecidiye locations should expand for overwidth passage upto 6.90 meters.

Technical Specs of YYS Bridge

Height	: 329 meters
Length	: 2.164 meters
Width	: 58.4 meters
Abutments	: 2 + 2
Horizontal Range	: 1408 meters
Basic Materials	: Steel and Concrete
Projected for	: 4+4 Lanes for Vehicles, 1+1 Railway System
Vertical Range	: 73 meters
Type	: Suspension Bridge
Weight of Bastion/Redoubt	: 870 Tonnes
Amount of Bastion/Redoubt	: 60
Amount of Wire Ropes	: 176

- YYS Bridge is one of biggest Bridge due to 329 meters of Height and 59 meters of Width.
- When established next phase, YYS Bridge able to accept 2 Sets of Railcar same time.
- Weight restriction is 54 tonnes as per legislation which limit ruled on 1973 when 1st Bridge opened for CAR Traffic. Weight Limit of YYS Bridge much more as per verbal info provided by IC ICDAS, Management Company therefore as Transportation companies we

oblige to use YYS Bridge means we deeply request to increase weight limit to 150 tonnes min base.

Speed Limits

- 3-1) Recently Speed limit is 50 Kms per hours, thus takes 7 days if drive by 50 kms between West and east borders of Turkey. We deeply request to increase speed limit upto 80 kms (at least 70 Kms) which will be benefit of short transit time to speed- up deliveries.
- 3-2) Short Transit time also to be benefit of Traffic Congestion.
- 3-3) Positive effect logically to be valid for Pollution and Carbon Foot Print to be less.

Comparison Table between Germany, Holland and Turkey			
	GERMANY	HOLLAND	TURKEY
Speed Limits	80 km/h	80 km/h	50 km/h

Permission of Highway Drive

- 4-1) Less traffic congestion in City Centers and Standart Road Network.
- 4-2) Risk of Accidents to be more less when compare with driving at standart road networking.

Comparison Table between Germany, Holland and Turkey			
	GERMANY	HOLLAND	TURKEY
Highway Allowed	Highway networking prefered.	Highway networking prefered.	Not allowed.

Night Drive

- 5-1) Truck, Trailer and Escort Car lighting much more effective during night drive when compare with Day time. Thus Positively effect Safety of Traffic.
- 5-2) Summer Heat in Turkey negatively affect Surface of the road and Asphalt melting some weeks (some roads) of Summer.
- 5-3) Nighth drive also positively affect Lifetime of Tyres and cooling of Engine to be less affected.

Comparison Table between Germany, Holland and Turkey			
	GERMANY	HOLLAND	TURKEY
Night Drive	Night Drive allowed with requirement of sufficient lighting by escort cars.	Night Drive allowed with requirement of sufficient lighting by escort cars.	Not Allowed.



Application of ETAG 032 as a new level of expansion joint assessment

K. Hakan Geyik

Mageba Yapı Sanayi ve Ticaret A.Ş.
CAYIROVA KOCAELI, Turkey

Simon Hoffmann

mageba Ltd.
Bulach, Switzerland

ABSTRACT

Even though the European Technical Approval Guideline ETAG 032 “Expansion Joints for Road Bridges” has been introduced already in 2013 only rather simple flexible plug and nosing joints have been granted an European Technical Assessment (ETA). Nevertheless many national standards and regulations like Czech TP 86, Austrian ÖNorm B4031 and Dutch RTD 1007 refer to ETAG 032 or copied basic parts of it.

Latest efforts by the European Organization for Technical Assessment (EOTA) resulted in the transition of ETAG 032 to the actual format of European Assessment Documents (EAD). These EADs provide a more comprehensive specification for expansion joints, which is expected to push much more for ETAs granted for various types of expansion joints.

The paper will introduce these EADs and show first applications of the assessments not limited, but in particular for complex expansion joint systems like modular and large cantilever finger expansion joints. This way a new level for assessment of expansion joints is reached, which exceeds significantly any other common national specifications for expansion joints in Europe or on an international level. Overrolling tests on special prepared test tracks with statistical evaluation of measured data serves as viable basis for the assessment of the dynamic behavior of expansion joints respectively their fatigue design. Fatigue tests analyze the fatigue resistance and durability supported by wear tests. Full size kinematic test for modular joints are presented that prove the movement performance for up to 1800 mm total movement capacity. Important findings from these applications are shared in regard of general consideration of ETAG 032.

Keywords: ETAG 032, expansion joint, testing

1 INTRODUCTION

1. Introduction

mageba has been the very first company holding an European Technical Assessment (ETA) according to ETAG 032 [1 to 8] for expansion joints made of steel and therefore has been the first supplier worldwide being able to provide such expansion joints in full accordance with ETAG 032. Basis for the related CE marking is ETA-17/0612 [9] granted 13.07.2017 by OIB (Austrian Institute of Construction Engineering) in combination with the “Certificate of Constancy of Performance” issued by the notified certification body according to the Construction Product Regulation (CPR) [10].

This way mageba has proven to fulfill general requirements regarding ETAG 032 applicable for various types of expansion joints including nosing RS type joints as well as modular joints with and without noise reduction sinus plates and cantilever finger joints. The particular assessment procedure for obtaining an ETA related to these types of expansion joints for road bridges has been initiated by mageba already in 2015 and finalized for ETA-17/0612 covering single seal nosing joints.

Mageba has continued efforts for assessment in particular of modular type LR expansion joints in constant adaptation to the latest drafts of the EADs [11 to 16]. This way mageba claims to be the only supplier for modular expansion joints that succeeded in all tests according to the final draft of EAD 120113-00-0107 [16] and currently being fully prepared for submittal of an ETA. These tests cover in particular – but are not limited to – the following:

- Static testing – mechanical resistance of the product represented by test methods for components
- Dynamic testing – resistance of fatigue and wear of the product represented by test method for components
- Dynamic assessment and field testing
- Fixing of sealing elements represented by test method for components
- Assessment of resistance to fatigue by testing
- Assessment of movement capacity

Such efforts and results of successful tests have been considered for other major projects referring in particular to design according to ETAG 032. Official approval of such compliance has been granted e.g. for the largest ever build modular joints with noise reduction sinus plates (LR23-LS100 with 23 seals) supplied by mageba to the Forth Replacement Crossing Bridge project in Scotland. Involved have been expert assigned by OIB for the structural expert statement regarding compliance to ETAG 032 respectively superseding EADs.

2. Current status of ETAG 032

While mageba prepared assessments including various tests according to ETAG 032 the transition of ETAG 032 (all parts) to European Assessment Documents (EADs) has been initiated as referenced in the listing “ETAGs and their numbering as EADs” published by EOTA [17]. Mageba as well as other suppliers for modular expansion joints contribute actively to the Working Group (WG) dealing with this transition. Even though the mandate of the WG relates to a transition solely ~~with~~ without technical changes to the document it became clear that the EAD will provide significant improvements in terms of distinctiveness. Consequently it is a clear benefit for customers and suppliers of modular expansion joints to wait for the citation of the transferred EAD instead continue on the soon superseded ETAG 032. Progress on EAD 120113-00-0107 [16] (superseding ETAG 032 Part 8 for modular expansion joints [8]) has been fast and citation by the European Commission is expected for spring 2020. Likewise all suppliers for modular expansion joints have shifted their focus to an ETA based on the new EAD and none has continued or even received an ETA referring to ETAG 032 Part 8.

3. Application of ETAG 032 in EU member states

The CPR defines EADs and ETAGs used as EADs as “harmonized European specification”, which is coordinated among all EOTA member states and shall not be conflicted by national standards. This way expansion joints with granted ETA according to ETAG 032 can be placed on the market in the European Economic Area (EEA) in general and national standards shall specify only the use and application and/or additional aspects not covered by ETAG 032. Assessment methods including Assessment and Verification of Constancy of Performance (AVCP) cannot be changed by national regulations.

Various national standards and regulations in EU member states refer to ETAG 032 or copied basic parts of it. Namely the following have been introduced:

- Czech TP 86 introduced 2009
- Austrian Önorm B4031 introduced 2018
- Dutch RTD 1007 introduced 2013
- Romanian AND 590 introduced 2016

Furthermore other national specification are currently under preparation. Such includes one of the oldest and most established specifications for expansion joints TL/TP FÜ [18] introduced already in 1992 and currently applicable in its 2005 revision [19]. A new revision of TL/TP FÜ based on ETAG 032 respectively the transferred EADs is expected to be published in 2020. Beyond the European Union respectively EOTA members (including e.g. Switzerland) many authorities recognize the value of ETAG 032 and have referenced it in various general and project related specifications. This way ETAG 032 gains international importance and has the potential to substitute other specifications like AASHTO LRFD Bridge Design [21] and Construction [22] specification more and more.

4. Role of the Technical Assessment Body and Notified Body

EOTA lists currently [23] 33 Technical Assessment Bodies (TAB) in the field of “Road equipment: Circulation fixtures”, which relates to ETAG 032 according to EOTA listing [24]. Few of them have expertise in the field of expansion joints for road bridges or can refer to reasonable history of involvement. OIB with executive members being involved in the development of ETAG 032 from the very beginning and providing the chair of the WG in charge for the transition of ETAG 032 to EADs is among one with the highest expertise in the field of expansion joints for road bridges. Apart of this particular expertise OIB is cooperating with other experts in this field supporting the assessment. Checking of design calculations is supported by independent specialists from Fritsch Chiari an Partner (FCP) e.g. providing sophisticated engineering services and survey with particular focus on expansion joints for decades. Testing is conducted by independent and renowned experts like the Materials Testing and Research Institute (MPA Karlsruhe). E.g. MPA Karlsruhe has conducted for various manufacturers tests based on different standards and national accreditations of expansion joints for road bridges within their 100 years of history in construction product testing.

Without such involvement of experts responsibilities respectively interfaces including a minimum “four eyes principle” between basic tasks like, testing, checking and assessment cannot be ensured or guided by otherwise mandatory quality assurance systems like EN ISO/IEC 17025 [25] for testing.

The same applies for the notified certification body (NB), which ensures third party survey based on control plans defined by the TAB granting the ETA. Currently 7 NBs have an accreditation and notification as NB for expansion joints for road bridges according ETAG 032. Few of them have experience in the field of road expansion joints or have been accepted as third party survey based on other national standards and regulations in the past like e.g. TL/TP FÜ. Various NBs survey manufacturers related to ETAs that have been issued by the same NB acting as TAB including the definition of control plans, which disregards the independence of the NB and stops revealing of mistakes in the interpretation of standards, assessment and even the ETA itself.

The coordination between the different experts within their particular focus (testing, engineering, assessment and survey) is considered as vital aspect to ensure full use of expertise and mutual control. Such has been an important principle in the past in the application of TL/TP FÜ in Germany e.g. including definition of dedicated test labs and checkers with sufficient level of expertise. CPR is shifting that responsibility now to the manufacturer and client as far as national standards and regulations do not provide additional aspects in this regard.

5. Static testing

Static tests regarding mechanical resistance of the product represented by a test method for components relate in particular to creep and relaxation of components used for modular joints. Prestress of the sliding system connecting centerbeams with support bars is a vital aspect in the overall performance of a modular expansion joint. All expansion joints face certain vertical upswing at the point the wheel loses contact with the load carrying elements like centerbeams or fingers. EAD 120113-00-0107 for modular joints requires to identify this upswing and dynamic factors from dynamic assessment based on field tests (compare 7.), while most other types allow for an upper threshold values of 30%. The special kinematic of modular joints does not allow to define such upper threshold values. The load impact on the sliding bearings result from the design load multiplied by identified dynamic factors acting to the prestressed sliding system of the connection of the centerbeam to the support bar and connection of the support bar to the structure at the support box. The uplift acting on the sliding springs is that load impact multiplied by the identified upswing value. Creep effecting the sliding bearing and relaxation effecting the sliding spring reduce the effective prestress for these connections and may result in decompression (gaping) if not considered. In particular fatigue resistance will not be given in case of hammering connections due to decompression. Testing covering service, fatigue and ultimate load conditions is described in detail in EAD 120113-00-0107, Annex C and requires the use of special chambers (compare Fig 1)) to consider temperature effects.

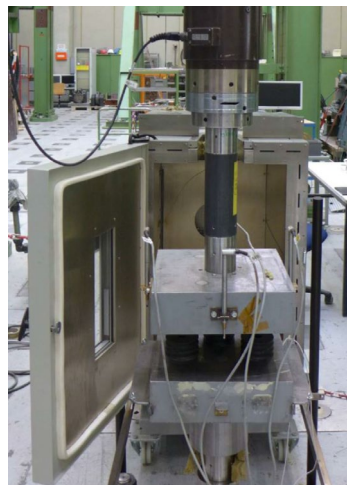


Fig. 1) Static test setup including climate chamber

6. Dynamic testing

Dynamic tests regarding resistance to fatigue and wear of the product represented by a test method for components relate in particular to sliding components used for modular joints. Wear and load impact challenge both the durability of modular expansion joints respectively maintenance of such joints as the related sliding bearings and sliding springs are considered as replaceable parts according Table 2 of EAD 120113-00-0107. Category “B” applies for these components, which shall provide an intended working life not less than 0,5 times the intended working life of the kit relating to minimum 25 years for these components based on recommended 50 years for the kit (overall expansion joint). Apart of the large accumulated movements related to such long working life it is clearly related to very high number of load cycles. Accordingly the second phase is recommended to cover unlimited fatigue life by testing for 5×10^6 cycles. Mageba has tested sliding springs and sliding bearings according to phase 1 described in EAD 120113-00-0107, Annex D for up to 9 km of accumulated sliding path with double amplitude of up to 1 m (compare Fig. 2a)) proving stable and low friction as well as succeeding without any sign of wear. Subsequent the sliding bearings have been tested (compare Fig. 2b)) according phase 2 for fatigue loads adjusted with results from dynamic assessment based on field tests (compare 6.). Such testing for 5×10^6 cycles resulted in less than 2,4 % change of height. Both phases require active temperature control of the entire test setup.



Fig. 2) a) Wear test setup and b) fatigue test setup both with active temperature control

7. Dynamic assessment and field testing

Dynamic assessment and field test relate in particular to the dynamic behavior of expansion joints, which are identified by overrolling tests per each type and system applicable to a range of similar behavior. Especially vertical dynamic impact, upswing, transfer of horizontal to vertical load and horizontal response ratio factors have significant impact on the loads that need to be considered for fatigue calculations as well as for loads applied in tests. Apart of EAD 120113-00-0107 [16] for modular joints all other EADs [11 to 15] related to expansion joints for road bridges provide default values, which can be applied instead of values identified by overrolling tests. Nevertheless results from dynamic assessment and field tests can be applied for most types almost identical to modular joints. For all such tests it is vital to fulfil requirements given by the applicable EAD in detail like in EAD 120113-00-0107, Annex E for modular joints. In particular all dynamic influences need special attention like evenness of medium quality ensured for the pavement minimum 30 m before and behind the installed expansion joint specimen. Proving that criteria requires defined prepared pavement as well as very special expertise and equipment in the field of roads surface survey and data processing. Similar applies to the dynamic measurements from different truck impacts on various speed, full

acceleration and full braking. Field measurements by the use of strain gauges, accelerometers and laser signals as well as statistical data evaluation requires particular expertise, which can be offered by few experts especially if such should cover experience related to dynamic assessment of expansion joints. It took mageba with various partners several weeks of test campaign to conduct these tests for various types of expansion joints such as nosing (single seal), cantilever finger and modular joints with and without noise reducing elements (compare Fig. 3)).



Fig. 3) Dynamic assessment and field test setup

8. Fixing of sealing elements represented by test method for components

Fixing of sealing elements represented by test method for components relates in particular to seal elements applied for nosing (single seal) and modular joints. Test are specified in EAD 120709-00-0107, Annex D and F respectively EAD 120113-00-0107, Annex F and address proper fixing and mechanical resistance as well as watertightness and cleanability. Specific cycles of partially combining longitudinal, transversal and vertical movement have to be conducted under permanent control regarding proper fixing and for some cycles filled with sand to simulate debris or water to check for watertightness. Such covers new and artificially aged components and as tested by mageba as well special connection details for waterproofing membranes (compare Fig. 4)).

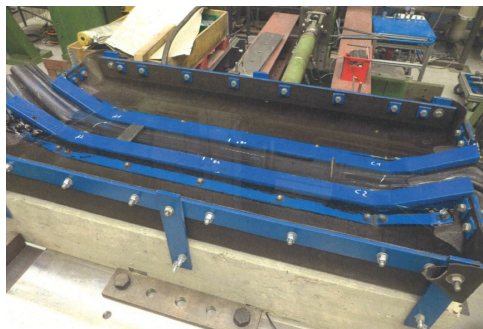


Fig. 4) Watertightness test for strip seals

9. Assessment of resistance to fatigue by testing

Assessment of resistance to fatigue by testing relates in particular to details, which are difficult to be assessed by calculation only like the anchorage of expansion joints to concrete structures. Taking into account that these elements cannot be replaced and an intended working life of 50 years is anticipated, the number of load cycles should cover unlimited fatigue resistance by testing for 5×10^6 cycles. Again test loads shall be based on fatigue loads adjusted according results from dynamic assessment based on field tests (compare 7.) in order to cover the effective behavior of the tested type

and system of expansion joint. Particular care is required regarding simulation of the wheel print for the load application (compare Fig. 5).



Fig. 5) Fatigue testing of anchorage

10. Assessment of movement capacity

Assessment of movement capacity is required for all types of expansion joints for road bridges and is specified in EAD 120109-00-0107, Annex D.3 (referenced by the other EADs). The test shall cover full movement capacity of the expansion joint in several cycles partially combining longitudinal, transversal and vertical displacement as well as rotations if relevant. In particular for very large movement capacity such testing is very demanding and requires very special test equipment. Mageba has used such equipment to test 18 gaps modular expansion joints with and without noise reduction elements and movement capacity of up to 1800 mm in longitudinal, 900 mm in transversal and 90 mm vertical direction (compare Fig 6)).



Fig. 6) Assessment of movement capacity

11. Conclusion

First applications of ETAG 032 respectively superseding EADs have shown its high level in regard of considered design requirements in comparison to other currently applied specifications for expansion joints for road bridges. This high design level in combination with demanding and extensive test procedures provide a new level of safety, robustness and durability of expansion joints serving the bridge owner and public in general. Still national specifications have in important role in defining the use and application of expansion joints according to ETAG 032 and additional aspects not covered by ETAG 032. These national specifications as well as ETAs shall refer to the EADs superseding ETAG 032 for the benefit of a more comprehensive specification and consequent fulfilment of the Construction Products Regulation (CPR). The Technical Assessment Body (TAB) has a special role as a key element in ensuring the declared performance according granted ETA. Considering the complexity of the assessment task it seems not only vital, but inevitable to involve

other experts as no TAB has the broad expertise covering formalities, engineering, testing, measuring and data processing (among many other challenges). Expansion joints and in particular their detailed testing is a very specific field with very few experts available, which the TAB needs to involve in coordination with the manufacturer of the expansion joint. Similar applies to the later Assessment and Verification of Constancy of Performance (ACVP) by the Notified certification Body (NB). The particular expertise and independence of the TAB and NB will give the basis for surveillance of the values declared by the supplier.

12. References

- [1] ETAG 032 Part 1 GENERAL, May 2013
- [2] ETAG 032 Part 2 BURIED EXPANSION JOINTS, May 2013
- [3] ETAG 032 Part 3 FLEXIBLE ASPHALTIC PLUG EXPANSION JOINTS, May 2013
- [4] ETAG 032 Part 4 NOSING EXPANSION JOINTS, May 2013
- [5] ETAG 032 Part 5 MAT EXPANSION JOINTS, May 2013
- [6] ETAG 032 Part 6 CANTILEVER EXPANSION JOINTS, May 2013
- [7] ETAG 032 Part 7 SUPPORTED EXPANSION JOINTS, May 2013
- [8] ETAG 032 Part 8 MODULAR EXPANSION JOINTS, May 2013
- [9] ETA-17/0612 mageba Tensa®Grip Type RS, granted 17.07.2017
- [10] Construction Product Regulation, Regulation (EU) No 305/2011 of March 2011
- [11] EAD 120093-00-0107 FLEXIBLE ASPHALTIC PLUG EXPANSION JOINTS FOR ROAD BRIDGES, December 2019
- [12] EAD 120109-00-0107 NOSING EXPANSION JOINTS FOR ROAD BRIDGES, December 2019
- [13] EAD 120110-00-0107 MAT EXPANSION JOINTS FOR ROAD BRIDGES, December 2019
- [14] EAD 120111-00-0107 CANTILEVER EXPANSION JOINTS FOR ROAD BRIDGES, December 2019
- [15] EAD 120112-00-0107 SUPPORTED EXPANSION JOINTS FOR ROAD BRIDGES, December 2019
- [16] EAD 120113-00-0107 MODULAR EXPANSION JOINTS FOR ROAD BRIDGES, December 2019
- [17] ETAGs and their numbering as EADs, EOTA Publication January 2019
- [18] TL/TP FÜ 92, Technical delivery and inspection specifications for watertight expansion joints, release 1992
- [19] TL/TP FÜ 05, Technical delivery and inspection specifications for watertight expansion joints, release 2005
- [20] TL/TP FÜ 20, Technical delivery and inspection specifications for watertight expansion joints, draft 2020
- [21] AASHTO LRFD Bridge Design specification, 8th Edition, September 2017
- [22] AASHTO LRFD Construction specification, 4th Edition, 2017
- [23] <https://www.eota.eu/en-GB/content/how-to-find-a-tab/55/>, last visited 18.02.2020
- [24] Categorization of ETAGs in the product areas according to Annex IV Regulation (EU) No 305/2011, January 2014
- [25] EN ISO/IEC 17025:2017 Accreditation of conformity assessment bodies

Bridge Maintenance



Qualifying Commercial Rapid Repair Media for Partial Depth Bridge Decks Repairs

Ali Banaei Pour, M.Sc.

Ph.D. Student and Graduate Research Assistant
Department of Civil, Environmental, and Architectural Engineering
University of Kansas, Lawrence, KS 66045-7609

Robert J. Thomas, Ph.D.

Assistant Professor
Department of Civil and Environmental Engineering
Clarkson University, Potsdam, NY 13699

Marc Maguire, Ph.D.

Assistant Professor
Durham School of Architectural Engineering and Construction
University of Nebraska-Lincoln, Omaha, NE 68182

Andrew D. Sorensen, Ph.D.

Assistant Professor
Department of Civil and Environmental Engineering
Utah State University, Logan, UT 84322-4110

Md. Abdullah Al Sarfin, M.Sc.

Ph.D. Student and Graduate Research Assistant
Department of Civil and Environmental Engineering
Utah State University, Logan, UT 84322-4110

ABSTRACT

Department of transportations' mandates to limit the impact of construction on the traveling public highlight the need for rapid bridge deck repairs. Numerous proprietary and non-proprietary rapid repair media have been developed to address this need; a systematic qualification of these materials is needed. Critical properties include setting time, rate of strength gain, compressive and tensile strength, workability, bond strength, dimensional compatibility (free and restrained shrinkage), and durability. This research study is aimed at evaluating eight commercial cementitious repair media for partial-depth repair of concrete bridge decks. A robust laboratory study of the mechanical performance and durability properties of the selected materials was conducted. More than 450 specimens were prepared according to manufacturer recommendations and tested at ages of 4 hours, 24 hours, 7 days, and 28 days to measure their setting time, compressive and splitting tensile strength, elastic modulus, autogenous and drying shrinkage, surface resistivity, and slant shear bond strength. The goal of this study is to identify the most influential factors in the success or failure of repair materials and projects as well as which tests are most helpful in the process of evaluation and selection of repair materials.

Keywords: Concrete, Repair, Rapid Repair, Rapid-set Materials, Material Testing

1 INTRODUCTION

Deck patching is an economical option for addressing deterioration in concrete bridge decks (Cervo and Schokker, 2010). Conventional portland cement-based concrete is a reliable repair material, but the requisite curing time delays reopening and requires detours or lane closures. Rapid repair of deteriorated bridge decks and pavements reduces construction costs and impacts on the public (Ram, 2013). Consequently, rapid-hardening, pre-packaged repair mortars or concretes have recently been in great demand. These are typically used so that the repaired structure can be reopened to traffic in as few as 2-4 hours after field placement (Ram, 2013; Cervo and Schokker, 2010; Rizzo and Sobelman, 1989; Goodwin, 2013). The primary categories of rapid-setting cement-based materials are magnesium phosphate cement, calcium sulfoaluminate (CSA) cement (Thomas et al., 2018), calcium aluminate cement, and other blended cements (Ram, 2013; ACI and ICRI, 1999; Cusson and Mailvaganam, 1996).

Compared to conventional Portland cement-based concrete, prepackaged cementitious rapid repair materials are easier to mix and are more compatible with the substrate, but they are costly and can be more susceptible to shrinkage (Yang et al., 2016). One of the major concerns in rapid repair of concrete is the premature failure of the repair system (Baluch et al., 2002), which is mainly caused by exposure to freeze-thaw cycles, aggressive chemical exposure, mechanical abrasion, loss of bond between the repair and the substrate, and dimensional stability of the repair material (elastic modulus, shrinkage, expansion, etc.). Most of the problems are related to durability and construction issues rather than structural failures (Ram, 2013). For this reason, proper selection and systematic performance evaluation of a repair material is of the utmost importance. Since a plethora of rapid-setting repair materials with a wide range of mechanical and physical properties are commercially available, selecting a suitable material is difficult.

In this study, eight commercial cementitious rapid repair media were investigated for application to concrete bridge decks. A robust laboratory study of mechanical performance and durability was conducted. Setting time, compressive and splitting tensile strength, static modulus of elasticity, autogenous and drying shrinkage, surface resistivity, and slant shear bond strength were tested. Most tests were performed at ages of 4 hours, 24 hours, 7 days, and 28 days. The objective was to identify the most influential factors and tests to be considered for an efficient material evaluation and selection in their repair projects.

2 EXPERIMENTAL PROGRAM

2.1 Materials, Mixing, and Casting

Eight rapid-set pre-packaged repair materials from five manufacturers were selected for investigation. Table 1 presents important properties of the selected repair materials. All materials were cement-based and one-component. Some contained fibers and some were pre-extended with coarse aggregates. M4 was extended 100% by weight with local No. 8 pea gravel. None of the materials required a primer to apply.

Materials were mixed and cast according to manufacturer recommendations. All materials were preconditioned to 70°F (21°C) before mixing. A 3 ft³ (0.085 m³) rotating drum mixer was rinsed with water, followed by removal of any excess water in it. An initial amount of water (different for each product), along with pea gravel for M4, was added to the mixer and the mixer was started. The repair material was added slowly and mixed for a time specified by the manufacturer (typically 1-3 minutes). The time at which water touched the cement for the first time was recorded. The mixing continued for a few minutes after adding the remaining water. After achieving a uniform consistency in the mixtures, casting of the specimens was started. Adding extra water to the mixture was strictly avoided.

Table 1 Summary of Properties of Selected Repair Materials

Property	Material							
	M1	M2	M3	M4	M5	M6	M7	M8
Contain Fiber?	Yes	No	No	No	Yes	No	No	Yes
Weight of Bag, lb	53.5	65	65	55	60	50	50	50
Pre-Extended?	Yes	Yes	Yes	No	Yes	No	No	No
Yield/Bag, ft ³	0.40	0.5	0.5	0.5	0.42	0.43	0.43	0.42
Required Water/Bag, L	1.89	2.4	2.6+0.24	2.8-4.3	2.8-3.3	2.6	2.6	3.07
Recommended Tempt. Range for Mixing, °F	40-120	> 45	> 40	45-90	45-90	> 40	> 50	> 40
Mixing Duration, min	7	3	3 (max)	1-3	3 (max)	3-5	3-5	2-3
Working Time, min	Varies	-	-	10-25	15-20	8	25	-

1 lbs. = 0.45 kg.; 1 ft³ = 0.0283 m³; 1 L = 0.001 m³; 1 °F = [32 + (5/9)]°C

2.2 Testing Program

The selected repair media were investigated for their mechanical and durability properties by performing the following tests at ages of 4 hours to 28 days. All measurements included three replicates.

2.2.1 Setting Time

Initial and final setting times were measured by Acme penetration resistance (ASTM C403) using fresh 6×6 cylinders.

2.2.2 Mechanical Properties

Compressive strength, static modulus of elasticity, and splitting tensile strength were measured in accordance with the relating ASTM specifications (C39, C496, and C469, respectively) using 4x8 in (100x200 mm) cylinders with three replicates per test at ages of 4 and 24 hours and 7 and 28 days.

Bond strength was measured by slant shear (ASTM C882 and C928). Three replicates were tested each at 4 hours, 24 hours, and 28 days. The substrate concrete had a design strength of 5000 psi (34.5 MPa) and the substrate cylinders were water cured for at least 28 days followed by being saw cut at 45° angle through the long axis into two equally-sized sections. Fresh repair material was poured on top of the substrate and the composite specimen was then moist cured.

2.2.3 Durability and Dimensional Stability

The surface electrical resistivity (AASHTO TP 95) of every cylinder was measured prior to mechanical testing.

Autogenous shrinkage was measured with the corrugated tube method (ASTM C1698) beginning at final set. Rapid setting times precluded sieving materials that included coarse aggregates or fibers, so autogenous shrinkage was only measured for those without (M4, M6, and M7).

Drying shrinkage (ASTM C157 and C928) of 3×3×16-in (75×75×400 mm) concrete prisms was measured after demolding at both 4 and 24 hours. Although the standard methods recommend testing beginning at 24 hours, rapid materials are meant to enter service after only 4 hours. Specimens were stored at 73±3°F (23±2°C) and 50±5% RH after curing. Length change was measured in short intervals for the first 6 hours after demolding, followed by daily and then weekly measurements for up to 28 days.

3 RESULT AND DISCUSSION

3.1 Setting Time

Figure 1-a shows the initial and final setting times of the repair media. Initial setting time corresponds to a complete loss of workability; final setting time corresponds to the start of strength development. Therefore, the setting time is a critical measurement that needs to be considered. The repair materials evaluated in this study showed varied setting times. The accuracy of the setting time measurement is affected by several factors, including material and ambient temperature.

Based on Figure 1-a, the initial setting time for all materials was between 20 and 35 minutes, except for M2 and M7. Both M2 and M7 had an initial setting time of more than one hour. All other materials become fully solidified in less than an hour. M4 had the lowest initial setting time (23 minutes), while for M2 reaching the initial set time took 72 minutes. In other words, M4 and M2 had the lowest and the highest working time, respectively. Similarly, M2 and M7 were the only materials with a final setting time of more than an hour. For all other materials, the final setting time was measured between 30 to 50 minutes. Here, M3 and M8 had the lowest final set time (28 minutes). For M2, becoming fully rigid took about 2 hours, similar to a conventional high early strength concrete.

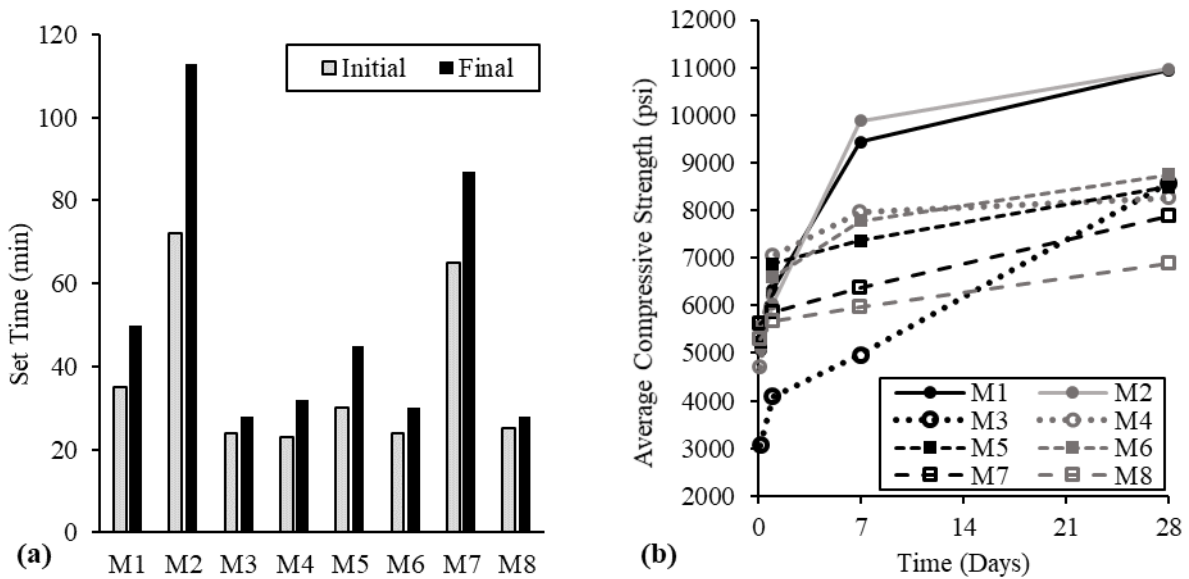


Figure 1: (a) Setting time, and (b) Average compressive strength of repair materials (1 psi = 0.0069 MPa)

The time between the initial and final set for most materials (75% of materials) was around 5 and 15 minutes. For M2 and M7, which had the highest initial and final setting time, reaching the final set was relatively gradual and took 20 to 40 minutes. Most materials started to gain strength rapidly, commonly in less than 45 minutes.

3.2 Compressive Strength

A SHRP-proposed classification system was adopted to categorize the selected rapid repair media based on the rate of strength development. Accordingly, very early strength (VES) materials develop at least 3,000 psi (20.7 MPa) compressive strength in 4 hours; high early strength (HES) materials achieve at least 5,000 psi (34.5 MPa) in 24 hours; and very high strength (VHS) materials achieve compressive strength over 10,000 psi (69 MPa) in 28 days (Yang et al., 2016; Goodspeed et al., 1996). Table 2 presents compressive strength results and SHRP classifications for the tested repair media.

Table 2 Average compressive strength of the repair materials at different ages (1 psi = 0.0069 MPa)

Product	Average Compressive Strength (psi)				SHRP Category
	4 Hours	24 Hours	7 Days	28 Days	
M1	5,067	6,334	9,442	10,942	VES, HES, VHS
M2	5,106	6,044	9,876	10,966	VES, HES, VHS
M3	3,065	4,088	4,967	8,573	VES
M4	4,709	7,050	7,971	8,266	VES, HES
M5	5,238	6,880	7,356	8,490	VES, HES
M6	5,545	6,600	7,781	8,747	VES, HES
M7	5,611	5,854	6,382	7,893	VES, HES
M8	5,293	5,660	5,956	6,879	VES, HES
VES: Very early strength HES: High early strength VHS: Very high strength					

Based on Table 2, all materials satisfy compressive strength requirements at very early ages, with the minimum and maximum at 4 hours being about 3,000 psi (20.7 MPa) and 5,600 psi (38.6 MPa), respectively. Thus, all materials fall into the VES category. All materials, except for M3, can be classified into HES category as their 24-hours strength is more than 5,000 psi (34.5 MPa). However, all materials meet the target strength at 24 hours, which is 4,000 psi (27.6 MPa). This is also true for target strength at 7 days, since all materials have at least 5,000 psi (34.5 MPa). The late-age compressive strength of all materials was also desirable (between 6,800 (46.9 MPa) and 11,000 psi (75.8 MPa)). The only materials that can be labeled VHS are M1 and M2. It should be noted that SHRP classification is helpful in terms of deciding on the repair volume and speed. VES materials quickly develop enough strength and are a good choice for a small repair area, while HES allows for the pavement to be reopened to traffic in 24 hours. When there is a substrate with a high compressive strength a VHS material is preferred, but it should be considered that high strength materials are often more susceptible to shrinkage cracking and related problems.

Figure 1-b shows the strength development of repair media; all materials satisfy the minimum compressive strength requirements but the rates of strength gain were very different. M1, M2, and M3 developed not only a noticeable compressive strength at early ages (more than 1,000 psi (6.9 MPa) from 4 to 24 hours), but also significantly and continuously gained strength after 24 hours. In these three materials, the late-age compressive strength (at 28 days) is nearly twice their 24-hour strength. M1 and M2 also have the highest 7 and 28-days strength among all materials. This could be due to the noteworthy hydration potential remaining in these materials after setting rapidly and quickly and indicates a desirable performance in terms of compressive strength at both early and late ages.

Conversely, M7 and M8 had a low strength gain at early ages and also insignificant strength development at late-ages, but still meeting the project compressive strength requirement very well. M4, M5, and M6 showed a considerable strength gain at early ages (about 1,500 psi (10.34 MPa) to 2,000 psi (13.8 MPa) increase), but the rate of strength gain beyond 24 hours in these materials is not as high as M1, M2, and M3. Nevertheless, M4, M5, and M6 showed desirable compressive strength gain and performance at both early and late ages.

3.3 Static Modulus of Elasticity

Modulus of elasticity is an indicator of the stiffness of a material, and one of the general requirements for the structural compatibility of repair materials is having an elastic modulus close to that of the substrate concrete (Quezada, 2018). If the substrate is assumed to be a typical, normal-weight concrete bridge deck with a nominal compressive strength of 5 ksi (34.5 GPa), then its elastic modulus is around 4,000 ksi (27.6 GPa) (ACI 318-14, 2014). Considering the elastic modulus of an aged concrete deck being more than 4,000 ksi (27.6 GPa), an E_c of 4,000 (27.6 GPa) to 5,000 ksi (34.5 GPa) can be considered as the desired range. The average elastic modulus of the rapid repair materials at different ages is presented in Figure 2-a.

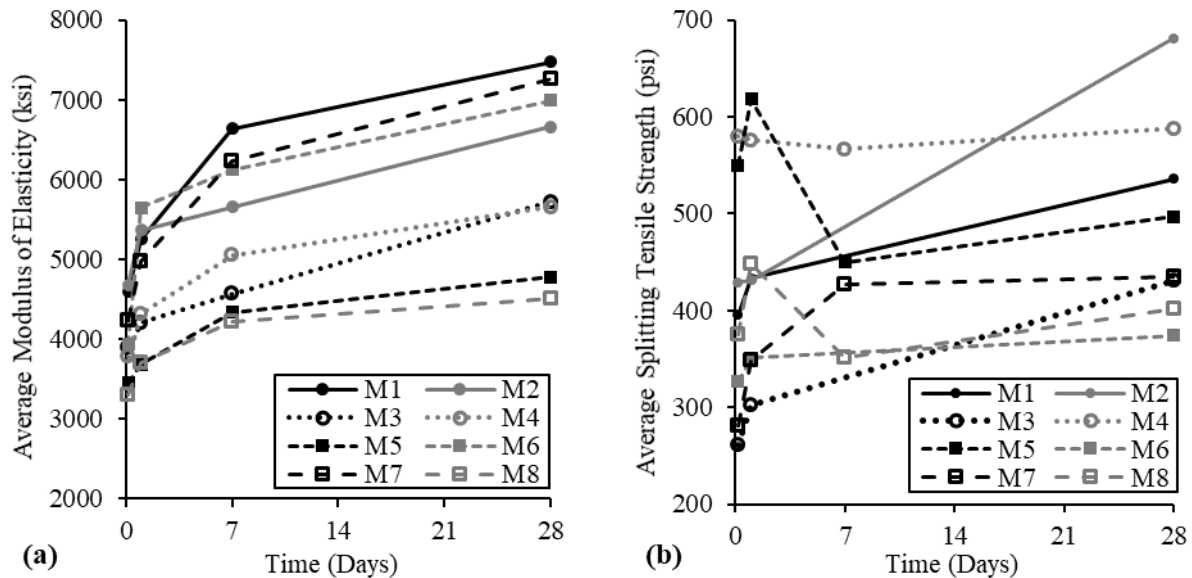


Figure 2: (a) Average elastic modulus, and (b) Average splitting tensile strength of repair materials (1 psi = 0.0069 MPa)

Based on Figure 2-a, the elastic modulus of the selected rapid repair materials at the time of exposure to traffic (4 hours) is between 3,300ksi (22.8 GPa) and 4,700 ksi (32.4GPa). M2 and M8 had the lowest and the highest E_c at 4 hours, respectively. At this age, only three materials (M1, M2, and M7) had an elastic modulus of over 4,000 ksi (27.6 GPa). At late-ages (28 days), the selected repair materials showed a E_c of 4,500 ksi (31 GPa) to 7,500 ksi (51.7 GPa), with M8 and M1 having the lowest and the highest value, respectively.

Similar to the compressive strength gain (Figure 1-b), different rates of elastic modulus development can be observed. M1 and M7 did not develop much elastic modulus at early ages, but had a dramatic development beyond 24 hours. These two materials also had the highest elastic modulus at 7 and 28 days. M2, M3, and M6 showed a similar trend, but their stiffness development beyond 24 hours is not as high as M1 and M7. M6 showed the highest increase in stiffness at early ages (4 to 24 hours) among all materials. M5 and M8 did not show a very noticeable stiffness development at neither early nor late ages. However, these two materials are the only materials that fall in the desired elastic modulus range of 4,000 ksi (27.6 GPa) to 5,000 ksi (34.5 GPa) at late ages.

3.4 Splitting Tensile Strength

The repair material should have a tensile strength equal to or greater than that of the substrate concrete (Quezada, 2018). For a normal weight concrete with a nominal 28-days compressive strength of 5,000 psi (34.5 MPa), the tensile strength is 400-500 psi (2.76-3.45 MPa) (ACI 318-14, 2014). Therefore, the repair materials should have a tensile strength of at least 400 psi (2.76 MPa) to

be considered acceptable. Figure 2-b presents the average tensile strength of repair materials at different ages. It should be noted that, due to some mixing and casting limitations, the splitting tensile test at the age of 7 days was skipped for M1, M2, M3, and M6.

Based on Figure 2-b, M3 and M4 had the lowest and the highest tensile strength at the critical age of 4 hours. Four materials (M1, M2, M4, and M5) satisfied the tensile strength requirement at this age, having a strength of about 4,000 psi (27.6 MPa) or higher. At late ages (28 days), all but one material (M6) had a tensile strength of higher than 4,000 psi (27.6 MPa). M2 had the highest tensile strength at 28 days. Different trends in tensile strength development can be observed in Figure 2-b. Similar to compressive strength results, M1 and M2 had the highest tensile strength development. M3, had the worst tensile strength development at early ages but managed to satisfy the strength requirement at 28 days. Some materials (M4, M5, and M8) did not continuously develop tensile strength. These materials showed a decrease in tensile strength from 24 hours to 7 days, but again developed strength beyond 7 days. This behavior is more noticeable in M5 and M8 which both contain fibers. M4, despite following the mentioned trend, maintained a high tensile strength all the time.

3.5 Surface Electrical Resistivity

Surface electrical resistivity is a measure of concrete chloride penetrability. A resistivity of <10, 10-15, 15-25, 25-200, and >200 indicates a high, moderate, low, very low, and negligible chloride penetration, respectively (Kessler et al., 2008). Average surface resistivity of all materials at different ages is presented in Figure 3-a. Based on Figure 3-a, M1, M2, and M3 had a moderate and M6 had low chloride penetration potential at the critical age of 4 hours. All other materials had very low chloride penetrability at the age of 4 hours. After 4 hours, all materials developed surface resistivity over time and their chloride penetration potential at 28 days was very low. The development in M1 was exceptional as its surface resistivity significantly increased beyond 24 hours, making its chloride penetrability at 28 days negligible.

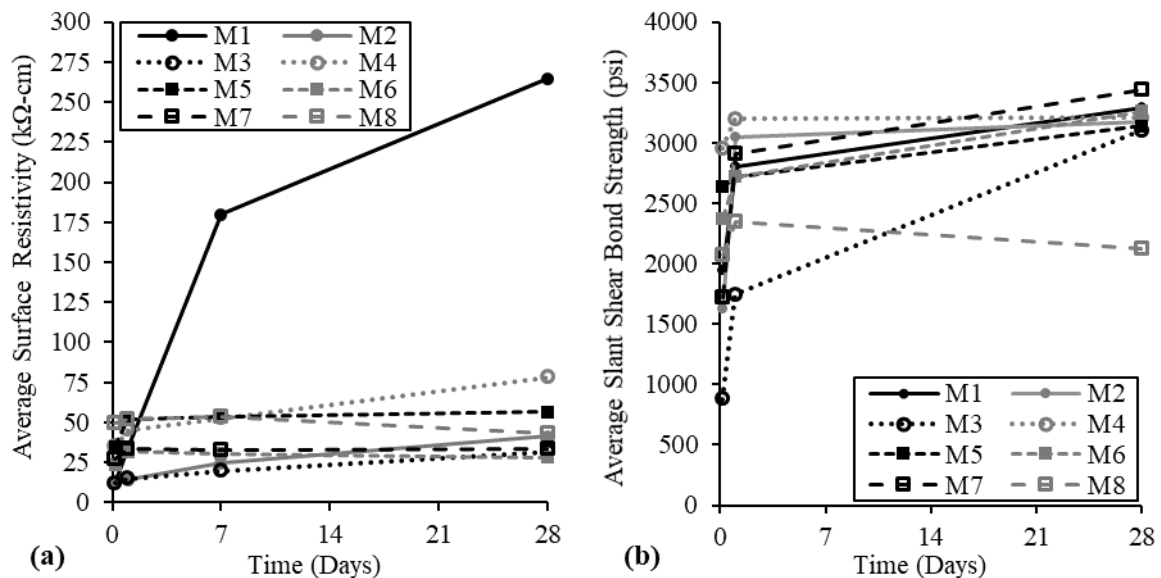


Figure 3: (a) Average surface resistivity, and (b) Average bond strength of repair materials (1 psi = 0.0069 MPa)

No other material gained a noticeable surface resistivity after the initial development, and based on Figure 3-a, they showed a similar steady increase in surface electrical resistivity over time. M6 and M8 showed a slightly decrease in surface resistivity at late ages, but their chloride penetration potential was still very low.

3.6 Slant Shear Bond Strength

The quality and strength of bond between the substrate concrete and repair material is of utmost importance. Practically, there is a state of shear at the repair-substrate interface, therefore the slant shear test was adopted to measure the bond strength of the selected repair media. According to ASTM C928, the required bond strength for rapid-set prepackaged repair materials is 1000 psi (6.9 MPa) and 1500 psi (10.34 MPa) at 1 and 7 days, respectively. Table 3 presents the average slant shear bond strength of the repair materials at different ages along with the failure mode observed in three specimens tested at each age.

Table 3 Average slant shear bond strength and failure modes of the repair materials (1 psi = 0.0069 MPa)

Product	Average Slant Shear Bond Strength (psi)					
	4 Hours	Failure Modes	24 Hours	Failure Modes	28 Days	Failure Modes
M1	1,943	R, R, R	2,797	R, S, S+R	3,285	S, S, S
M2	1,625	R, R, R	3,047	S, S, S	3,174	S, S, S
M3	878	R, R, R	1,742	R, R, R	3,099	R+S, S, R+S
M4	2,954	B, B, S	3,198	S, S, S+R	3,209	S, S, S
M5	2,632	B, B, B	2,720	B, S+B, B	3,136	R, S, S+R
M6	2,373	R, R, R	2,722	B, R+S, R+S	3,260	S+R, S, S
M7	1,718	B, R, R	2,913	S+R, R+B, R+B	3,434	S, S, S
M8	2,071	B, B, B	2,343	B, S+B, R+B	2,117	B, R+B, B
R: Repair material failure S: Substrate concrete failure B: Bond failure						

Based on Table 3, the lowest and the highest bond strength at the critical age of 4 hours was observed in M3 and M4, respectively. At the late-ages (28 days), all but one material (M8) had a bond strength of over 3,000 psi (20.7 MPa). The early age bond strength of repair materials varied noticeably, but the 28-days bond strength for all materials was very close, except for M8. Similar to splitting tensile strength, M8 showed an increase-decrease trend and its late-age bond strength was the considerably lower than all other materials.

Figure 3-b shows that all materials also satisfy the 7-days bond strength requirement of ASTM C928. M3, which had the lowest bond strength at 4 hours, had the most significant bond strength development among all materials. M2 and M7 had the highest bond strength development from 4 to 24 hours, but M2 did not developed much bond strength beyond 24 hours. This was also true with M4, which had the highest bond strength at early ages (4 and 24 hours), but developed a negligibly beyond 24 hours. M1, M5, M6, and M7 showed almost a same rate of bond strength development beyond 24 hours. As discussed previously, in can be observed in Figure 3-b that M8 followed an increase/decrease trend, similar to its splitting tensile strength development behavior. It had also the lowest 1- and 28-days slant shear bond strength.

Another observation was in failure modes in which materials showed all possible failure patterns, including bond failure, repair material failure, substrate concrete failure, and a combination of the three failure modes. Figure 4 illustrates the typical failure modes observed in the slant shear test. In this study, in four out of eight repair materials (M1, M2, M3, and M6) bond failure was observed in one specimen only. Other materials (M4, M5, and M7) experienced bond failure at early ages but not at late ages. M8 is the only material having bond failure at both early and late ages. Based on Table 4, M5 and M8 had the highest number of bond failures. M2 is the only material having only repair or substrate failure modes. M2 also had the highest number of substrate failures, long with M4. M3 had the highest number of repair material failures.



Figure 4: Failure modes observed in the slant shear bond strength tests: (a) Bond failure, (b) Substrate concrete failure, (c) Repair material failure, and (d) Combination of failures

3.7 Autogenous Shrinkage

Figure 5 shows the average autogenous shrinkage of the three materials at different ages.

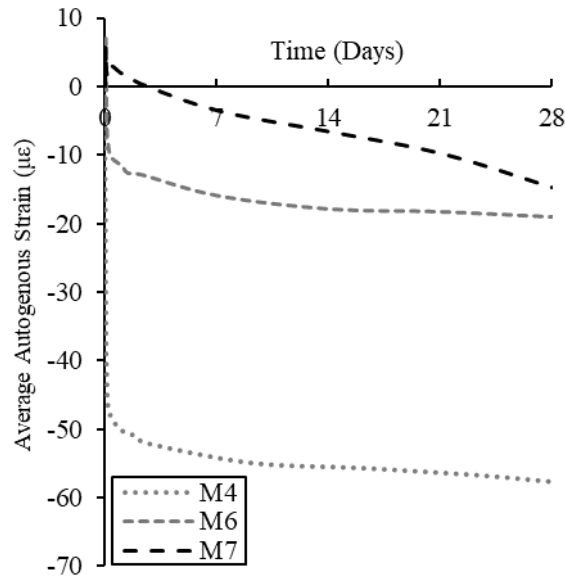


Figure 5: Average autogenous shrinkage of materials 4, 6, and 7 at different ages

It can be observed in Figure 5 that a significant portion of the total autogenous deformation occurred in the first 2-3 days. This observation is especially discernable in M4, in which the rate of autogenous strain development beyond two days is very steady with a slow pace. M4 also had the highest autogenous deformation at all ages, with about -50 and -60 $\mu\epsilon$ at 24 hours and 28 days, respectively. Nonetheless, a deformation of -60 $\mu\epsilon$ is still negligible, calling for further investigation through drying shrinkage test. Another observation in Figure 5 is that M6 and M7 initially and at very early ages showed expansion, but started to shrink afterwards. There are two possible reasons for this phenomena, namely early heat of hydration which causes thermal expansion, and use of shrinkage compensating admixtures which cause expansion to offset the material shrinkage (Yang et al., 2016). It should be noted that the only difference between the two materials is that M7 has a higher initial and final setting time, so the material with more working time developed lower autogenous deformation.

3.8 Drying Shrinkage

A dimensional (volume) stability requirement between the repair material and the substrate concrete is the long-term shrinkage of the repair material being equal to or greater than that of the substrate (Quezada, 2018). ASTM C928 requires the allowable decrease in length change after 28 days to be -0.15% ($-1,500 \mu\epsilon$), for air-cured test specimens. Crack development due to repair material shrinkage can reduce durability and cause premature failure of the repair system. Therefore, materials with high shrinkage cracking potential should be avoided. The shrinkage performance can be improved by methods such as internal curing (Yang et al., 2016) and coarse aggregates extension. The free dry shrinkage results are illustrated in Figure 6.

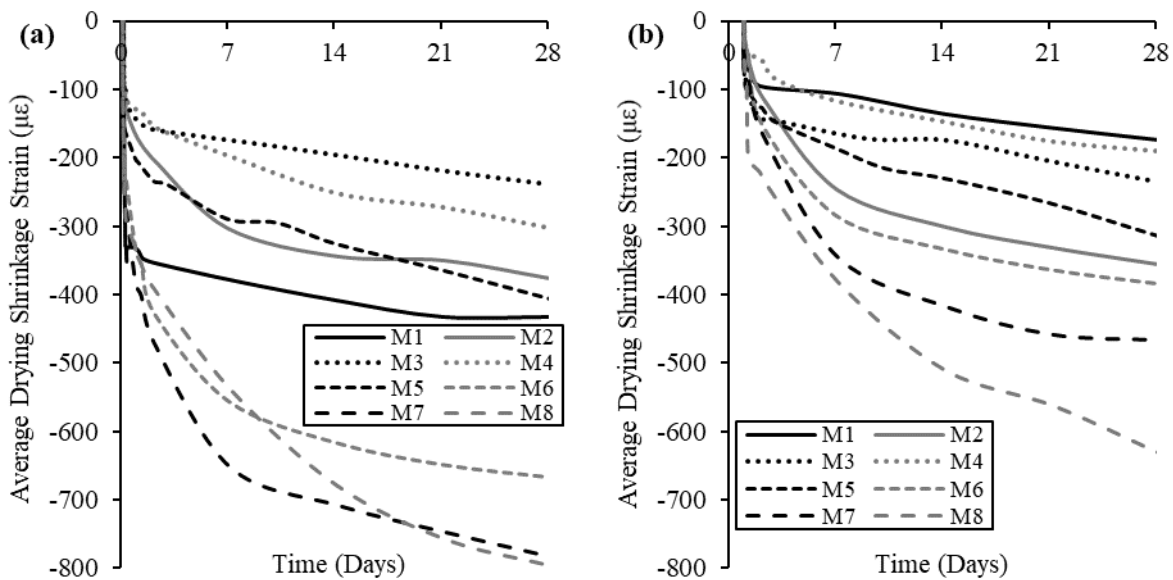


Figure 6: Average drying shrinkage of repair materials at different ages, demolded at: (a) 4 hours, and (b) 24 hours

Based on Figure 6-a, the selected repair materials showed different rates of drying shrinkage development which reflects the fact that they are composed of a variety of cementitious constituents and admixtures. Therefore, the entire free shrinkage development behavior should be considered and not just a specific point in time. M3 showed the best length change performance, as it developed the lowest drying shrinkage at almost all ages. Conversely, M7 and M8 displayed the highest length change due to free dry shrinkage. M7 and M8 also had a poor mechanical performance in terms of compressive strength, with M8 having also a very poor splitting tensile strength, modulus of elasticity, and slant shear bond strength. M1 and M2, having the highest compressive strength and very high elastic modulus, tensile strength, and bond strength, also showed an acceptable length change development. A substantial portion of the drying shrinkage occurred in the first few days, similar to what was observed in the autogenous shrinkage. Specifically, the majority of free shrinkage occurred in the first 2-4 days, for M1 to M5. These five materials had noticeably less free dry shrinkage than M6 to M8. Nonetheless, even M6 to M8 with the highest drying shrinkage satisfy the ASTM C928 requirement, with a 28-days length change of about half the specified limit ($-1,500 \mu\epsilon$).

Another observation in Figure 6-a is two different drying shrinkage development behavior. M2 to M5 showed an overall very low drying shrinkage at all ages. They had a small drying shrinkage within the first few hours, possibly due to temperature loss, followed by a slow and steady rate of shrinkage growth over time. M6 to M8 had a rapid and large increase in drying shrinkage within the first few days, followed by a continuous and gradual increase in length change over time. M1 showed a combination of the aforementioned shrinkage development behaviors; it displayed a noticeable and rapid increase in free dry shrinkage in the first two days, but had a very slight shrinkage growth beyond that point.

4 CONCLUSIONS

Eight commercially available cementitious repair media were investigated for rapid repair of concrete bridge decks. A robust laboratory study of mechanical performance and durability properties of the materials was conducted to measure their setting time, compressive and splitting tensile strength, elastic modulus, autogenous and drying shrinkage, surface electrical resistivity, and slant shear bond strength at ages of 4 hours to 28 days. Considerable variation was observed in the performance of the selected materials.

It was found that all repair materials evaluated in this study can be exposed to traffic after 4 hours and can meet the requirement of their compressive strength being equal to or greater than that of the substrate concrete. At the critical age of 4 hours, materials had a compressive strength of 3000-5600 psi (38.6 MPa). At late ages (28 days), the compressive strength of repair materials was 6,800-11,000 psi (46.9-75.8 MPa).

The time between the initial and final set for most materials was found to be between 5 and 15 minutes, and materials commonly started to gain strength in less than 45 minutes. The elastic modulus of the repair materials at 4 hours and 28 days was 3,300-4,700 ksi (22.75-32.4 GPa) and 4,500-7,500 ksi (31-51.7 GPa), respectively. Four materials showed a splitting tensile strength of about 4,000 psi (27.6 MPa) or higher at 4 hours, while all but one material had a tensile strength of higher than 4000 psi (27.6 MPa) at late ages. The chloride penetration potential of the materials at late ages was found to be very low.

Seven materials had a slant shear bond strength of over 1,600 psi (11 MPa) at 4 hours, while all but one material showed a bond strength of over 3,000 psi (20.7 MPa) at 28 days. Also, all possible failure modes were observed in the slant shear test; bond failure, substrate concrete failure, repair material failure, and a combination of the three failure modes. In four out of eight repair materials, the predominant failure mode was substrate and/or repair failures.

With regard to dimensional stability, all materials generally had a satisfactory performance but with different trends of autogenous (sealed) or drying shrinkage development. The highest observed autogenous shrinkage was 60 $\mu\epsilon$. At 28 days, five materials had a free dry shrinkage of between 200 and 400 $\mu\epsilon$, while for the other three materials it was between 600 and 800 $\mu\epsilon$, well below the ASTM C928 limit of 1,500 $\mu\epsilon$. It is recommended to use methods such as coarse aggregate extension or internal curing to reduce a high shrinkage cracking potential.

Overall, and based on the initial lab performance observations provided in this paper, M1 and M8 showed the best and the worst performance in terms of both mechanical and durability properties, respectively.

5 ACKNOWLEDGEMENT

The authors gratefully acknowledge the support from Utah Department of Transportation.

6 REFERENCES

- [1] ACI (American Concrete Institute) and ICRI (International Concrete Repair Institute). Concrete Paving Technology—Guidelines for Partial Depth Repair. In *Concrete Repair Manual*, Farmington Hills, MI: ACI/ICRI, 1999, pp. 467–478.
- [2] Baluch, M. H., M. K. Rahman, and A. H. Al-Gadhib. Risks of Cracking and Delamination in Patch Repair, *Journal of Materials in Civil Engineering*, 2002. 14(4): 294–302.
- [3] Cervo, N. M., and A. J. Schokker. Bridge Deck Patching Material Evaluation. *ASCE Journal of Bridge Engineering*, 2010. 15(6): 723-730.
- [4] Cusson, D., and N. Mailvaganam. Durability of repair materials. *Concrete International*, 1996. 18(3): 34-38.
- [5] Goodspeed, C., S. Vanikar, and R. Cook. High-Performance Concrete (HPC) Defined for Highway Structures. *Concrete International*, 1996. 18(2): 62–67.
- [6] Goodwin, F. Early-Age Repair Material Properties and Early Age Repairs. *ACI Web Session*, ACI Spring 2013 Convention, Minneapolis, MN, 2013.
- [7] Kessler, R. J., R. G. Powers, E. Vivas, M. A. Paredes, and Y. P. Virmani. Surface Resistivity as an Indicator of Concrete Chloride Penetration Resistance. *Concrete Bridge Conference*, St. Louis, MO, May 4-7, 2008.

- [8] Quezada, I. Investigating Rapid Concrete Repair Materials and Admixtures. *Dissertation*, Utah State University, Logan, UT, 2018.
- [9] Ram, P. V., J. Olek, and J. Jain. *Field Trials of Rapid-Setting Repair Materials*. Publication FHWA/IN/JTRP-2013/02. Joint Transportation Research Program, Indiana Department of Transportation and Purdue University, West Lafayette, IN, 2013.
- [10] Rizzo, E. M., and M. B. Sobelman. Selection Criteria for Concrete Repair Materials.” *Concrete International*, 1989. 11(9): 46–49.
- [11] Thomas, R. J., M. Maguire, A. D. Sorensen, and I. Quezada. Calcium Sulfoaluminate Cement. *Concrete International*, 2018. 40(4): 65-69.
- [12] Yang, Z., H. Brown, J. Huddleston, and W. Seger. Performance evaluation of rapid-set prepackaged cementitious materials for rehabilitation of surface distress of concrete transportation structures. *PCI Journal*, March-April 2016. 81-96.
- [13] Yang, Z., H. Brown, J. Huddleston, and W. Seger. Restrained Shrinkage Cracking and Dry Shrinkage of Rapid-Set Prepackaged Cementitious Materials. *ASCE Journal of Materials in Civil Engineering*, 2016. 28(6): 04016014.



Major Upgrade of Istanbul Iconic Suspension Bridges

Dyab Khazem

Parsons
 New York, USA

Huseyin Kopkalli

Parsons
 New York, USA

.....

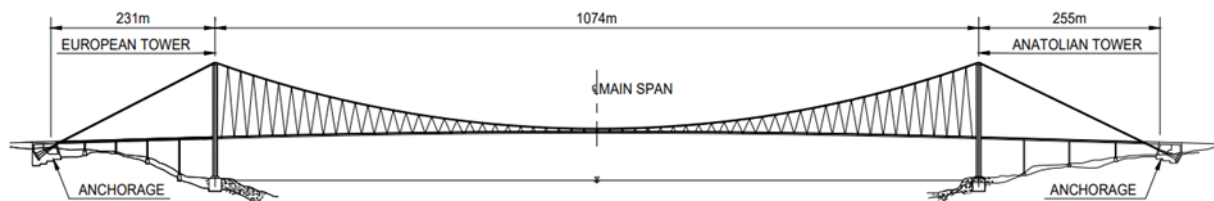
ABSTRACT

This paper discusses major upgrades made to the iconic first and second Bosphorus bridges in Istanbul, incorporating the state-of-the-art in in-depth inspection, monitoring, preservation and life extension techniques. An upgrade that would extend their service life for the next century. for the twenty first century. The inspection of both bridges, which were built in 1973 and 1984, revealed the need for rehabilitation and modernization to current international standards. This included the replacement of the hangers, cable bands, cable reinforcement, reinforcement near the towers, cable preservation (dehumidification system). KGM selected Parsons to perform the design work and the construction supervision for one of the largest bridge rehabilitation projects in Turkey.

Keywords: suspension, cables, hangers, dehumidification, seismic

1 INTRODUCTION

The first Bosphorus Bridge is a suspension bridge over the Bosphorus Strait in Istanbul, Turkey. It has a main span of 1074m and was opened to traffic in 1973. The Bosphorus Bridge is one of only 3 major suspension bridges in the world that was designed and constructed with inclined hangers, with the others, by the same designer, being the Severn and Humber Bridges in the UK. (see Figures 1&3)



AS DESIGNED HANGER ARRANGEMENT

Figure 1 The original first Bosphorous Bridge with inclined hangers

The second Bosphorus Bridge or the Fatih Sultan Mehmet (FSM) Bridge was completed in 1988 and was the second bridge over the Bosphorus Strait. It has a main span of 1090m and was the 15th longest suspension span bridge in the world at the time. There is no suspended side span on the

bridge. The overall width of the bridge is 39.4m and it carries four (4) lanes of traffic in each direction (see Figure 2). The average daily traffic is about 200,000 vehicles/day.

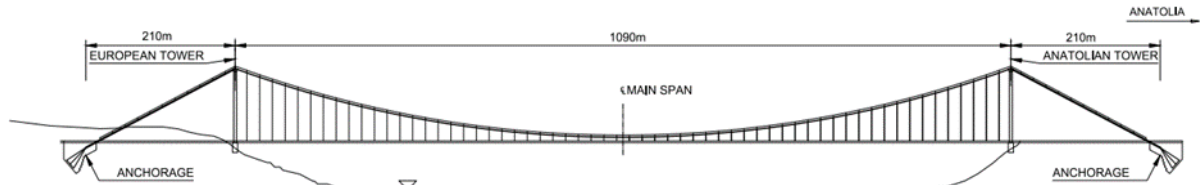


Figure 2 : The Second Bosphorus Bridge (Fatih Sultan Mehmet) designed with vertical hangers by the same designer 30 years later

2 SUSPENSION SYSTEM - MAIN CABLE EVALUATION

As part of the Bosphorus Bridge major rehabilitation project, (2014 through 2016), the scope of work included an in-depth evaluation of the main suspension cables at 14 locations for the first time since the bridge was opened to traffic in 1973. This paper provides a very comprehensive investigation by Parsons -New York, and a rigorous forensic testing program of corrosion impact by the renowned corrosion testing laboratory for bridge cable at Columbia University in New York. This paper documents the inspection, testing and evaluation of the main cable as well as recommendations for appropriate mitigation strategies. [1]



Figure 3: Original cable construction of the first Bosphorus Bridge using the arial spinning method

In general, the inspection revealed various levels of corrosion, ranging from heavy ferrous corrosion on the exterior and near surface wires, to moderate corrosion of the bottom half of the cable cross section (stage 3 - 4), with 4 being the worst corrosion stage where cracking is possible.

During the typical inspection of all 14 locations, only few broken wires were found at and near cable bands. The main culprit identified as the source of water ingress into the main cable, was the sealing details of the cable bands without caulking grooves at the interface with the wire wrapping. This was mitigated by replacing all cable bands with improved sealing details and clamping capacity.

During the unwrapping of the main cable, as part of the cable rehabilitation works, 62 broken wires and sever local corrosion was found near the South Asia tower. This condition was not expected and represented the worst condition found along the entire cable. As a result, an in-depth inspection was performed at all eight saddle locations adjacent to the towers and under cable band locations.

The cable interior was inspected at all locations and photographic documentation of each of the grooves was performed to document the corrosion condition deep within the cable. In addition, wire samples representing the various corrosion stages were extracted from within the cable for testing per NCHRP Guidelines report 534 with additional advance analysis and testing for fracture, fatigue and hydrogen effects. (See Figure4)

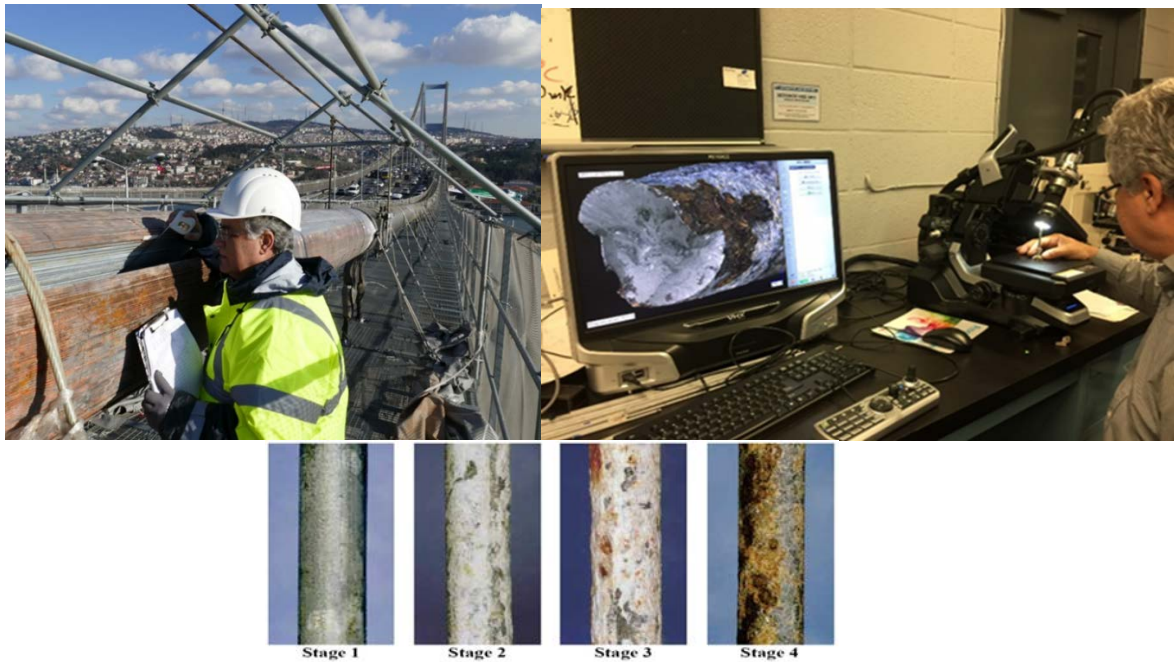


Figure 4: Main cable inspection and laboratory wire corrosion testing

Wire samples were extracted and shipped to Columbia University for testing. Testing was conducted in collaboration with Parsons and included not only tensile test but also ductility fatigue and fracture testing. Test data was used in the cable strength modelling using 2 methods, per the statistical NCHRP Guidelines method and a more advanced finite element modelling techniques for an added level of confidence.

The factor of safety of the main cable varied along the one cable from the original 2.22 to 1.99 at the tower location. The NCHRP Guidelines as well as well-established international practices for suspension bridges require that remedial measures be taken when the factor of safety falls below 2.15.

2.1 Cable Reinforcement (Auxiliary Bi-pass System Near Tower Saddle)

1. The worst condition was limited to the segment of cable near the tower. It was determined that splicing the 62 broken wires near the saddle was not feasible and did not fully restore the original main cable factor of safety of 2.2, due to significant loss of strength and ductility of the rest of unbroken corroded wires. These wires with advance stages of corrosion 3-4, are 2-3 layers deep into the cable totalling 850 -1100 wires. The main culprit for these broken wires was corrosion-induced hydrogen embrittlement and stress corrosion cracking. This resulted in reduction of the factor of safety to a low level of 2.0. Testing of the broken wires at revealed high level of hydrogen. As such, it was recommended to reinforce the main cable locally by installing an auxiliary bypass system to restore its capacity. See Figure 5.

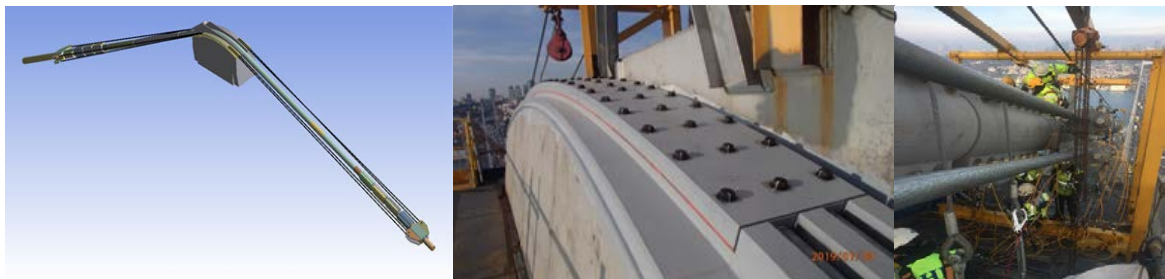


Figure 5 : Main cable auxiliary bypass system of locked coil strands at tower locations

The system consisted of 4 locked coil strands passing over the existing saddle and anchored to the good section of the main cable via bolted clamps. See figure 5

2.2 Corrosion Mitigation by Dry Air Injection (Dehumidification)

To stop further corrosion in the future and preserve the current factor of safety it was decided to design a state-of-the-art dehumidification system which was developed by Parsons in collaboration with Columbia University. The system consists of dry air injection ports at predetermined locations including the anchorage chambers. A main cable dehumidification system was installed as part of the new cable protection system. The design and function of the system was based upon the latest research and testing performed by Parsons in conjunction with Columbia University in New York City on a full size cable test specimen. (See Figure 6) [2]



Figure 6: Cable corrosion research and dehumidification utilizing internal sensors on full scale cable mock-up at Columbia University

The system has injection ports at the anchorages, towers and main span third points. Exhaust ports are located at the back-span mid points, the main span midpoint, and the main span quarter points. The dehumidifiers are located in the anchorages, tower top struts and the box girder. In the anchorages, the cable strands are in an enclosure consisting of polyethelene sheets supported by tensioned strands. (See Figure 7) This reduces the volume of air needing dehumidification and makes the system more efficient.[3]



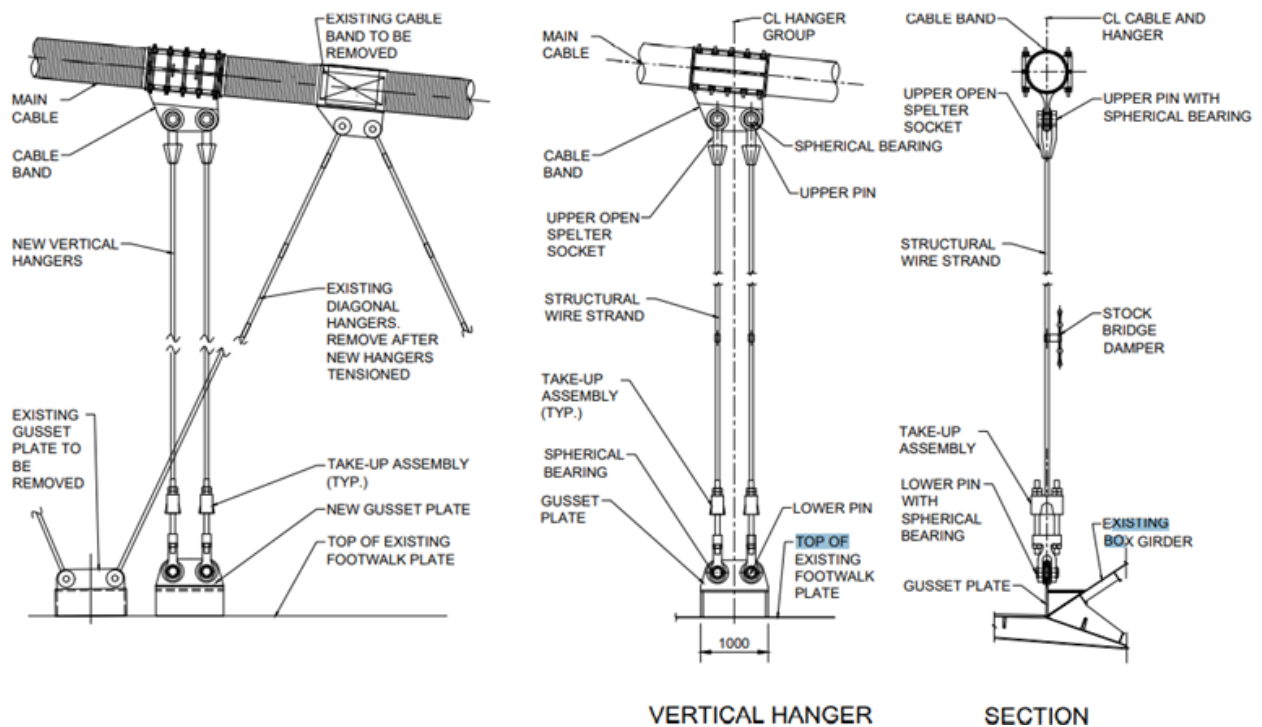
Figure 7: Dry air injection and exhaust port locations and air-tight elastomeric wrapping /sealing

At the towers, the existing cable sleeves were replaced with new airtight stainlesssteel sleeves and the saddle top plate was replaced with a stainless plate with neoprene gaskets to again provide an airtight seal. The injection/exhaust ports consist of a 3mm plate stainless steel housing with plexiglass port windows. (See Figure 7) At these locations, the cable is wedged open with zinc wedges at six equal radial locations. Temperature and humidity sensors are installed at these wedged locations within the cable in order to continuously monitor the atmospheric conditions The main cable is

wrapped with the traditional galvanized wire wrapping, without the use of any type of paste applied to the cable wires. An elastomeric wrap (D.S. Brown Cableguard) is then applied over the wire wrapping in order to provide an airtight system. A polyurethane elastomeric caulking is then applied at all joints and interfaces in the cable bands, shrouds and ports.

2.3 Suspender Replacement and Reconfiguration

The existing hangers on the Bosphorus Bridge are 62mm diameter structural strands that are inclined (See Figure 1). Issues with existing inclined hangers include unequal forces (near zero to near double design forces), broken wires, cable band bolts bent and overstressed, and lower gusset plates overstressed. The vertical hanger system consists of a pair of 55mm diameter structural stands, a new cable band and a new lower gusset plate attached to the box girder at each new hanger location (see Figure 5). The new vertical hangers are located at locations that are different from the existing so that they can be installed with the existing hangers in place. There is a total of 30 vertical hangers in each half and side of the main span, or a total of 120 on the bridge. The typical hanger spacing is 17.9m. The results of the evaluation of the alternatives indicated that the vertical hanger option would cost 50% less than the inclined hanger option and that the work could be performed in 50% of the time as compared to the inclined hanger option. Consequently, the vertical hanger design was



implemented with the approval of KGM.

Figure 8: New vertical hangers were installed and tensioned prior to the removal of the inclined hangers under traffic load.



Figure 9: final bridge configuration with vertical hangers



Figure 9: Original inclined hangers and new vertical hanger configurations show good aesthetics

3 SECOND BOSPHORUS BRIDGE (FATİH MEHMET SULTAN)

The Fatih Sultan Mehmet (FSM) Bridge was completed in 1988 and was the second bridge over the Bosphorus Strait (see Figure 2). It has a main span of 1090m and was the 15th longest suspension span bridge in the world at the time. There is no suspended side span on the bridge. The overall width of the bridge is 39.4m and it carries four (4) lanes of traffic in each direction (see Figure 2 and Figure 3). The average daily traffic is about 200,000 vehicles/day.

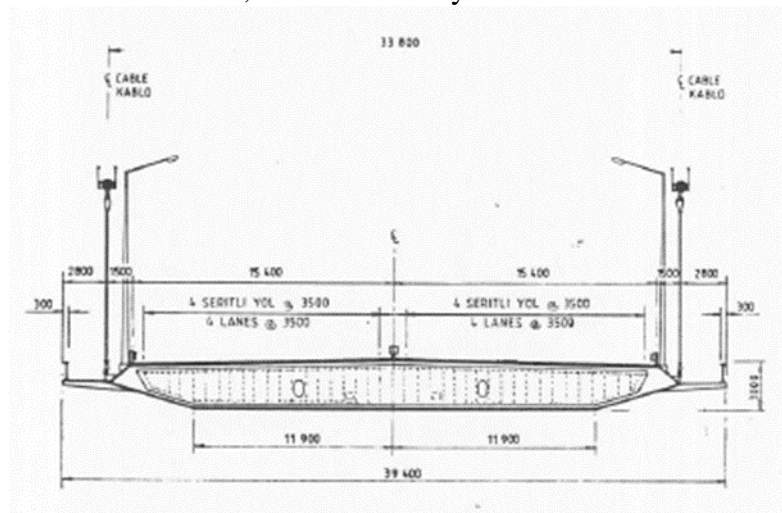


Figure 10: FSM Bridge Cross Section

Concern over the condition of the bridge hangers was raised, when Parsons reported that the hanger at panel point 29 on the north Asia side was deformed and the protective sheathing of the ropes were cracked and deformed. Subsequently, KGM acted promptly and tasked Parsons to (1) urgently replace the ropes of the damaged hanger and conduct a full visual inspection of all hangers ropes. Subsequently, corrosion was detected within most of the bridge hangers. (see figure 5)



Figure 10: Polyethylene sheath and trumpet (left) and the flat top surface of the lower socket (right)

4 SUSPENSION SYSTEM REHABILITATION

Concern over the condition of the bridge hangers was raised in December 2015, when Parsons reported that the suspension hanger 29 on the north Asia side was deformed and the protective sheathing of the suspension ropes were cracked and deformed. Subsequently, KGM took the proper action and tasked Parsons to (1) urgently replace the ropes of hangers 28, 29, and 30 on the north Asia side, as it was recognized they posed an immediate threat to the stability of the bridge; and (2) remove the lower portion (300mm) polyethylene sheathing of all the remaining hangers to conduct a full visual inspection of all hangers ropes, which occurred in April 2016.

A global finite element (FE) model of the FSM bridge was developed to analyze the structural response to the design loads and calculate the design forces on the hangers under the various updated loading scenarios such as live load, wind and current seismic criteria including accidental hanger loss were investigated. (see figure 11)

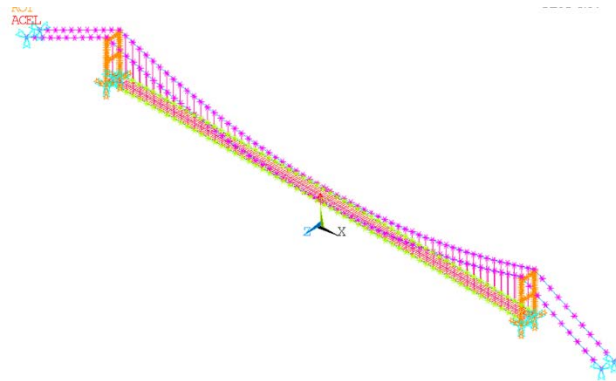


Figure 11. Global 3D model using ANSYS for various load cases per Euro&AASHTO Codes

The new innovative hanger design was based on the successful solution Parsons adopted for the first Bosphorus Bridge's vertical hangers. Unlike the original design the new designed hangers are equipped with built in provision for jacking to adjust length and tension for jacking and tensioning adjustment, as well as low friction spherical bearings to allow for movements. The hangers are open spiral strands with Class C galvanizing on the outer layer. The target design life of the new hangers is 80 years. (see figure 12)

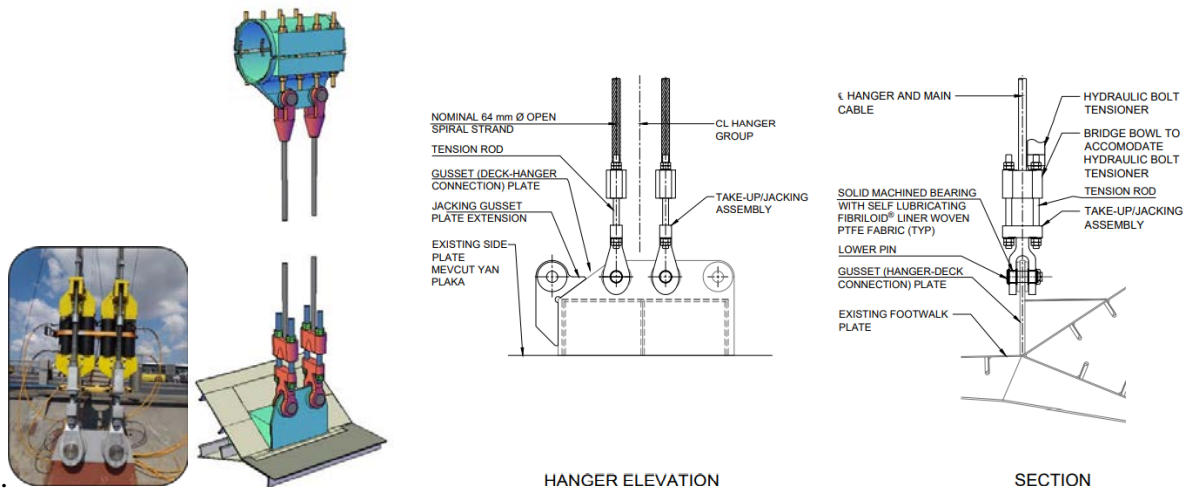


Figure 12. New Hanger details similar to the first Bosphorus Bridge with new built-in provision for length and tension adjustment

5 CONCLUSION

Preservation and life extension of these two iconic landmark suspension bridges was proven successful in upgrading these bridges to the 21st century standards. One of the major items of work was the in-depth evaluation of the main cables, replacement of the inclined hangers on the Bosphorus Bridge. Initial studies and evaluation had shown that the use of vertical hangers, as compared to inclined hangers, would provide better structural performance. Further, the vertical hangers cost 50% less and since the work could be performed in 50% of the time as compared to the inclined hanger option therefore, the vertical hanger design was implemented. Another major item of work was the implementation of a cable dehumidification system in order to better protect and preserve the main cable wires. The design of the system was based upon the research performed by Parsons at Columbia University in New York City and is the first such implementation on a suspension bridge. provided at the end faces to allow caulking for proper sealing. The side faces of the existing cable bands are toothed to help retaining the main cable's wires.

The towers were reinforced at the bottom with the installation of vertical stiffeners and at several intermediate locations by adding diaphragms. The vertical hangers and dampers significantly reduced the seismic demands on the tower legs.

The rehabilitation of the second bridge (FSM) with similar advanced corrosion protection and suspension system extended the service life of the bridge for another century if properly maintained.

6 ACKNOWLEDGEMENT

The authors would like to acknowledge KGM management and maintenance teams for their exceptional support, and guidance during the design and construction, which made this project possible. Many thanks to the contractors IHI/Makyol JV for their cooperation.

REFERENCES

- [1] Rehabilitation of the Bosphorus Bridge, Serzan and Khazem, (2016) Istanbul Bridge Conference
- [2] Khazem & Betti (2013) Monitoring Suspension Bridges as an Asset Management Tool. Second Conference on Smart Monitoring, Assessment and Rehabilitation of Civil Structures.
- [3] Khazem, Betti, Paskova & Webber. Advances in The State of The Art of Suspension Bridge Cable Dehumidification. The 9th International Cable Supported Bridge Operators Conference ICSBOC 2016, Halifax, Nova Scotia, CANADA



Operation reliability index for maintenance decision making in bridges

Sadegh Lajevardi
Helder Sousa
Paulo B. Lourenço
José C. Matos
Daniel V Oliveira

Department of civil engineering/ISISE research centre/ University of Minho
Guimareas, Portugal

.....

ABSTRACT

Maintenance management developed by several approach to optimize cost recently. Meanwhile decision making during operation is difficult task for managers to keep them safe as well as stakeholder demands satisfaction and costs with regard to resources limitation. This paper presents an approach for decision making process to select alternatives based on their costs. For this manner, the uncertainty of defect probability combine with other availability and performance features to find priority of maintenance equipment and their reliability. This multi-dimensional decision making do not deal with the essential imprecision of subjective judgment based on quantitative evaluation. To demonstrate the use and capability of the model, a case study is presented. In this case, results shows the quality value combined by delay as an effectiveness parameters (91.08) and then decision tree will complete it by risk and reliability factors.

Keywords: Reliability, Bridge, Maintenance, decision making.

1 INTRODUCTION

Maintenance decision making is an important issue for managing resources with optimization vision. Decision making had been applied in several fields rely on mathematical tools and statistical approach. This maintenance management has been developed In order to find reliability and combine maintenance decision making with an emphasis on their ability to predictive [1]. In this field, big data analysis tools considered for representing their application in decision making [2]. If maintenance work packages considered as a project, these methods are an agile method for keeping infrastructure safe and sustainable [3, 4, and 5]. Data-driven decision-making also applied Building information modelling (BIM) and Geographic Information System (GIS) are integrated to support the acquisition and update of data required for the proposed RCM process [6]. Life-cycle cost analysis (LCCA) is another tools for maintenance planning [7]. Failure Mode and Effect Analysis (FMEA), Fault Tree Analysis (FTA) and Bayesian network (BN) is also applied for maintenance management with emphasis on risk and reliability decision tools [9, 10 and 11]. According to a recent classification and risk assessment application, research in this field of area investigates the integration between

Structural Health Monitoring (SHM) and Reliability Centered Maintenance (RCM). RCM is used for project management as an agile approach.

2 METHODOLOGY

For maintenance management it is necessary to consider three level of decision making layer. The first layer attempt to find the priority of members with regard to their quality level and their repair cost. For this step visual inspection database has been applied. For the next step it is necessary to choose the overall importance state and bridges comparison before the network and their state in the past. For this manner, present research apply Overall Railway Infrastructure Effectiveness (ORIE) to in this step of decision making. The final decision making step rely on maintenance method selection based on decision tree method. Case study

This research focuses on a bridge in Tehran subway which was located in a main line. For this reason, delay and operation time suppose in real case for a period of time. The case study analysis in a period of time which was start in the first month of winter till the end of that month. Some other items such as delay and operation time suppose in this real case based on the next slide table.

Table 1 Proposed item

Proposed item	Quantity	Unite
Delay for defected equipment	30	Min/Month
Delay for unserviceable status	240	Min/Month
Operation time	31500	Min/Month
Scheduled plan	31980	Min/Month
Head	4	Min
Average person in each car	40	Person
Number of Car in each train	8	-
Average ticket price without subsidy	2	\$
Operation revenue	5040000	\$
Operation revenue with delay	5035200	\$
Operation revenue with unserviceable status	5001600	\$
Operation revenue with run to fail status	0	\$

2.1 Hypothesis

For this research it is necessary to represent the condition during the operation and case analysis. Therefore, the operation time start half pas five till twenty-three at the night. Based on the operation time, the Allocated Up Time (UT - minute per month) has been calculated. During a month there is a delay for maintenance due to unexpected infrastructure failure for half an hour, which has been considered as Down Time due to Infrastructure Failures (DTF). This maintenance activity has been done between 10 Am to 10:30 Am. Scheduled plan for train and other diesel vehicles considering as Scheduled Total Train Operating Time (TTOT) for a month two hours more than UT for round the clock. Delay due to speed reduction was considered six hours in that month based on the recorded events. Every emergency maintenance has been done during the night when the service operation had been stopped.

2.2 Calculation

Overall Railway Infrastructure Effectiveness will calculate the comparison base for second level of maintenance decision making. This index has been calculate the comparison tool based on the infrastructure equipment's availability (A), the infrastructure performance rate (P), and the infrastructure quality rate (Q). Based on bellow formula ORIE of this bridge has been calculated.

$$Q = \frac{Q_{val}}{Q_{lim}} \quad \text{if } Q_{val} < Q_{lim}$$

$$Q = 1 \quad \text{if } Q_{val} \geq Q_{lim}$$

Formula (1)

$$P = \frac{TTOT}{TTOT + TDNMR + TDSR}$$

Formula (2)

$$A = \frac{UT - (DTIF + DTOM)}{UT}$$

Formula (3)

$$ORIE = A \times P \times Q$$

Formula (4)

The quality rate (Q) is a function of the measured Q value (Qval) and its deviation from the stated Q limit (Qlim). In OEE and ORIE calculations, the quality rate varies between 0% and 100%. Therefore, the quality rate is not supposed to exceed one in the ORIE calculations as well, although the measured Q value can have a higher value than the stated Q limit if the track section standard is higher than the stated objectives.

For the next parameter (P), It is necessary to calculate the formula (2) based on some index rely on delay and operation times.

- TTOT = Scheduled Total Train Operating Time
- TDNMR = Train Delays due to No Maintenance Required
- TDSR = Train Delays due to Speed Reductions.

The availability (A) related to infrastructure failure which is a function of the allocated uptime (UT) and unplanned downtime due to infrastructure failure (DTIF) and unplanned downtime due to overdue maintenance activities (DTOM)

2.3 Results

As you could see in follow table, Beam, drainage and abutments are the highest value in this case based on Quality state and the cost for repairing.

Table 2 Equipment status and their cost repair

No	Item	Members	Defect	Total (number/length)	Qval	Material cost (\$)	Repair action cost (\$)	Total cost per equipment
1	Railway track	Rail	100	7800	99	45	74.87	119.87
2		Fastening	2	520	100	1	0.83	1.83
3		Guide rail	0	260	100	0	0.10	0.50
4		Travers	9	130	93	70	113.97	183.97
5		Ballast	1350	70200	98	3	547.87	550.87
6		Track subgrade	250	7800	97	0	2,000.00	2,000.00

		Welding and joint	1	260	100	20	66.67	86.67
8	Deck	Expansion joint	0	10	100	10	333.33	343.33
9		Foundation isolation	0	4	100	10	233.33	243.33
10		Barrier	0	7800	100	100	266.67	366.67
11		Beam	2	7	71	70	200.00	270.00
12		Drainage	2	5	60	5	166.67	171.67
13	Pier	Elastomeric bearing support	0	7	100	100	2,666.67	2,766.67
14		Pier cab	0	7	100	4	200.00	204.00
15	Retaining wall	Abutment	1	2	50	0	1,000.00	1,000.00
16	Foundation	Pedestal	0	7	100	0	3,333.33	3,333.33
17		Footing	0	7	100	0	2,333.33	2,333.33
Total Qval	92	Total cost repair	13,976.03					

This table result consider for the first step of maintenance decision making. For the next step it is necessary to calculate the ORIE for this case study. The Overall Railway Infrastructure Effectiveness value has been illustrated in follow table which consider the delay for availability, quality and the members' performance. This item will help decision makers for finding the degradation models and finding the bridge priority to compare other bridges in the rout.

Table 3 ORIE index

Railway bridge	Factor	Unit	Quantity	Factors	Total (ORIE%)
A	UT	(min/month)	31500	1.00	91.08
	DTIF	(min/month)	30		
	DTOM	(min/month)	0		
P	TTOT	(min/month)	31980	0.99	
	TDNMR	(min/month)	0		
	TDSR	(min/month)	360		
Q	Qval	(metre)/(meter)	92	0.92	
	Qlim	(metre)/(meter)	1		

The final decision making step rely on maintenance model determining. It is supposed 4 level or 4 models for maintenance method in this research.

✓ Run to fail level

In this level the equipment operate without any interval inspection and any preventive maintenance which is represented the poorest level of maintenance.

✓ Unserviceable level

This level representing the lowest level of preventive maintenance with emergency maintenance and several operation disorders and delay.

✓ Defected level

This medium level of quality lead to several defect with some seldom operation disorders.

✓ Prefect level

This costly maintenance which is prepare a high quality based on combination of condition monitoring for sensitive equipment and interval inspection for important and risky equipment.

This methods in three level of maintenance decision making, will demonstrate the capacity of the usage of this analysis model, for a case study with combination of decision tree and Overall Railway Infrastructure Effectiveness.

Based on the calculation, expected revenue for each level of maintenance with regard to delay calculated based on bellow table.

Table 4 Expected revenue

Item	Amount	Unit
Operation revenue	5040000	\$
Operation revenue with delay	5035200	\$
Operation revenue with unserviceable status	5001600	\$
Operation revenue with run to fail status	0	\$

Based on follow figure, we have the uncertainty of events which illustrate by percentage in each condition. Bellow the percentage of failure probability, the revenue based on table 4 illustrated and monitoring cost with opposite sign calculate the final value for each condition.

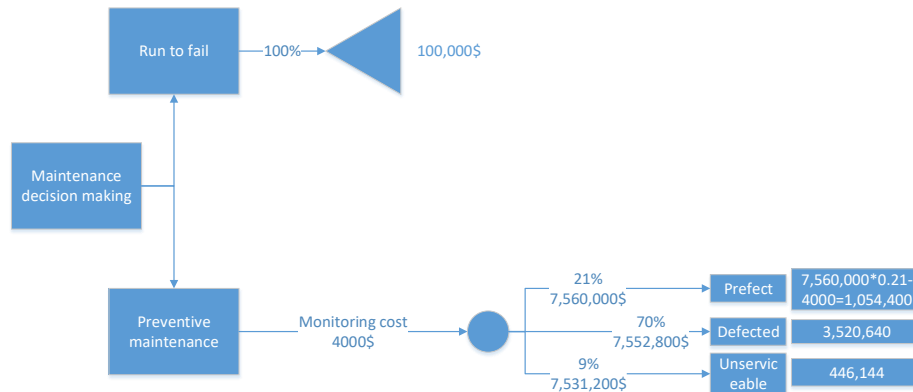


Figure 1: Caption of Example Figure

REFERENCES

Use 10-point Times New Roman font for the references and list them at the end of the paper. Include the following information (as applicable).

- [1] Mi, S., Feng, Y., Zheng, H., Wang, Y., Gao, Y., & Tan, J. (2020). Prediction maintenance integrated decision-making approach supported by digital twin-driven cooperative awareness and interconnection framework. *Journal of Manufacturing Systems*, (August), 0–1. <https://doi.org/10.1016/j.jmsy.2020.08.001>
- [2] Frankova, P., Drahosova, M., & Balco, P. (2016). Agile Project Management Approach and its Use in Big Data Management. *Procedia Computer Science*, 83(Ant), 576–583. <http://doi.org/10.1016/j.procs.2016.04.272>
- [3] Špundak, M. (2014). Mixed Agile/Traditional Project Management Methodology-Reality or Illusion, *Procedia - Social and Behavioral Sciences*, 119, 939–948. <http://doi.org/10.1016/j.sbspro.2014.03.105>
- [4] Rasnaxis, A., & Berzisa, S. (2016). Method for Adaptation and Implementation of Agile Project Management Methodology. *Procedia Computer Science*, 104(December 2016), 43–50. <http://doi.org/10.1016/j.procs.2017.01.055>
- [5] Oyebanji, A. O., Liyanage, C., & Akintoye, A. (2017). Critical Success Factors (CSFs) for achieving sustainable social housing (SSH). *International Journal of Sustainable Built Environment*. <https://doi.org/10.1016/j.ijsbe.2017.03.006>
- [6] Ma, Z., Ren, Y., Xiang, X., & Turk, Z. (2020). Data-driven decision-making for equipment maintenance. *Automation in Construction*, 112(July 2019), 103103. <https://doi.org/10.1016/j.autcon.2020.103103>
- [7] Zuluaga, S., & Sánchez-Silva, M. (2020). The value of flexibility and sequential decision-making in maintenance strategies of infrastructure systems. *Structural Safety*, 84(September 2019), 101916. <https://doi.org/10.1016/j.strusafe.2019.101916>
- [8] Chemweno, P., Pintelon, L., Muchiri, P. N., & Van Horenbeek, A. (2018). Risk assessment methodologies in maintenance decision making: A review of dependability modelling approaches. *Reliability Engineering and System Safety*, 173(June 2016), 64–77. <https://doi.org/10.1016/j.ress.2018.01.011>
- [9] MS Lajevardi, J Matos, Paulo B. Lourenço; (2018). Quality control index survey for railway bridge health monitoring, *IABSE Symposium 2019 Guimarães*
- [10] B Conde, JC Matos, DV Oliveira, B Riveiro; (2020). Probabilistic-based structural assessment of a historic stone arch bridge, *Structure and Infrastructure Engineering*, 1-13
- [11] HS Sousa, F Prieto-Castrillo, JC Matos, JM Branco, PB Lourenço; (2018). Combination of expert decision and learned based Bayesian Networks for multi-scale mechanical analysis of timber elements, *Expert Systems with Applications* 93, 156-168



GPR AND AERIAL PHOTOGRAMMETRY APPLIED TO MANSORY ARCH BRIDGE ASSESSMENT

Samuel Neves

Programa doutoral em Geo-tecnologias aplicadas a construção, energia e industria, Universidade de Vigo, Escola de Engenharia de Minas, Campus Lagoas - Marcosende, 36310
Vigo, Espanha

Simona Fontul

Laboratório Nacional de Engenharia Civil, Av. do Brasil 101, 1700-066
Lisboa, Portugal

Mercedes Solla

CINTECX, Universidade de Vigo, GeoTech research group, Campus Lagoas – Marcosende, 36310
Vigo, Espanha

ABSTRACT

Several stone arch bridges are listed historical monuments in Portugal, which are valuable tourist attractions or local landmark. Many these ancient structures are the oldest constructions still in use within the transportation infrastructure and as a result of the increase in traffic load and their age they have undergone some structural decay. Ground penetration radar has been shown to be valuable in evaluating the state of conservation of ancient bridges in order to preserve their historical character. In this work, the stone Bridge over Tuela river, near of Mirandela (Portugal) was surveyed by using a 500 MHz frequency antenna. In addition, an aerial photogrammetry survey was performed, together with GNSS measurements, in order to get the 3D model of the bridge. Results show how GPR mapping provides reliable information from historical, archaeological and structural points of view, which combined with 3d models result in a powerful tool to monitor and assess the status of conservation of the bridge. All the information produced is noteworthy knowledge for archaeologists, architects and civil engineers as it can be used to take decisions about stability and for future strengthening measures.

Keywords: Georadar, Geophysics, Cultural Heritage, Bridge, 3D models

1 INTRODUCTION

Ancient stone masonry arch bridges are still commonly in use within the transport infrastructure. Many of these structures require special attention and monitoring. Increases in traffic load and intense vibrations since they were designed can result in structural decay [1-2]. Therefore, ongoing diagnosis of their changing structural integrity is required to provide information in order to help with their preservation and restoration [3]

In the last several decades, there has been a continuous increase in the use of non-destructive testing (NDT) to evaluate civil engineering structures [4-5]. Among other NDTs, ground penetrating radar (GPR) has been widely used for evaluating masonry bridges [6-13]. These studies have provided promising information about hidden geometries (e.g. hidden arches, former shapes, etc.),

bridge foundations, ring stone thickness, moist zones and fill conditions, as well as cavities in stonework.

The aim of the work is to assess the state of conservation inside of the stone bridge using the georadar technique corrected by the 3D digital model given by aerial photogrammetry.

2 STONE BRIDGE OVER RIVER TUELA

It was prospected the stone bridge over Tuela river, near of Torre de D. Chama. This bridge is still on operation, connecting two villages. The bridge was built by the Roman empire, later it was the target of several retrofitting interventions. The bridge was built in granite and contain six arcs, each arc has 4,4 m span. The bridge has 100 m length and 6,20 m width maximum. The level of water is above 6,5 m bellow of the level o the top of the bridge. Near to this bridge an anepigraph milestone was found, it would integrate the Roman way that of the present Léon and Astorga went to Zamora and Salamanca.

During the Middle Ages, an important regional road axis would pass through here from Guimarães to Bragança. To the east is also the section of a cobbled path about 800 m long and which forked about 300 m from the bridge.



Figure 1: Location of stone bridge over the Tuela river (Portugal).

3 METODOLOGY

3.1. AERIAL PHOTOGRAMMETRY

The aerial photogrammetry survey was carried out with the DJI Phantom 4 PRO UAV, which has a camera onboard, with a sensor of 20 Mpixels. This vehicle has a GPS positions, which allows georeferencing each aerial image to improve the workflow processing. It is very light and easy to take-off and landing; the drone can be launched by hand and no additional equipment is required. It flies and lands autonomously using UGCS [17] aerial flight plan.

We used at field:

a) ground control software UGCS to plan the flights in the laptop over the study area and controlled the drone's trajectory during flights.

b) ground control points (GCP) to increase the precision and place the current geographic referencing, such as, ETRS89 – TM06 Portugal. This operation was performed using GNSS Leica Rover GS15 with CS15.

After data collected, data processing was performed with Agisoft PhotoScan Professional [16] to generate orthophotos, digital elevation models and 3D models. Then, the Autocad architectural and topographical drawings from 3D model of the stone bridge were created.

3.2. GROUND PENETRATING RADAR

The equipment used was the Zond 12e advanced georadar [14], from the RadarSystems.

Due to the work being carried out in a rural / urban environment and the possibility of signal contamination by telecommunications, shielded antenna of 500 MHz was used to minimize the effect of noise on the georadar record. The acquisition mode was in time with 56 samples per second with time window of 60 ns. Three GPR profiles were conducted along the axis of the bridge (two profiles near to the spandrel walls and 1 profile centered with cross section of the bridge to along the longitudinal axis). The profiles were georeferenced using markers obtain by GNSS Leica Rover GS15 with CS15. The GPR allow to connect GNSS to GPR but a NMEA protocol license was needed to share geographic information devices.

After acquisition data, the profiles were subjected to post-acquisition digital processing through the Reflexw software [15], which allowed improving the image visualization and adding information about the depth and length of the profiles and grids. This operation consisted in correcting the amplitude with the depth, removing general and specific interferences, applying filters to correct the positioning of the antennas, to check the positioning and the geometric shape of the reflections.

4 RESULTS AND DISCUSSION

To achieve the aim of this work, first was needed individually analyse the GPR radargrams and to compare with the measured geometry of the bridge. **Erro! A origem da referência não foi encontrada.** shows, as example, that the radargram has some variability along the bridge length. The blue dash line shows the lateral variation given by time travel of the electromagnetic waves in the medium. When comparing the blue dash line with bridge geometry, changes on dielectric properties along the profiles can be observed. These variations can be caused by moisture, joints between stone blocks or vegetation. For a better understanding, electromagnetic waves velocities constrained by the bridge geometry were calculated.

Other geophysical features were also found: the red squares that point out hyperboles caused by holes inside the bridge bearing (E1 – E2 sections). This method has proven to be reliable for detection of holes or pipes in stone bridges.

Aligned with each arch (on bridge geometry), the radargram shows the hyperbolas from the top and bottom of each arch (yellow arrows indicates the ring stone thicknesses). The hyperbolas are characterized by: i) high amplitude wave on the bottom of the vault ashlar, at the interface with the air; ii) lower amplitude wave (inside of ring stone of the arch) and iii) another high amplitude wave, at the bottom of the ring stone, at the interface with air. The GPR wave travel time between the top and the bottom of the ring stones were measured (RS in Table 1) and compared with the real thickness of the ring stones from photogrammetry (L1 in Table 1). Similarly, the travel time of electromagnetic waves between the pavement surface and the location of the top of rings stone was measured (T1 in Table 1) and then compared with the real thickness from geometry (L2 in Table 1). The wave velocity and the dielectric constant for each section at arch were then calculated. Theses parameters can provide information on the conservation status inside the bridge and enable the location of pathologies.

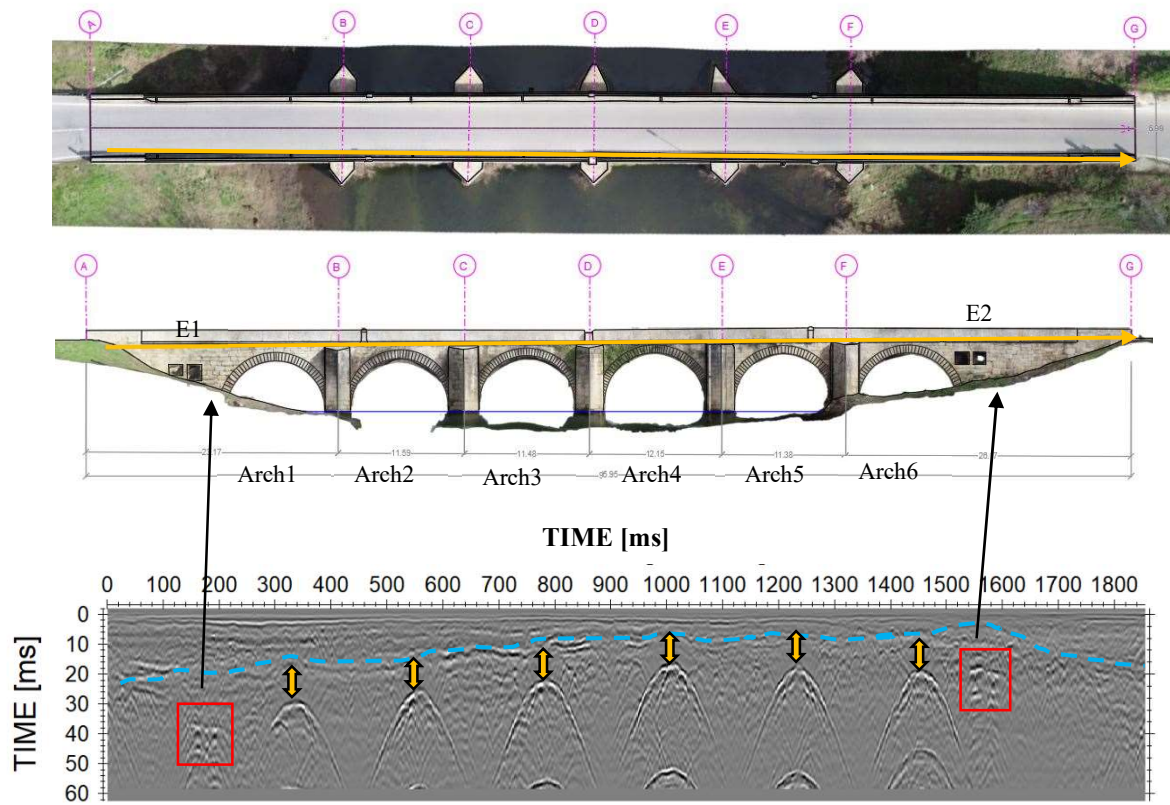


Figure 2: Radargram processed from profile 1 and bridge geometry near right bridge (edge).

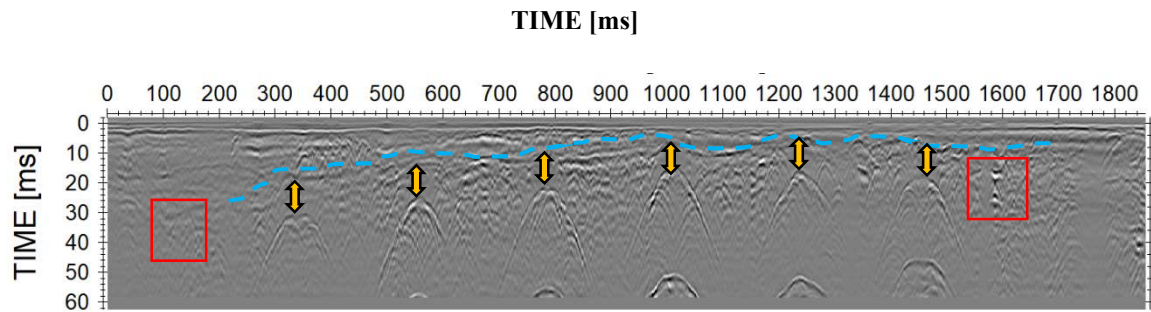


Figure 3: Radargram processed from profile 2, on middle of cross-section bridge.

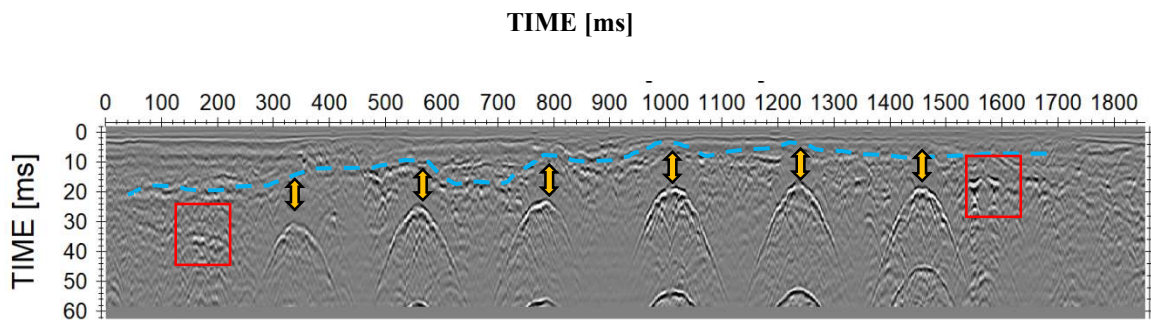


Figure 4: Radargram processed from profile 3 near left bridge (edge).

Table 1 shows the waves velocity and dielectric constant for each section. The dielectric constant ranges between 1 and 81, being 1 for air and 81 for freshwater. Results presented on Table 1 shows the dielectric constants obtained. It can be observed that the values are in accordance with the ones given by literature for the construction material of the bridge (granite), vary between from 5 to 7 [18]. Lower dielectric constants correspond to dry sections or void (depend the level of reflections on radargram). Higher dielectric constants represent wet section or higher level of humidity.

These results are helpful for bridge assessment, enabling a better understanding of the conservation stage of the bridge, and analyse it in more detail.

Table 1: Dielectric constants obtained by section.

Section	E1	Arch1	Arch2	Arch3	Arch4	Arch5	Arch6	E2
T1 (ns)	38	16	13	10,5	9	8	10	17
L2 (m)	2,21	1,11	0,89	0,76	0,48	0,57	0,54	1,16
V (cm/ns)	11,7	14,0	13,9	14,7	11,1	14,7	11,2	13,7
Er [1-81]	6,6	4,6	4,7	4,2	7,3	4,2	7,2	4,8
RING STONE								
RS (ns)		12,5	11	11,5	7	9	8	
L1 (m)		0,76	0,78	0,69	0,74	0,73	0,73	
V (cm/ns)		12,4	14,4	12,2	21,5	16,5	18,6	
Er [1-81]		5,9	4,4	6,1	2	3,3	2,6	

At the bottom of the radargram, the hyperbolas caused by the interface between air and the water surface (river's level) are also observed.

5 CONCLUSION

This work aimed to assess the conservation status of a stone bridge over Tuela river, using GPR and 3D digital model.

This study showed that the joint interpretation of GPR and geometric information from photogrammetry enable a more accurate interpretation of GPR measurements and a better diagnosis of bridge condition. In this way, changes of moisture and material heterogeneity can be detected through different values of the dielectric constant obtained when superposing the eave travel time with the bridge geometry. So, lower dielectric constants show dry sections or void (depend the level of reflections), while higher dielectric constants indicate wet section or higher level of humidity. Both anomalies are important to assess bridge condition. Also, GPR signal allows to detect and locate other features, discontinuities of the bridge structure, such as holes inside the bridge bearing, represented in the radargrams by hyperboles.

The data showed that there are also lateral variations of the dielectric constants. These variations can be provided by humidity, joints between stone blocks, or vegetation.

These results are useful for bridge assessment, as allow the engineers to understand the state of conservation of the bridge and analyse in more detail, mainly the internal condition, that is difficult to be diagnose with traditional inspection methods.

Further research is to develop a Building Information Modelling (BIM) or similar integration methodology, which allows us to join all the data on the same platform.

REFERENCES

- [1] Forde MC,1998. "Bridge research in Europe", Construction and Building Materials, 12(2-3):85-91.

- [2] Bhandari NM, Kumar P., 2006. "Structural health monitoring and assessment of masonry arch bridges", In: *Advances in Bridge Engineering*; 2006, p. 115-132.
- [3] Vecco, M. A definition of cultural heritage, 1010. "from the tangible to the intangible". *Journal of Cultural Heritage*, 11, pp. 321-324.
- [4] Popovics JS, 2003. "NDE techniques for concrete and masonry structures", *Prog. Struct. Engng. Mater*, 5:49-59.
- [5] Leucci G, Cataldo R, Nunzio G., 2007. "Assessment of fractures in some columns inside the crypt of the Cattedrale di Otranto using integrated geophysical methods". *Journal of Archaeological Science*, 34(2):222-232.
- [6] McCann DM, Forde MC., 2001. "Review of NDT methods in the assessment of concrete and masonry structures", *NDT&E International*, 34:71-84.
- [7] Colla C, Das PC, McCann D, Forde M., 1997. "Sonic, electromagnetic and impulse radar investigation of stone masonry bridges", *NDT&E International*, 30(4):249-254.
- [8] Flint RC, Jackson PD, McCann DM., 1999. "Geophysical imaging inside masonry structures", *NDT&E International*, 32:469-479.
- [9] Pérez-Gracia V., 2001. "Radar de Subsuelo. Evaluación para Aplicaciones en Arqueología y en Patrimonio Histórico-Artístico", PhD Thesis. Universidad Politécnica de Cataluña.
- [10] Fernandes F., 2006. "Evaluation of two novel NDT techniques: microdrilling of clay bricks and ground penetrating radar in masonry". PhD thesis. Universidade do Minho.
- [11] Arias P, Armesto J, Di-Capua D, González-Drigo R, Lorenzo H, Pérez-Gracia V., 2007. "Digital Photogrammetry, GPR and Computational Analysis of structural damages in a medieval bridge", *Engineering Failure Analysis*, 14:1444-1457.
- [12] Lubowiecka I, Armesto J, Arias P, Lorenzo H., 2009. "Historic bridge modelling using laser scanning, ground penetrating radar and finite element methods in the context of structural dynamics", *Engineering Structures*, 31(11):2667-2676.
- [13] Solla M, Lorenzo H, Novo A, Rial FI, 2010. "Ground-penetrating Radar Assessment of the Medieval Arch Bridge of San Antón", Galicia, Spain. *Archaeological Prospection*, 17(4):223-232
- [14] RadarSystems, 2017. "Prism2 User's Manual PDF Manual v2.60", From <http://www.radsys.lv> Prism 2. 65 pp.
- [15] Sandmeier KJ, 2020. "ReflexW manual v.9.5", From <http://www.sandmeier-geo.de>. Sandmeier Scientific Software. 709 pp.
- [16] AgiSoft PhotoScan Professional (Version 1.2.6), 2016, From <http://www.agisoft.com>.
- [17] UGCS software, 2020. From <http://www.ugcs.com>.
- [18] Daniels, D. 2004. "Ground Penetrating Radar", 2nd Edition, The Institution of Electrical Engineers.



Long-Term Anti-Corrosion Protection of Al-Mg Plasma Arc Thermal Spray Applied to Bridge Bearings in Harsh Environments

Tolga Onal

Kawakin Core-Tech Co., Ltd.
Saitama, Japan

Javier Lopez Gimenez

Kawakin Core-Tech Co., Ltd.
Saitama, Japan

Takehiko Himeno

Kawakin Core-Tech Co., Ltd.
Saitama, Japan

ABSTRACT

During the last decades, the important consequences of corrosion have become a significant problem worldwide. Corrosion protection of bridges, including their key structural components like bridge bearings, seems of capital importance to ensure the long-term durability of the structure and a low life cycle cost.

The current paper describes and compares the performance of widely used corrosion protection coatings, e.g. paint and hot-dip galvanizing, and Al-Mg Plasma Arc Thermal Spray when applied to bridge bearings under highly corrosive environments. Conducted accelerated corrosion tests simulating harsh environmental conditions carried out in bearing specimens reveal the stable and durable anti-corrosion coating obtained with the Al-Mg plasma arc thermal spray technology.

Keywords: corrosion protection, bridge bearing, hot-dip galvanizing, thermal spray, corrosion test

1 INTRODUCTION

Bridges are one of the most important components of modern transportation systems, playing a critical role in the transportation networks within cities, or modern highway networks. Corrosion is one of the most determining factors affecting the deterioration of bridges, causing not only visual degradation, but also affecting their security and serviceability. Given the cost, and importance of these civil infrastructures in our daily life, it seems necessary to apply reliable corrosion methods, which can ensure their serviceability during a long-life cycle with minimal maintenance. In order to achieve this goal, it is crucial that the important structural members of the bridge are effectively protected against the detrimental effects of corrosion.

One of the most critical structural components of a bridge is its bearing supports. Among other functions, these devices support the weight of the deck, and accommodate longitudinal displacements and rotations of the superstructure. Bridge bearings are often located in areas that are poorly ventilated, and have the potential to collect large amounts of dirt, debris, and moisture or standing water. All these factors usually lead to corrosion and deterioration problems as the ones described in Fig. 1. In addition, bridges located in marine environments, e.g. near port facilities, which are very common in infrastructure development plans, present a higher risk of corrosion. The presence of strong corrosive agents such as salt air can accelerate steel corrosion, and demands the application of stable and durable coatings to prevent bridge deterioration.

In Japan and all around the world, there are innumerable cases of bridges affected by corrosion, which has triggered the study and active implementation of new anticorrosive technologies worldwide. In the current paper, the focus is on the protection technologies applied to bridge bearings. Special attention is paid to new protective coatings investigated to improve the durability of

conventional paint and galvanized coatings in highly corrosive environments. The performance of these technologies is studied through accelerated corrosion tests, of which results will be presented.



Figure 1: Corrosion Damage in Bridge Bearings Installation Area

2 ANTI-CORROSION METHODS FOR BRIDGE BEARINGS

2.1 A Brief Approach to Corrosion Protection Systems

In order to avoid the appearance and development of corrosion in steel surfaces, the most common approach is to provide a protective coating layer. Its purpose is to physically avoid water and oxygen to come into contact with the steel, therefore avoiding the formation of rust. Among these methods, paint coatings have been widely studied, and heavy-duty coatings have been proposed and applied in bridges exposed to marine environments. However, regarding its durability, this technology presents the following issues.

- The protective layer is degraded due to its exposure to wet and dry cycles of direct sunlight and rainwater. Therefore, regular repainting and maintenance are necessary. This is particularly troublesome for bridge bearings since their location complicates regular inspections and re-coating operations.
- In painted structures rust starts in areas where the coating has been damaged, exposing the steel surface. Bridge bearings, characterized by complicated shapes, are difficult to be evenly coated, and any damage occurred during transportation or installation can easily trigger the appearance of rust starting in these damaged areas.

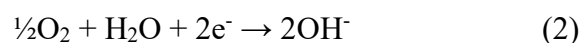
Paint coating only forms a protective layer, but other technologies have been developed to, in addition, provide sacrificial protection. This is achieved by coating the steel surface with another metal which is easier to be corroded. Hot-dip galvanizing and a more advanced technology, the thermal spraying technique, are based on this principle, and their mechanisms for corrosion protection will be explained in the next sections of this paper.

2.2 Mechanism of Sacrificial Protection

As previously stated, the appearance of rust requires the presence of both water and oxygen. The corrosion process is very similar to a battery since it will result in a flow of electrons between anodic and cathodic sites (Fig. 2). Corrosion of iron (Fe) starts when an iron atom in the outmost layer comes into contact with water, losing some electrons and becoming a positively charged ion (Fe^{2+}), which allows it to bond to negatively charged atoms.



The other part of the reaction must involve water and oxygen, and it can be represented by



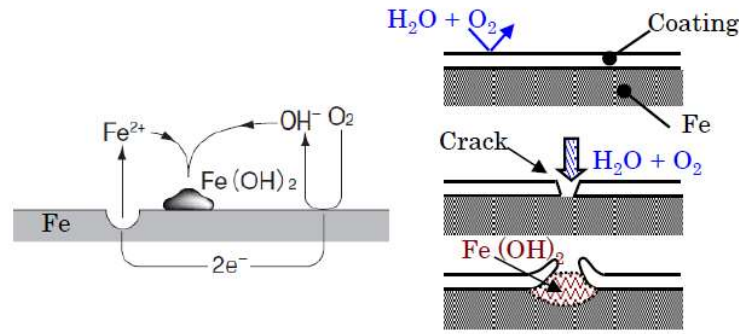


Figure 2: Mechanism of Rust Formation

This negatively charged material can combine with the iron and electrons produced in the first reaction, producing iron hydroxide $\text{Fe}(\text{OH})_2$. This ferric hydroxide (rust) deposited on top of the steel surface is porous, with poor protection capacity, and as long as water and oxygen are provided the oxidation process will continue. This is the reason why painted steel surfaces will rapidly corrode once the coating is damaged, and the base metal is exposed.

However, when steel is coated with a more reactive material, like zinc in the case of hot-dip galvanizing, rust develops faster in the coating, as described in Fig. 3, providing sacrificial protection.

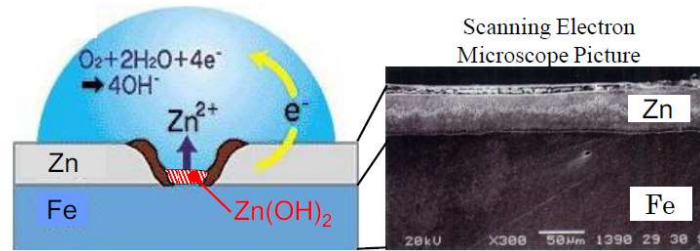
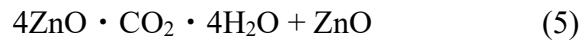


Figure 3: Sacrificial Protection

Similarly to the previous case, the above two reactions produce as a result zinc oxide $\text{Zn}(\text{OH})_2$. Since Zn can release electrons (ionize) easier than Fe, this method prevents the oxidation process (rust formation) of Fe. This is called sacrificial protection.

In this case, the zinc oxide produced in this process is a dense oxide film that works as a passivation layer.



The stability of this protective film, makes it difficult for air and water to trespass it, providing a new protection layer that covers the scratches and confers long-term corrosion protection.

2.3 Appropriate Metal Choice for Sacrificial Protection

Table 1 presents the electrochemical series, which is a classification of metals according to their tendency to lose electrons to form positive ions. Metals with higher ionization tendency than Fe will corrode more easily and therefore prevent the corrosion of the steel surface. The metals with higher ionization potential are K, Ca, and Na, but they rapidly react with liquid H_2O (explode), which makes impractical their use as protective coatings. This is the reason why the selected metals for anti-corrosion coatings are Zn, Al, and Mg.

Table 1 Electrochemical Series

Metal	K	Ca	Na	Mg	Al	Mn	Zn	Cr	Fe	Ni	Sn	Pb
Potential (V)	-2.92	-2.76	-2.72	-2.32	-1.66	-1.18	-0.76	-0.71	-0.47	-0.27	-0.14	-0.13
	Higher tendency to oxidize ← → Lower tendency to oxidize											
Reactivity with air	Oxidize very easily				Creates and oxide film on the surface							
Reactivity with water	React vigorously			React with steam but not with water, oxidizing						Not reactive		

2.4 Technologies to Create a Protective Film

Once a metal with high ionization tendency has been selected it is necessary to create a strong coating layer of this molten material, which will protect the base metal against corrosion.

A typical approach to obtain this coating layer is hot-dip galvanizing. In this method, as shown in Fig. 4, the base metal to be protected is immersed in a kettle or vat containing molten zinc. Since the melting point of Zinc is 420 °C, the vast majority of materials can be coated using this method, with the exception of high strength materials. However, it is a complicated process which has to be performed in a galvanizing plant, thus site application is not possible.

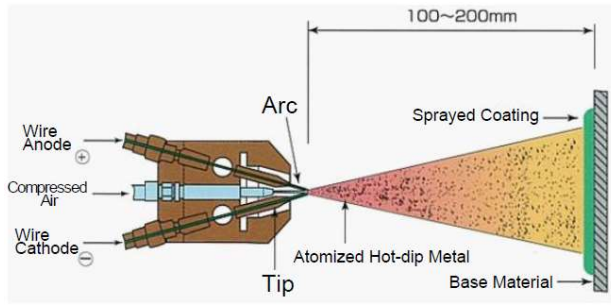


Figure 4: Hot-Dip Galvanizing

Hot-dip galvanizing using aluminum has also been developed, but the high melting point of Al (600 °C) is an important disadvantage. High temperatures can affect some materials creating distortions and strength degradation. Besides, the necessity of a big tank capable of withstanding these high temperatures will increase the cost. As a consequence, aluminum is not used alone for hot-dip galvanization, but alloyed with Zinc to reduce the mentioned disadvantages.

The next metal in the electrochemical series is magnesium, which also has a high melting point, in this case equal to 650 °C. For similar reasons, and despite its high corrosion protection capability, it is not used in hot-dip galvanizing.

In order to make the most of the excellent anti-corrosion protection characteristics of aluminum Al-Mg plasma arc thermal spray method is proposed. Plasma Arc Thermal Spraying is a process in which a modified gas or electric arc welding equipment equipped with compressed air is used to melt and project a metal wire onto a steel surface, as shown in Fig. 5. In this method, surface preparation is a critical step necessary to ensure a very good adherence between the steel base and the sprayed coating layer. There are several metals which can be sprayed following this technique, including Zn, Al, and Mg. The fact that a metal like Mg, with outstanding corrosion protection characteristics, can be employed in this method to create a protective layer seems to be an advantage.



(a) Scheme of thermal spraying technique

(b) Application of thermal spraying

Figure 5: Plasma Arc Thermal Spraying Technique

3 COMPARISON OF ANTI-CORROSION PERFORMANCES

As described in the previous sections, several anticorrosion protection strategies for metals have been studied, developed, and applied during the last decades. In order to evaluate and compare the anti-corrosion performance of these protection technologies, accelerated corrosion tests with salt spray were performed. The results of these tests are described and discussed in the following chapters of this paper.

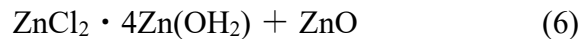
3.1 Test Specimens

Test pieces treated with four different anti-corrosion coating strategies were prepared. These methods are fluorine resin paint coating, Zinc hot-dip galvanized coating, Zn-Al thermal sprayed coating, and Al-Mg plasma arc thermal sprayed coating. An accelerated corrosion test was performed for 9 months (6,000 hours), including wet (salt spray) and dry stages. These stages were cycled automatically so the samples undergo the climate changes that they would experiment in real environmental conditions [1].

3.2 Test Results

The test results are shown in Table 2. After 2.3 months (1,500 hours) of exposure in the accelerated test, rust was observed in the cross-cut areas of the samples coated with fluorine resin paints, where the steel surface was directly exposed to the corrosive agents.

Despite its sacrificial protection capability, red rust developed in the hot-dip galvanizing test pieces after 1,000 hours. The test conditions, which include salt spray stages to simulate marine environmental conditions, lead to the formation of unstable white rust.



















This corrosion product is highly hygroscopic, thick under wet conditions, and powdery under dry conditions. Consequently, the passivation layer cannot properly be adhered to the steel surface, and thus zinc is rapidly decomposed. This might be the cause of the loss of the anti-corrosion protection properties of the Zn observed in these specimens during the accelerated test. Similar behavior and conclusions can be obtained from the Zn-Al coated specimens but, in this case, the rust formation started a bit later (after 4.5 months). This beneficial delay in rust occurrence could be caused by the combination of zinc with aluminum.

On the other hand, test specimens coated with Al-Mg plasma arc thermal spray showed a highly stable protection layer during the whole duration of the accelerated test, which was 9 months (or 6,000 hours). During that time no rust formation could be observed, even in the cross-cut area of the plate-like test specimens. This highlights the suitability of Al-Mg to provide an effective corrosion protection under marine environmental conditions. Therefore, and according to the obtained results

from the accelerated test, Al-Mg coating exhibits excellent anti-corrosion protection, which can be six times more durable than the obtained with hot-dip galvanizing.

Table 2 Accelerated Test Results

	Start	2.3 months	4.5 months	9 months
Fluorine Resin Paint				
Zn Hot-dip Galvanizing				
Zn-Al Thermal Spray				
Al-Mg Plasma Arc Thermal Spray				

4 APPLICABILITY TO BRIDGE BEARINGS

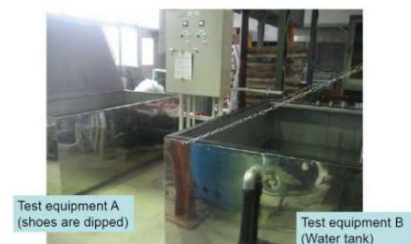
The previously described test was carried out in plate-like test specimens. Due to the complex shape of bridge bearings, it seems necessary to carry out similar tests in these complicated structures, to evaluate the influence of this factor in the performance of the coating methods. In order to achieve this goal, rubber bearing specimens (Fig. 6(a)) were subjected to accelerated corrosion tests simulating harsh environmental conditions [2].



(a) Test specimens



(b) Dry warehouse



(c) Tanks

Figure 6: Corrosion Test to Bearing Models

4.1 Test Outline

As shown in Fig. 6, two tanks and a dry warehouse were used to simulate wet and dry cycles respectively. The test pieces were alternately placed in both environments for a set amount of time, and the development of corrosion in the test pieces was examined. The specimens were treated with Zn thermal spray, Al thermal spray, and Al-Mg plasma arc thermal spray methods in order to carry out a comparative analysis.

4.2 Test Results

As shown in Fig. 7(a), rust appeared and was rapidly developed in the test specimen coated with Zn thermal spray. The test piece coated with aluminum, a metal with a higher tendency to lose electrons than Zn, corroded but in a lower extent, as it can be appreciated in Fig. 7(b).

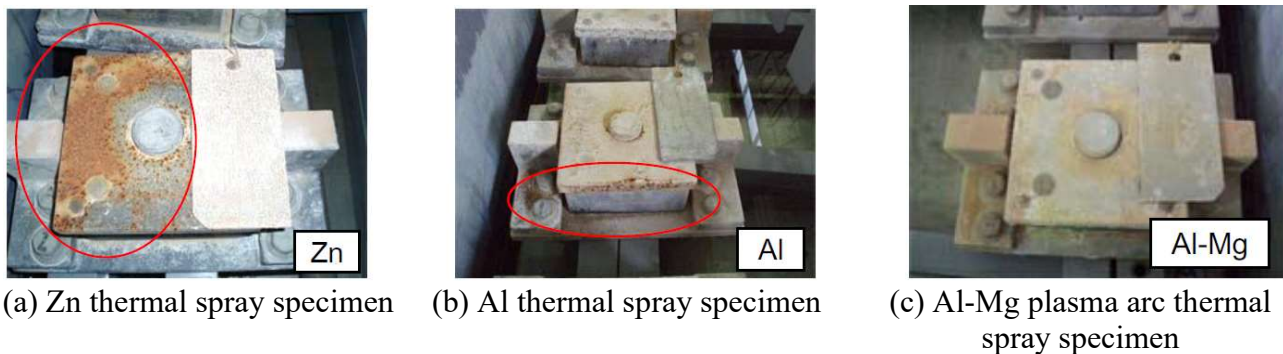


Figure 7: Results of the corrosion test to bearing models

In the Al-Mg specimens, although some traces of rust can be observed on the surface, they were not developed in these test pieces. The rust that appeared in the previous bearings remained inside the tank and was adhered to the Al-Mg bearings once they were dipped in the tub. Therefore, the test results confirmed the stability and satisfactory performance of Al-Mg plasma arc thermal spray, when applied to the actual components of bridge bearings under corrosive environments.

The plate-like test pieces, shown in Fig. 7 placed on top of the bearings, were prepared at the same time and with the same coatings as the bearing-like test pieces. However, unlike the bearing specimens, their anti-corrosion performances are quite similar. Because of this and other reasons, it is advisable to carry out long term outdoor exposure tests, in order to confirm the anti-corrosion performance of the studied coatings.

5 CONCLUSION

In the current paper, different anti-corrosion protection methods for bridge bearings such as paint coating, hot-dip galvanizing, Zn thermal spray, Al thermal spray and Al-Mg plasma arc thermal spray were described. The accelerated tests simulating harsh environmental conditions and actual components of bridge bearings carried out in order to compare their anti-corrosion performance, highlighting the stable and long-term protection capability of Al-Mg plasma arc thermal spray method.

REFERENCES

- [1] Kyushu Electric Power Co., Ltd.: Research for Application and Usage of Surface Treatment Technology, Techno Report, June 2004.
- [2] University of the Ryukyus / Kawakin Core-Tech Co., Ltd.: Report of the Joint Study of the Corrosion of Bridge Bearing under Marine Environment, January 2010.

Seismic Analysis of Bridges



Structural Analysis of Seismically Isolated Curved Bridge According to Turkish Earthquake Code

Elif Yıldırım

Bogazici University, Department of Earthquake Engineering
Istanbul, Turkey

Elif Güngör

Başaran İnşaat
Istanbul, Turkey

ABSTRACT

The main goal of this study is to obtain dynamic response of an example curved seismically isolated bridge according to Turkish Earthquake Code for Bridges with Seismic Isolation and Dampers (TECB-SI 2020). Nonlinear time history analyses are performed since the code is guided that for isolated curved bridges and bridges located on soil class D. Lead rubber bearings are used as seismic isolation system in this bridge. For nonlinear time history analysis, seven ground motion datasets containing two orthogonal horizontal components are processed and scaled. These records are used for upper bound and lower bound nonlinear time history analyses. Also, application direction of the records is rotated with 90 degrees and all analyses are repeated. Thus, 56 nonlinear dynamic analyses are performed. Structural responses are evaluated to determine column and isolator design. Requirements based on the code for factory production control and prototype tests of lead rubber bearing are also proposed.

Keywords: Curved bridge, Lead rubber bearing, Nonlinear time history analysis.

1 INTRODUCTION

The purpose of seismic isolation systems used for bridges is to separate the superstructure from substructure with vertically stiff but horizontally flexible element. When an isolated structure is subjected to an earthquake, the deformation occurs in the isolators rather than the substructure elements. Flexibility in horizontal direction enables the natural period of the system to increase and the earthquake forces are consequently decreased. In addition, seismic isolators have hysteretic energy dissipation system to limit relative displacements. Therefore, seismic isolators transfer forces to the substructure by reducing the earthquake forces.

In this study, seismically isolated curved bridge located in Istanbul, Turkey is selected to be investigated in accordance with Turkish Earthquake Code for Bridges with Seismic Isolation and Dampers (TECB-SI (2020)). Lead rubber bearings in circular shape are used as seismic isolation system in this bridge. Nonlinear dynamic analyses using upper bound and lower bound characteristics of isolator shall be performed to design this example bridge according to the code. Before nonlinear dynamic analyses, response spectrum analyses are performed for preliminary design. Main goal is to design columns and seismic isolation system on the basis of structural dynamic responses and propose details about the isolator design limits and isolator testing.

2 LEAD RUBBER BEARINGS

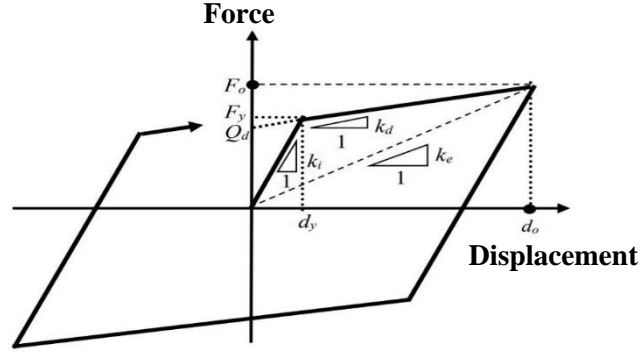


Figure 1 Bilinear force-displacement behavior of LRB

Lead rubber bearings are basically composed of rubber layers, reinforcing inner steel plates, lead core and bottom and top vulcanized steel plates to connect the isolator to anchorage plates. Rubber layers and steel plates provide flexibility in horizontal direction and rigidity in vertical direction respectively. Lead core contributes energy dissipation by transforming kinetic energy to heat energy under earthquake excitation and gives adequate rigidity for service loads such as wind and braking. Bilinear force-displacement curve representing nonlinear hysteretic behaviour of the typical seismic isolation system is given in Figure 1, where Q_d is characteristic strength, K_1 is elastic stiffness, K_d is post-elastic stiffness, K_e is the stiffness at the displacement of d_o , F_y effective yield strength, d_y is yield displacement. Characteristic strength (Q_d) is related to the area of lead core (A_L) and the effective yield stress of lead (σ_L) as given in Eq. 1.

$$Q_d = A_L \sigma_L \quad (1)$$

The value of effective yield stress of lead varies from cycle to cycle because of heating of lead core. Constantinou et al. (2011) suggests the average of effective yield stress of lead in the range of 10 to 12 MPa depending on the size of the lead core, bearing size, loading and manufacturing details. Values in this range can be used in analytical design of LRB. Post-elastic stiffness (K_d) is related to shear modulus of rubber (G), the bonded rubber area (A), and the total rubber thickness (T_r) as given in Eq. 2. Constantinou et al. (2011) stated that shear modulus of rubber depends on the rubber compound, loading conditions, and the amplitude and frequency of motion. Average shear modulus value in three cycles of motion is typically in the range of 0.45 – 0.90 MPa for isolators.

$$K_d = \frac{GA}{T_r} \quad (2)$$

2.1 Upper and Lower Bound Properties of Lead Rubber Bearings

The properties of seismic isolators vary in their service lifetime due to various reasons such as the effects of aging and contamination, the heating, loading, and scragging effect during seismic motion, and manufacturing conditions. These factors affect the horizontal stiffness parameters of isolator. Whereas isolators are initially designed using nominal mechanical properties under seismic and non-seismic conditions, structural analyses should be performed considering both upper and lower bound values of Q_d and K_d .

Property modification factors are categorized in TECB-SI (2020) as the effects of temperature (λ_{sc}), aging (λ_y), wearing during service movement (λ_{as}), contamination (λ_k), manufacturing quality (λ_{irt}) and testing factor (λ_{test}). All these property modification factors are given for low damping elastomeric bearings, high damping elastomeric bearings, and lead rubber bearings separately in

TECB-SI (2020) Table 7.1 and Table 7.2, for upper bound and lower bound respectively. These factors are used to determine upper bound ($\lambda_{üst}$) and lower bound (λ_{alt}) factors based on Eqs. 3-4 as given in TECB-SI (2020). Then, they are multiplied with Q_d and K_d to take into account stiffness change of LRB during lifetime. While the determining upper bound property, β factors for each effect is taken according to bridge importance class given in TECB-SI (2020) Table 7.3, unlike the other seismic codes. The largest shear force demands on the piers and abutments and the largest displacement demand on the isolators are determined using upper bound analyses and lower bound analyses, respectively. The number of rubber layers and the lead core sizes are then set by a trial-and-error procedure to achieve the required seismic performance.

$$\lambda_{üst} = [1 + \beta_{test}(\lambda_{test,üst} - 1)] \times [1 + \beta_{ürt}(\lambda_{ürt,üst} - 1)] \times [1 + \beta_{sc}(\lambda_{s,üst} - 1)] \times [1 + \beta_y(\lambda_{y,üst} - 1)] \times [1 + \beta_{aş}(\lambda_{aş,üst} - 1)] \times [1 + \beta_k(\lambda_{k,üst} - 1)] \quad (3)$$

$$\lambda_{alt} = \lambda_{test,alt} \times \lambda_{ürt,alt} \times \lambda_{s,alt} \times \lambda_{y,alt} \times \lambda_{aş,alt} \times \lambda_{k,alt} \quad (4)$$

Upper bound and lower bound analysis coefficients are consequently calculated as given in Table 1.

Table 1 Upper bound and lower bound analysis coefficients

Upper Bound Analysis Coefficient		Lower Bound Analysis Coefficient	
$\lambda_{max,Qd}$	1.54	$\lambda_{min,Qd}$	0.86
$\lambda_{max,Kd}$	1.28	$\lambda_{min,Kd}$	0.9

3 DESCRIPTION OF EXAMPLE SEISMICALLY ISOLATED CURVED BRIDGE

In this study, seismically isolated 3-span curved bridge located in Istanbul is considered. This bridge has post-tensioned cast in place box girder superstructure supported on reinforced concrete columns. The bridge consists of piers with the total height of 12 m and deck having a width of 9 m. The roadway alignment over the bridge is sharply horizontally curved with 70 degrees. The bridge is isolated with two isolators on piers and abutments. Three-dimensional drawing of the bridge can be seen in Figure 2; piles underneath the foundation are not demonstrated.



Figure 2 Three-dimensional drawing of the bridge

The bridge is classified as standard – normal bridge (KOS-2) in terms of its usage and importance level based on bridge classification system given in TECB-SI (2020) Section 1.6 and 1.7. The code also lists bridge analysis classes for isolated bridges in Section 3.3. These bridge classes contain complex bridges, single-span bridges, and other bridges. Curved bridges having angle between radius lines boundaries of the curvature greater than 8 degrees, and soil conditions with the class of D and E are classified as complex bridges. Therefore, this isolated curved bridge is considered as complex bridge. Under these circumstances, nonlinear time history analysis shall be performed according to TECB-SI (2020) Table 3.1 for this example bridge.

4 STRUCTURAL ANALYSIS OF CURVED BRIDGE

Three dimensional finite element structural model is generated on SAP 2000 as shown in Figure 3. Superstructure deck is modelled using shell elements, column sections are modelled with frame elements. Material properties of bridge deck and columns are C40 and C30 concrete, respectively. Each column section has 1.5 m diameter, 30 ϕ 28 mm longitudinal reinforcement and ϕ 18/10 mm transverse reinforcement. Column cross section is modelled using Mander confined concrete model of C30 for the core concrete considering reinforcement details, and reinforcing steel model for B420C. 30% of the gross section stiffness is used for the effective bending stiffness of the columns based on moment curvature relationship under service loads. No stiffness reduction is made in shear and axial stiffness of the column elements. To ensure the immediate occupancy performance level is acquired, plastic hinges are defined at column ends. For bridge deck, 50% of the gross section stiffness is used for in-plane and out-of-plane bending and shear behaviour and 20% of the gross stiffness is taken as effective torsional stiffness as suggested in the code.

Lead rubber bearings are modelled as a bilinear smooth hysteretic element with bi-directional interaction for nonlinear analyses. SAP 2000 utilizes elastic stiffness, yield force, and the ratio of post-elastic to elastic stiffness to be able to define the behaviour.

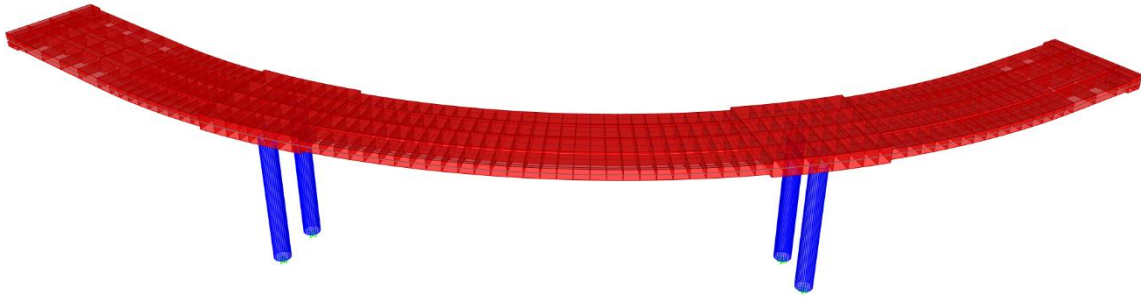


Figure 3 Three-dimensional finite element model of the curved bridge

4.1 Response Spectrum Analysis

In this study, response spectrum analysis is performed in order to compare the results with the nonlinear time history analysis. Seismically isolated bridges designed in conformity with TECB-SI (2020) shall ensure immediate occupancy performance level under DD-1 ground motion level. DD-1 is a very rare earthquake with a probability of exceedance of 2% in 50 years with a return period of 2475 years. Thus, DD-1 ground motion level with the return period of 2475 years is the design earthquake for seismically isolated bridges. Horizontal response spectral acceleration coefficient for short period, S_s and for 1sec period, S_1 are determined using site specific seismic hazard map (AFAD). Then, design response spectrum is constructed for local soil site condition which is class D.

For response spectrum analysis, nonlinear behaviour of isolators are modelled with effective stiffness of the element at the actual displacement. Each isolator is modelled with a separate link element with different effective stiffness values due to different displacement demand, even though same isolator is used for all. Effective period of the bridge T_{eff} is calculated separately for upper bound and lower bound analysis.

Energy dissipation system of the isolator is considered with equivalent linear viscous elements based on the energy dissipated per cycle at the actual displacement. The %5-damped elastic response spectrum is reconstructed dividing spectral acceleration values for period values larger than $0.8T_{eff}$ by damping reduction factor (B_s). B_s is calculated with the empirical equations defined in the code based on effective damping ratio of the system (ξ_e). Final displacement at isolators are achieved by iterating assumed effective stiffness and damping reduction factor.

4.2 Nonlinear Time History Analysis

Nonlinear time history analyses are performed using seven sets of acceleration records compatible with the design response spectrum and scaled within a range of $0.75T_{eff}$ and $1.25T_{eff}$ at upper bound and lower bound analyses.

Table 2 Selected Ground Motion Datasets

Event ID	Earthquake Name	Magnitude	R_{jb} (km)	V_{s30} (m/sec)	Mechanism
1	"Imperial Valley-06"	6.53	10.45	231.2	strike slip
2	"Landers"	7.28	23.62	353.6	strike slip
3	"Kobe_ Japan"	6.9	17.85	256.0	strike slip
4	"Kocaeli_ Turkey"	7.51	13.6	281.9	strike slip
5	"Tottori_ Japan"	6.61	28.81	293.4	strike slip
6	"Darfield_ New Zealand"	7	18.4	194.0	strike slip
7	"El Mayor_ Mexico"	7.2	10.31	242.0	strike slip

PEER NGA Database is used to select ground motion records. The best fitted ground motion time histories are selected and classified taken into account the earthquake magnitude, focal mechanism and site conditions and to fit the design code spectrum. Table 2 presents information about selected ground motion datasets. Ground motion datasets are processed for filtering and scaling. SEISMOMATCH (2016) software is used to scale the records. Response spectra for scaled accelerograms and code based design response spectrum are demonstrated in Figure 4. It is confirmed that the mean response spectra of the scaled ground motions is not smaller than the design spectrum ordinates for all periods.

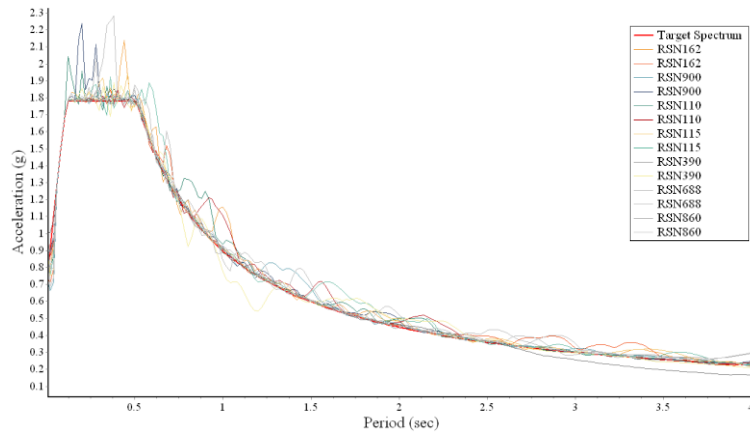


Figure 4 Response Spectra of Scaled Records

As in all nonlinear methods, in the initial step of the calculation, nonlinear static calculation is conducted under non-seismic loads. Nonlinear time history analyses are initiated on the basis of these internal forces. Two orthogonal components of the ground motion set are employed simultaneously in each analysis. 14 upper bound dynamic analyses and 14 lower bound dynamic analyses are carried out. Then, the application direction of records is rotated with 90 degrees and then analyses are repeated. After all, 56 time history analyses are performed and evaluated to consider above conditions. The average of the maximum absolute values of the structural response results obtained from each analysis are calculated to be utilized in the design.

Since all column sections are same with the diameter of 1.5 m, same P-M interaction diagram is provided for all columns. Axial loads and corresponding moment values obtained from dynamic analyses are plotted on the diagram as given in Figure 5.

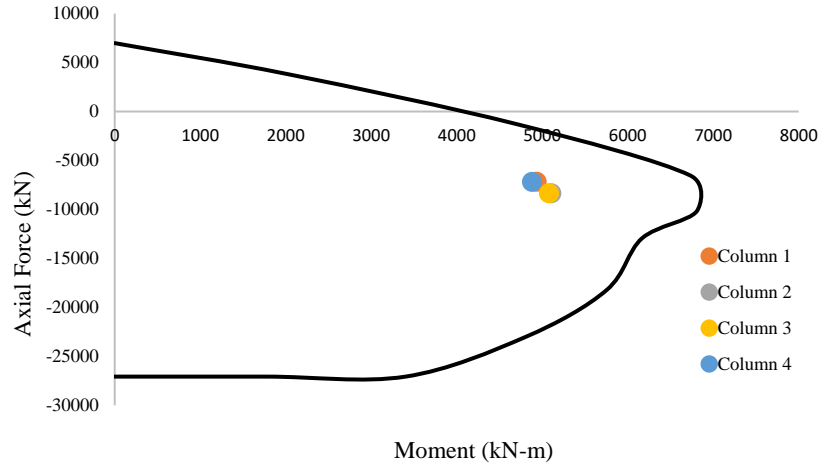


Figure 5 P-M Interaction Diagram for Column Cross Sections

Figure 6 demonstrates that force-displacement hysteresis curves of lead rubber bearing at abutment 1 in X and Y directions separately obtained from dynamic lower bound and upper bound analyses. The reason why abutment 1 is chosen that maximum displacements are occurred there in the bridge. Three of time history load cases results with maximum displacements are selected to show force displacement hysteresis curve during the analysis in order to be seen clearly.

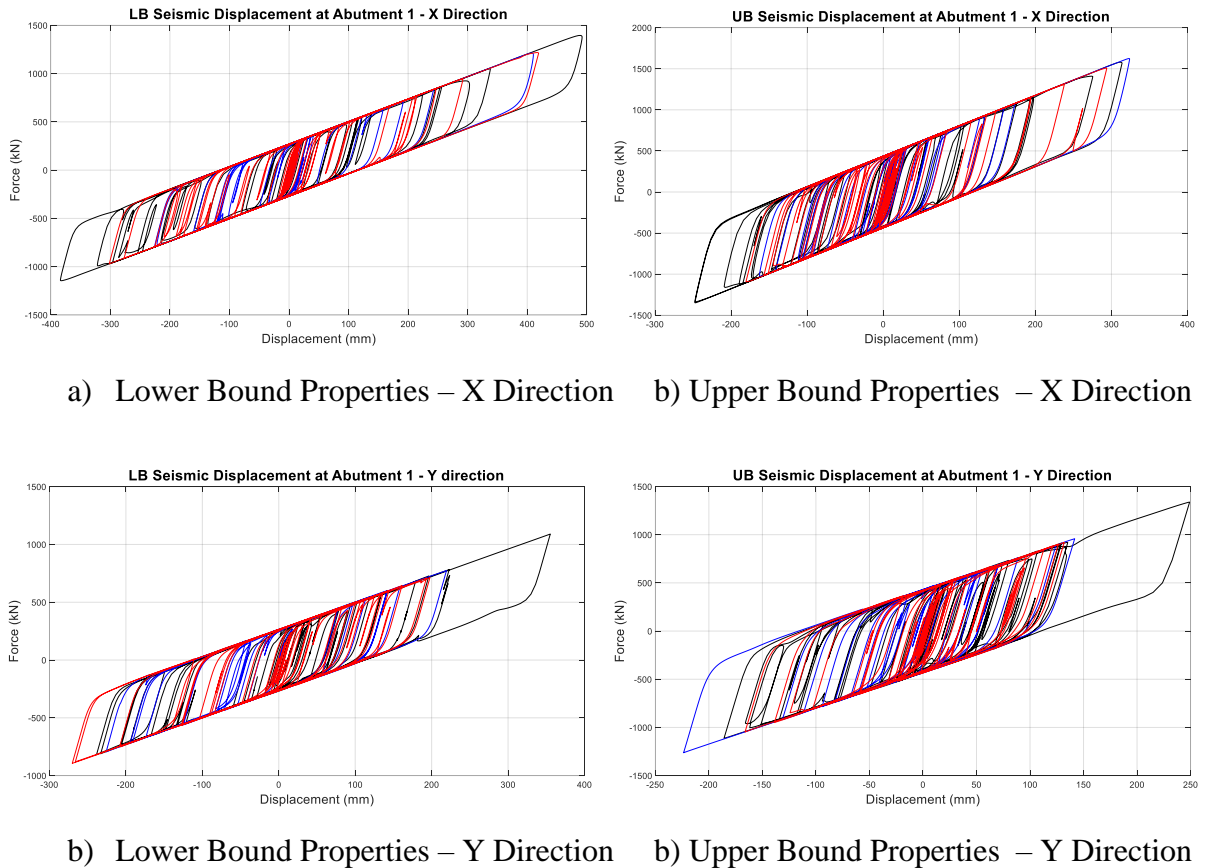


Figure 6 Force Displacement Hysteresis Curves of LRB at Abutment 1

5 LEAD RUBBER BEARING SHEAR STRAIN AND BUCKLING LIMITS

In TECB-SI 2020, service displacement for non-seismic case (d_s) is calculated as the sum of dead load (d_δ), live load (d_H), post tensioning (d_{AG}), shrinkage(d_R), creep ($d_{s\bar{U}}$) and thermal action

(d_{SC}) (Eq 6). The service displacement for seismic case (d_{SD}) is calculated as the sum of dead load ($d_{\bar{0}}$), post tensioning (d_{AG}), shrinkage (d_R), creep ($d_{S\bar{U}}$) and the half of thermal action (d_{SC}) (Eq 7).

$$d_S = d_{\bar{0}} + d_H + d_{AG} + d_R + d_{S\bar{U}} + d_{SC} \quad (6)$$

$$d_{SD} = d_{\bar{0}} + d_{AG} + d_R + d_{S\bar{U}} + 0.5d_{SC} \quad (7)$$

The design displacement capacity of isolator is the sum of amplified seismic displacement (d_1) and service displacement for seismic case (d_{SD}) that cannot be less than the service displacement for non-seismic case (d_S) (Eq 8). The amplified seismic displacement is given by Eq. 9 where d_0 is the seismic displacement in analysis. The structural safety factors, γ_{g1} and γ_{g2} depends on the bridge analysis class and bridge importance class. In our study, safety factors for complex bridges and KOS-2 bridges are 1.10 and 1.05 respectively.

$$d_T = d_1 + d_{SD} \geq d_S \quad (8)$$

$$d_1 = d_0 \gamma_{g1} \gamma_{g2} \quad (9)$$

Buckle et al. (2006) stated that a set of strain limits in the elastomer must be satisfied since the isolator is subjected to the gravitational loads and corresponding rotations under large seismically induced lateral displacements. All codes has own shear strain limits for elastomeric seismic isolators. In our code, shear strain caused by static axial load ($\gamma_{N, sb}$) is limited by 3.0 and total shear strain shall be less than 5.0 (Eqs. 11-12). For an additional check, the sum of shear strain caused by total axial loads (γ_{ND}), total displacement (γ_T), and half of rotations under service axial loads (γ_{θ}) while seismic excitation shall be less than 5.50 (Eq. 13). Shear strain caused by amplified seismic displacements is limited to a value depending on bridge analysis class (γ_{KOS}) that gives a value of 2.25 in this study (Eq. 14). The value of γ_{KOS} are taken as 2.0, 2.25 and 2.5 according to the bridge analysis class KOS-1, KOS-2 and KOS-3, respectively. In this study, allowable shear strain caused by amplified seismic displacement (γ_D) is 2.25. Also, shear strain caused by service displacement (γ_S) shall be less than 1.0. The shear strain limits are as follows:

$$\gamma_{\theta, d\bar{0}} \geq 0 \text{ ise } (\gamma_{N, sb} + \gamma_{S, sb} + \gamma_{\theta, st}) + 1.75 \times (\gamma_{N, d\bar{0}} + \gamma_{S, d\bar{0}} + \gamma_{\theta, d\bar{0}}) \leq 5.0 \quad (11)$$

$$\gamma_{\theta, d\bar{0}} < 0 \text{ ise } (\gamma_{N, sb} + \gamma_{S, sb} + \gamma_{\theta, st}) + 1.75 \times (\gamma_{N, d\bar{0}} + \gamma_{S, d\bar{0}}) + \gamma_{\theta, d\bar{0}} \leq 5.0 \quad (12)$$

$$\gamma_{ND} + \gamma_T + 0.50 \times \gamma_{\theta} \leq 5.50 \quad (13)$$

$$\gamma_D \leq \gamma_{KOS} \quad (14)$$

$$\gamma_S \leq 1.0 \quad (15)$$

where $\gamma_{N, sb}$, $\gamma_{S, sb}$, $\gamma_{\theta, sb}$ are shear strains respectively due to the effect of static axial load, lateral displacement from static loads and rotations imposed by static axial loads; $\gamma_{N, d\bar{0}}$, $\gamma_{S, d\bar{0}}$, $\gamma_{\theta, d\bar{0}}$ are shear strains due to the cyclic loading. Shear strain caused by amplified seismic displacement is the most critical check of LRB design which is given in Table 4. Above mentioned other shear strain checks are also confirmed.

Table 4 Shear Strain Limit Check

Location	A1		P1		P2		A2	
Seismic displacement (d_0) (mm)	327	324	170	176	147	153	293	291
Amplified displacement (d_1) (mm)	378	374	196	203	170	177	338	336
$\gamma_D = \frac{d_1}{n \times T_e} < 2.25$	1.80	1.78	0.93	0.97	0.81	0.84	1.61	1.60

The isolators in both deformed and undeformed configurations need to be checked against the possibility of instability. The calculation of buckling loads are critical and important which are based on the works of Stanton and Roeder (1982), Roeder et al. (1987) and Kelly (1993). If the isolator system is in the undeformed state and loaded only in the vertical direction, the factor of safety against buckling is calculated as dividing buckling axial load capacity for undeformed shape (N_b) by the total

load due to dead plus live load. If the isolator system is in the deformed state, the factor of safety against buckling is calculated as diving buckling axial load capacity for deformed shape (N_b') by total axial load in seismic case. The factor of safety should be at least 3 for undeformed state and 1.5 for deformed state. After all these checks, final design of LRB is determined and Table 5 demonstrates inner details in conjunction with K_I , K_d , Q_d and F_y .

Table 5 Lead Rubber Bearing Design

	Upper bound	Nominal	Lower bound
LRB Diameter (mm)	900	900	900
Lead Core Diameter (mm)	200	200	200
Total Rubber Thickness (mm)	210	210	210
Bearing height (mm)	287	287	287
Characteristic Strength (Q_d) (kN)	483.81	314.16	270.18
Yielding Force, F_y (kN)	537.60	349.10	300.20
Post-elastic Stiffness (K_d) (kN/m)	3318	2592	2333
Elastic Stiffness (K_I) (kN/m)	33175	25918	23326

6 FACTORY PRODUCTION CONTROL TEST AND PROTOTYPE TEST

According to TECB-SI (2020), factory production control tests are performed on each produced bearing in manufacturer plant or laboratory approved by engineer and prototype tests are performed for two full-size isolators of each type in independent laboratory or university laboratory. Single type of isolator is chosen for all isolation system because the code requires two type tests for each one. If we chose two types, four prototype tests should have been performed and it would be resulted in large percentage of total bearing cost.

Factory production control tests consist of two tests: compression capacity test under maximum vertical load capacity and combined compression-shear test. In combined test, the isolator is subjected to compression under dead load plus live load and three cycles of sinusoidal displacement of amplitude equal to the amplified seismic displacement (d_1).

Prototype tests are very essential and they have to be performed for each project prior to serial production. These tests are used to evaluate the main parameters of the isolator in order to compare them with the values used by engineer for design. Table 6 presents prototype test protocol and test sequence according to TECB-SI (2020).

Table 6 Prototype test protocol for isolators

	Test Name	No of Cyles	Vertical Load Description	Notes
1	Thermal Test	20	DL+0.2LL	Max thermal displacement, Velocity<5mm/sec
2	Wind Test	20	DL	Max wind load, test duration minimum 40sec
3	Braking Test	20	DL	Max braking load, test duration minimum 40sec
4a	Seismic Test	3	DL	0.25*d ₁
4b		3		0.50*d ₁
4c		3		0.75*d ₁
4d		3		1.0*d ₁
5	Seismic Test- Repeated	3	DL	0.25*d ₁ ; 0.50*d ₁ ; 0.75*d ₁ ; 1.0*d ₁
6	Wind Test- Repeated	20	DL	Max wind load, test duration minimum 40sec
7	Braking Test- Repeated	20	DL	Max braking load, test duration minimum 40sec
8a	Stability Test	-	0.9 DL	d ₁
8b		-	DL+LL	d ₁

7 CONCLUSION

In this study, TECB-SI (2020) is implemented for the analysis and design of an isolated bridge with highly curved alignment. Lead rubber bearings are used as seismic isolation system in this bridge. Since this type of bridges are classified as complex bridge based on bridge analysis classification in accordance with TECB-SI (2020), nonlinear time history analyses with minimum seven scaled datasets shall be carried out. Response spectrum analysis is also performed before nonlinear analyses in order to make preliminary design of LRB.

Since mechanical properties of isolators are changed throughout their lifetime, characteristic strength and post-elastic stiffness of LRB are modified based on upper bound and lower bound coefficients given in the code. 14 upper bound dynamic analyses and 14 lower bound dynamic analyses are carried out. Then, the direction of records is rotated with 90 degrees and then analyses are repeated. After all, 56 time history analyses are performed and evaluated. The average of maximum absolute values of each record are assessed as design based internal force and displacement. Shear forces obtained from upper bound analyses and displacements obtained from lower bound analyses are evaluated. LRB design is checked based on amplified seismic displacement and service displacements in accordance with shear strain and stability checks given in the code. Shear force capacities of columns are also checked based on transferred shear forces from isolators to the columns. Plastic hinges defined at the column ends are also evaluated whether plastic rotations are observed or not. The results reveal that columns remain elastic; therefore, immediate occupancy performance level is achieved.

TECB-SI (2020) also proposes factory production control and prototype test plans for seismic isolators. In this paper, the requirements of these tests are also mentioned.

REFERENCES

- [1] AFAD, The Disaster and Emergency Management Presidency, Turkish Hazard Map. <https://tdth.afad.gov.tr/TDTH/>
- [2] Buckle, I.G. Dicleli, M. Constantinou and Ghasemi, M. H. (2006), "Seismic Isolation of Highway Bridges."
- [3] Constantinou, M. C., Kalpakidis, I. V., Filiatrault, A., & Lay, R. E. (2011). LRFD-based analysis and design procedures for bridge bearings and seismic isolators. MCEER.
- [4] Kelly, J.M. (1993), *Earthquake-Resistant Design with Rubber*, Springer-Verlag, London.
- [5] PEER Ground Motion Database, NGA-West2 Shallow Crustal Earthquakes in Active Tectonic Regimes <http://ngawest2.berkeley.edu>
- [6] Roeder, C.W., Stanton, J.F. and Taylor, A.W. (1987), "Performance of Elastomeric Bearings", Report No. 298, National Cooperative Highway Research Program, Transportation Research Board, Washington, D.C.
- [7] Stanton, J. F. and Roeder, C. W. (1982), "Elastomeric Bearings Design, Construction, and Materials", NCHRC Report 248, Transportation Research Board, Washington, D.C.
- [8] Turkish Directorate General of Highways (2020). Turkish Earthquake Code for Bridges with Seismic Isolation and Dampers

Historical Bridges

The Bridge as a Witness to life, a Friend to people and an Essential piece of a city

Hulya Sonmez Schaap,

Senior Bridge Engineer, B.Sc., M.Sc., FIEAust, CPEng

Books about the history of bridges start with suspension bridges made from ropes and end with suspension bridges made from steel cables. It may look like “no progress” other than the materials but indeed there is a considerable step up from 50 to 2000m.

These books are not complete without such stories as that of the Roebling family who inherited the construction of the Brooklyn Bridge, a rescue attempt by a professor Farquharson of a dog called Tubby while Galloping Gertie was pulling apart and how the London bridge piers were so obstructive that the riverboats should “shoot the bridge” to pass under. (Gies, 1963; Steinman and Watson, 1957).

This paper will mention similar stories and people’s interactions with bridges together with engineering features while focusing on bridges of so called Asia Minor.



Anonymus Timber Bridge from Anatolia (Photo: Internet)

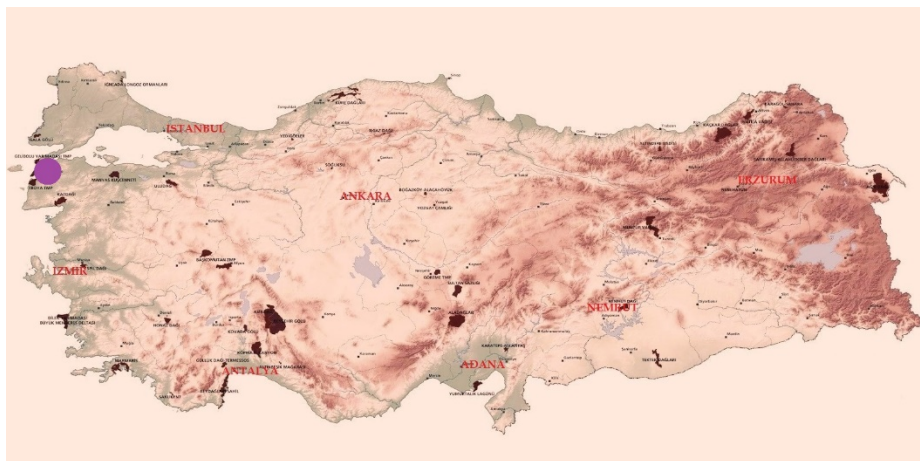
The first to mention is an 850BCE dated bridge in Smyrna. It is registered in the Guinness World Records (2017) as “the oldest datable bridge in the world still in use”. Even though it is hard to find justification other than all the bridge history books agreeing on it! It is called Caravan Bridge, having carried the caravans over the river Meles. The current bridge is a single 8.5m span made of stone. (Tyrell, 1911)



Caravan Bridge over Meles, Smryna (İzmir)-1865

(Engraving by Buch, Moritz <http://eng.travelogues.gr/>)

The setting of this bridge is famous as the birthplace of Homer, the semi-legendary author of epic poems the Iliad and the Odyssey. History, or fable, tells us that his mother Critheis named him Melesigenes because she bore him on the banks of the Meles. (Griffin, 1990)



Modern day Türkiye and Main Cities with Hellespont Crossing (Base Map Internet)

This spot was the custom's gate of Smyrna and travellers would stop here for rest and enjoy the pretty scenery of the Meles. A traveller's description gives a good impression: "...one-arched bridge and two or three large weeping willows hang over its margin. Under the shade of these trees the Turks collect in parties to smoke; and the Meadow of Caravan Bridge, for so the place is called: Mall of Smyrna" by Broughton (1810).



Pontoon Bridge place unknown (Photo: Internet)

Another crossing with a story is the ancient Hellespont, known today as the Dardanelles. The Persian Emperor Xerxes had to cross this spot to march his army from Anatolia to the European side. He bridged the strait two times in 480BCE. 5th century historian Herodotus describes these bridges in detail. Each time, they constructed two bridges, probably to accommodate the long length of the army. The first time, one bridge made using flax and the other with papyrus. After their collapse, they constructed the bridges a second time using flax and papyrus together for each bridge. They laid ships and triremes alongside each other and let down great anchors. They then secured them with cables from land, placed logs of wood and laid it with the earth. Fences were put on either side so the horses would not be frightened. (Godley, 1920)

When the first bridges swept away in a storm and Xerxes heard of this, he commanded that the Hellespont to be whipped with 300 lashes and pair of fetters to be thrown into the sea, which then becomes a tradition. Many movie scenes have shown people who lost their families in rivers similarly lashing the rivers to show their anger.

Herodotus narrates another story from the year 546BCE. When Croesus, King of Lydia, had a reason to fight with the Persian Emperor Cyrus, he sent emissaries to oracles to inquire whether he should send an army against the Persians. The judgement given to Croesus by each of the oracles was the same: if he should send an army against the Persians he would destroy a great empire.

Blinded with pride, he misinterpreted the message and started a war against the Persians but was then unexpectedly defeated by Cyrus. As a result Croesus lost his Empire.

When he questioned the oracles with blame, they responded to him by saying "...he ought, if he had wanted to plan well, to have sent and asked whether the god spoke of Croesus or of Cyrus' empire".

Herodotus describes the army's river crossing: "...when he came to the river Halys (Kızılırmak), he transported his army across it by the bridges..." He also mentions the common belief that Thales of Miletus, a renowned mathematician of the day, divided the river into two channels to cross it. Thales supposedly started from a point upstream from the army camp, dug a deep semi-circular trench to the rear of the camp and passing it, thus the soldiers were transported over fordable streams. (Gilli, Yamaç, Tok 2014)



Çeşnigir Bridge over Halys River (Photo: Internet)

This spot is now home to one of the unique stone bridge of Anatolia, called Çeşnigir Bridge. It is not dated exactly but classified to be from the Seljuk period dated around 1100 CE. The bridge was in very poor condition and was renovated during 2001. It has a very authentic appearance with many half circle openings randomly placed on the spandrel wall. Bedding itself onto the rock, it follows a broken line for its route which is typical to bridges during this era. (Çulpan, 1975)



Çeşnigir Bridge over Halys River (Photo: <http://www.yerelrehberim.com>-2010)

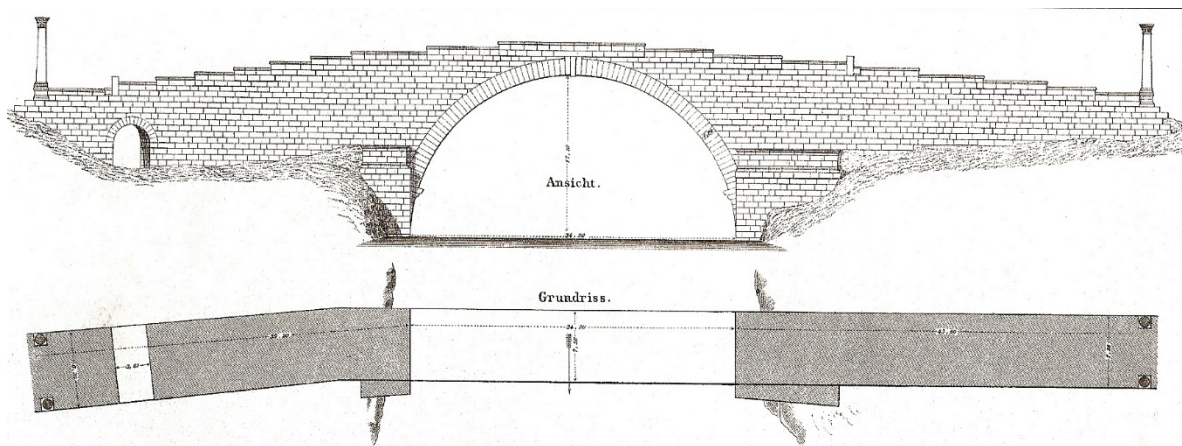
The Romans and Seljuks left many remarkable structures to Anatolian lands. One of the significant Roman bridges is the Cendere bridge crossing over the Chabinas (Cendere) River in the southeastern region. This bridge was a gift from four cities for the honour of the Empire.

200 BCE dated Cendere Bridge has a span of 34m with 7.5m width but interestingly only 4.5m in the clear passage between the parapets. Its appearance is dominated by the stepped parapets leading to the crown of the bridge. The parapets are detailed well to keep a pattern and to comply with the gradient of the bridge. Toward the end, they are stopped with pedestals, one of which is used for inscriptions. The bridge had 4 columns of 9-10m height at either side of its entrances. Each column was dedicated to a family member of Emperor Septimius Severus and held a statue of that person. The ones on the south side dedicated to Septimius and his wife Julia Domma, and the other two dedicated to their sons, Caracalla and Geta. (Çulpan, 1975)



Cendere Bridge over Chabinas River (Photo: İvestadiyaman 2017)

Cendere Bridge tells us a classic story of the battle for the crown. The two sons of the Emperor, Geta and Caracalla, were always in strong opposition to each other. Caracalla ended these arguments by murdering his brother. “Mortally wounded, Geta died, drenching his mother's breast with his blood”. Consequently, Geta’s column was removed from the bridge and his name chiselled from the inscription to delete his memory from history. (Herodian- 1961)



Cendere Bridge over Chabinas River (Başgelen-1999)

Nowadays this amazing bridge is still intact with its nice yellow stone color and 3 remaining columns.

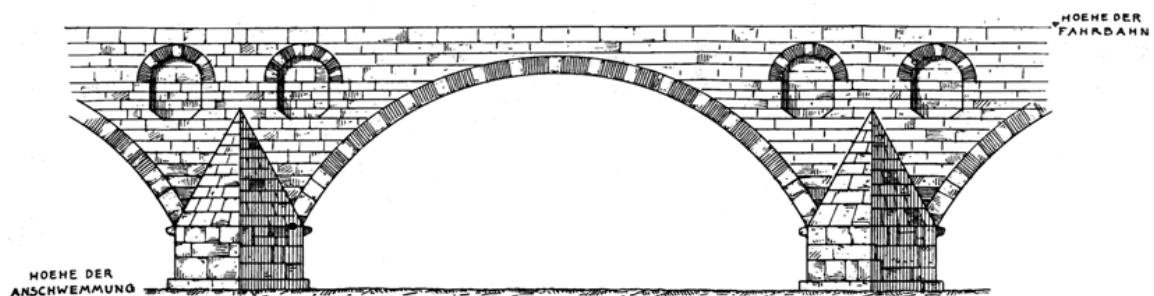
The next bridge was a lucky present for me. I was on the way to a bridge hunt and stopped in a village to get directions. A person called Mustafa offered to show me a local bridge which was a special one for him. First, we saw a roman bridge called Çakırca which served for the ancient roadway to İznik (Nicaea) and is currently cut off from the road network. Then we went to İnikli Bridge. Mustafa told me the story of a big flood in the region which he escaped from by parking their car on the bridge. (KantarAtlas, 2015).



İnikli Bridge in İznik (Photo: Kantaratlas-2005)

The bridge is nearly sunk in vineyard nowadays. It belongs to a unique group of bridges with its alternating brick and stone arches and this feature continues for the entire width of each arch. This type of construction is typical of the Byzantium period dated from 500-600, with similar examples in the vicinity.

When I first saw the bridge, I thought that old amphoras had been recycled this way, but soon realized that this was the design. Five similar bridges are recorded in the vicinity where tile is used in construction.



Sultançayır Bridge over Makestos (Susurluk) Creek, (Wiegand-1904)

More importantly, the bridge arch is segmental and one of the earliest examples of this type. A Segmental arch is one with the rise smaller than the radius of the semi-circle arch. Thus providing more space underneath the bridge. The openings between the main arches reduce the weight and the amount of material.

A bridge with a similar character is the Beşköprü, crossing over a formidable river called the Sangarius (Sakarya). Beşköprü Bridge is one of the achievements of Emperor Justinian, who was famous for the construction of the Hagia Sophia. The bridge was part of another ambitious canal project to utilize the Sangarius for sea transport and also regulate its flood. There are numerous theories on the design purposes of the bridge and the mystery of its use. The facts are that the arches are segmental and have two rows; both can be regarded as features to this group of bridges. (Whitby, 1985)



Beşköprü Bridge over Sangarios (Photo: Kantaratlas-2005)

Even though it is now well hidden in grassland over the old (perhaps artificial) basin of the Sangarius, it does not lessen in its magnificence owing to its dimensions and original architecture. There was a triumphal arch with a spiral staircase leading to the top at one entrance and another arch with half dome roof on the other end of the bridge. An ‘epigraph’ is mentioned to have been placed on the triumphal arch. This epigraph was written for the rivalry of Justinian with the river by the construction of the bridge. (Şahin, 1999)

Byzantium bridges had another distinctive feature as they had symbols of Christianity, especially on the keystones. Karamağara Bridge is one of them and it is an early pointed arch application. Its arch is ornamented with an anecdote from their holy book. Letters on each voussoir read “God protect your coming and going all the times’. When the bridge came in danger of being sunk under the dam lake of the Euphrates, the arch voussoirs of the bridge were dismantled and carried to a Museum. (İlter, 1967)

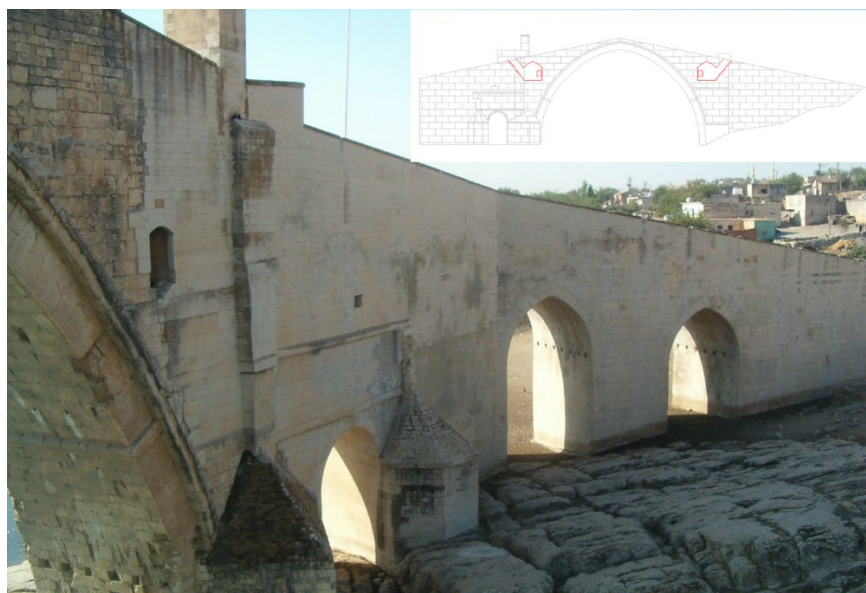
During the 10th century, Anatolia was home to the Seljuks and then the Anatolian Beyliqs who settled at various locations. The Beyliqs settled for short durations and were nomadic by nature. Their bridges also had similar characteristics. They did not follow certain rules and were also often constructed with the cranked plan, variable widths and spans, regularly resting on the ruins of older bridges.

Some of the Beyliqs already had their own techniques and cultures. One of these groups was the Artquids, a Turkmen dynasty that ruled in Eastern Anatolia. They left significant monuments and one is the engineering feat of the magnificent Malabadi Bridge with its clear span of 38.60m. It was constructed between 1145 and 1154 to cross the Batman River which leads to the river Tigris. (İlter, 1978)



Malabadi Bridge - Year 1918 (Karabekir 2017)

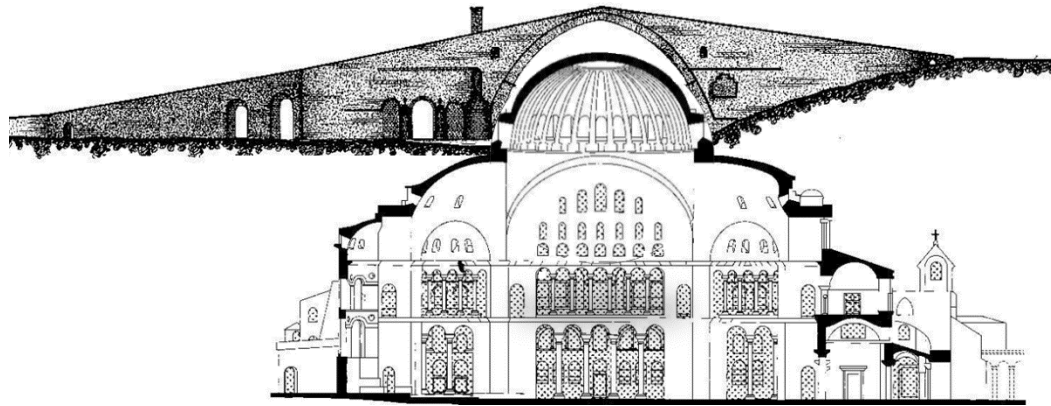
The chambers on either side were incorporated mainly to reduce weight on the arch. Stairs provide access to these rooms via an entry structure of a person's height on either end of the bridge. These rooms are 4.5 x 5.3m each; they have been home to travelers, fishermen, singers and also engineers who constructed the nearby bridge in 1956. (Köpriyet, 2014).



Malabadi Bridge - Year 1918 (Photo and Skech: Kantaratlas-2005)

This bridge has been a stop for many travellers. A famous one from Ottoman times called Evliya Çelebi showed his amazement by saying: "When it comes to describing this bridge; language is poor and the pen is broken!". (Dağlı and Kahraman, 2001)

Another traveller, Albert Gabriel, who visited the bridge in 1932, provides a good visual description that "the Hagia Sophia's largest dome of 33m can be inserted under the bridge". (Gabriel, 1940)



Gabriel's Description of Bridge with Hagia Sophia' 33m dome (Sketches: Internet and Ilter-1972)

On plan view, the bridge is not straight and this is referred to as a common method to slow attacks on cities for defence purposes. At the same time, arch thrust is set directly perpendicular on rock formations giving greater stability. The cranked plan also provides a greater area to resist and spread the floodwaters.

There are stretchers on the spandrel walls at regular intervals which enhance the seismic behaviour of the masonry structures, a feature especially important for the Anatolia region being an active seismic zone.

Nowadays, it is not possible to visit the bridge without a group of kids accompanying you all the time and telling the story of the bridge followed by a famous folk song. (Alagöz, 1975)

According to this song, the bridge has been connecting communities and especially two lovers. In it, Malabadi was the place where the story of a brave man started and ended. "He gave his heart to a girl from the opposite clan. They met on the bridge every day. Her father did not let them marry and killed them on the bridge. Guns boomed, the lovers went silent. Malabadi Bridge has been a grave to them ever since".

There is a collection of bridges with unique characters and different features distributed all over Anatolia. This unification in bridge architecture can be observed during the time of the Ottoman Empire which was one of the Beyliq groups who ruled Anatolia for the next 500 years. Some of which remarkable achievements belong to Sinan, who was the Royal Chief Architect-Engineer during the reign of Sultan Suleiman. Two of these are Moglova Bridge and Büyükçekmece Bridge. (Bozkurt, 1952)



Moglova Aquaduct (Laurens 1847)

Eastern Culture does not traditionally credit individuals and accordingly one should stay humble and not in the picture. Sinan describes himself as “mûr-i nâtüvân” meaning “poor ant” and refuses to place his signature on mosques which he also believed belong to God. Interestingly however he did place his signature on the inscription of Büyükçekmece Bridge. (Şenalp, 1988)



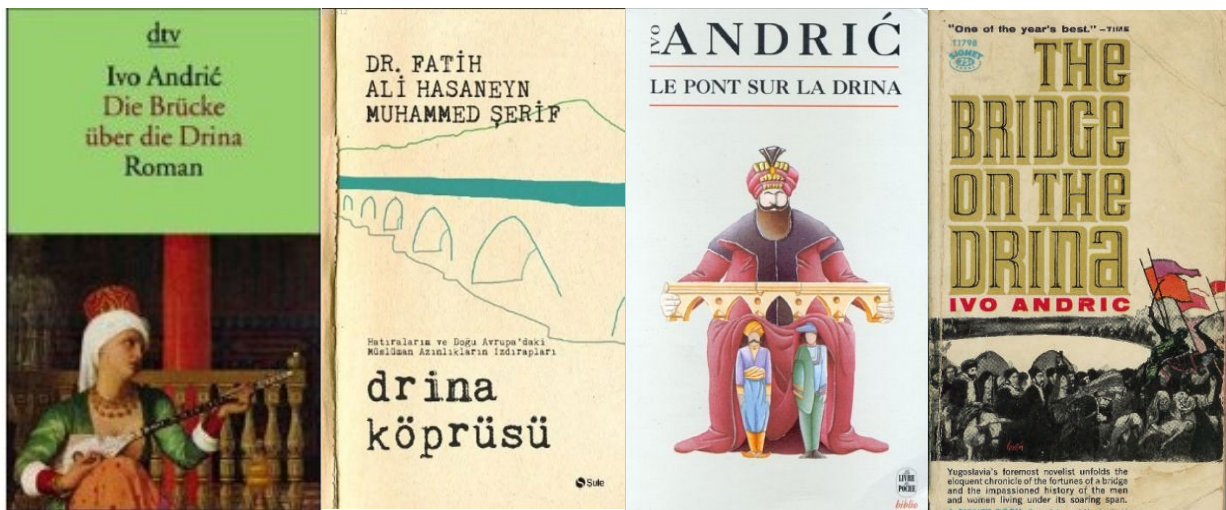
Büyükçekmece Bridge: Top: 4 Bridges connected with Islands, Left-Bottom: İncirpazarı Tower and Right-Bottom: Balcony Console Detail (Photo: Kantaratlas-2005)



Büyükçekmece is a bridge in 4 parts each connecting on artificial islands which were also constructed as part of the bridge. This also provides leeway for excessive floodwaters with least obstruction. It shows typical examples of Ottoman bridge architecture with inscription towers, balconies and bollards at the entrances. The spans are crossed with pointed arches and piers are surrounded by pointed or rounded cutwaters. (Kantaratlas, 2014)

Miniature with the Büyükçekmece Bridge from Sahnâme Selim Han (1581) (İşmen 1972)

The Ottomans left outstanding monuments in the Balkans and a distinctive one is Drina Bridge, also attributed to Sinan. Drina Bridge has been the starring character of a book called, “The Bridge on the Drina”. This book narrates the stories and life around the bridge starting from the construction of the bridge in 1571 until its destruction in 1914. Ivo Andrić won the Nobel Prize for literature for the epic force of his novel in 1961. (Edwards, 1959)



Different Covers of the Book: “The Bridge on the Drina” by Ivo Andrić (From Internet)

First published in 1945, the story of the whole nation and the region is explained through the life of the bridge with the bridge itself becoming a character of the story through its interaction with people's lives. An old tradition of human sacrifices to a River God, who was made angry by the construction of the bridge, starts the book. Water leakage from holes on spandrels is described as the milk of a mother whose baby has been sacrificed for the bridge. Then the bridge becomes a playground for kids who try to run away from the people hiding inside the bridge.

It also became a part of life as it welcomed settlers to have coffee and discuss the political and other issues of the day.



The Bridge on the Drina, Bosnia and Herzegovina, (Photo: Internet)

Then, Westerners conquer Sarajevo. The cultural and social differences of occident and orient are narrated in their treatment of the bridge. Oriental culture did not know how long the bridge was but they lived over the bridge, drinking coffee and discussing political issues. Occidents came and first they measured and surveyed the bridge, looked after it, assigned soldiers at the entrances but rarely did they sit over the balconies. The book ends with the death of one of the main characters, Hafiz Pasha which correlates with the collapse of the Bridge.

The fall of the Ottoman Empire can also be marked with a bridge over the Maritsa (Meriç), in Edirne. Meriç bridge construction took over 10 years and the Sultan struggled to finance the project. The 1847 dated bridge presents the mature features of Ottoman bridges with cutwaters, bollards, drainage details and especially an impressive artwork that is the marble inscription tower. (Çulpan, 1975)



Meriç Bridge over Maritsa, Edirne (Photo: <http://www.kulturportali.gov.tr>)



Meriç Bridge Inscription Tower Details and Ceiling (Photo: Kantaratlas-2005 and Internet)

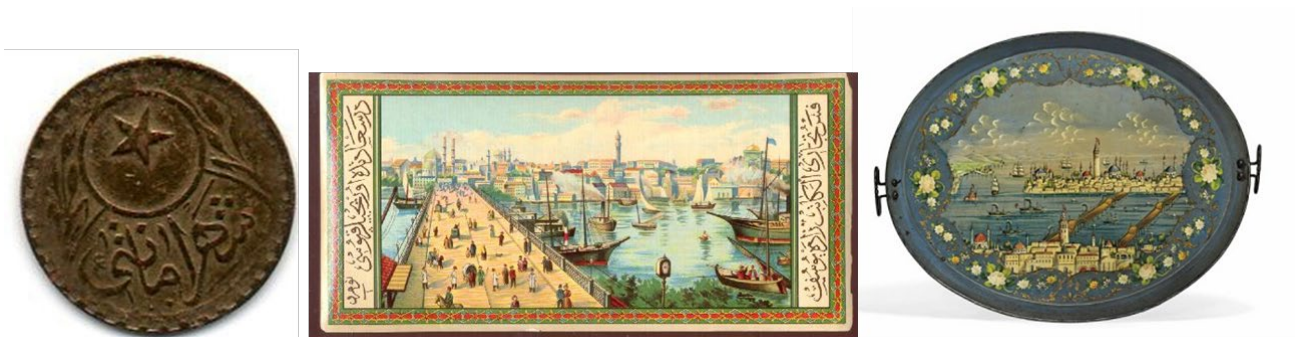
During its decline, the Ottoman Empire had many projects carried out by foreign companies with special contracts, called “imtiyaz” meaning ‘privileges’. One famous one was the 1912 Galata Bridge. It was designed by the German Firm, MAN, manufactured in Nurnberg and transported to Constantinople. It was a pontoon bridge with a swing “door” opened by rotating around a pin point by the pull of a ship. This bridge survived 33 years after which some parts gone missing, the rest sunken and departed to a resting place in the Golden Horn. (Özyüksel, 2014)



1875 Galata Bridge (later the 1912 Unkapanı Bridge) (Catalog 1905)

The history of the Golden Horn and its bridges is a book of its own with main character being the 1912 Galata Bridge. (Evren, 1994)

Besides being home to locals, visitors and fishermen, it has been a stage for important scenes from movies, played vital roles in national events like being a host to the funeral of Atatürk. It was decorated with an arch during the visit of foreign politicians and used as a character in criticizing politics. This inhabited bridge caught fire in one of its shops in the year 1992 while the current Galata Bridge was under construction.



Toll Tolken, Fez Label and Tray for Golden Horn Bridges (Photo: Internet)

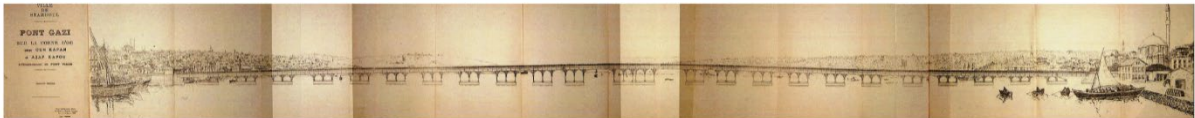
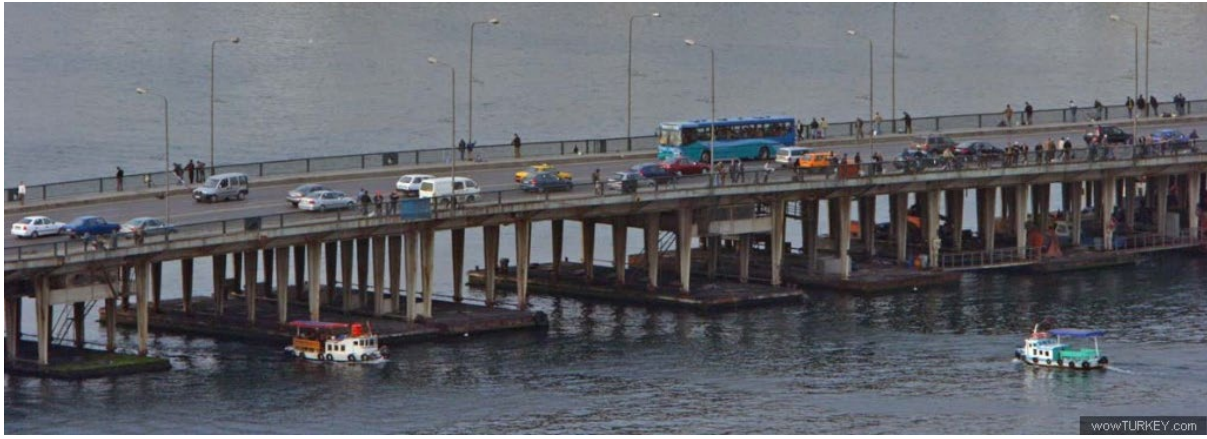


Funeral of Nation's Leader, Atatürk, 19 November 1938 crossing the Galata bridge
(Photo: Internet)

A famous poem about the 1912 Galata Bridge was written by Orhan Veli, who was a forerunner of modern Turkish poetry.

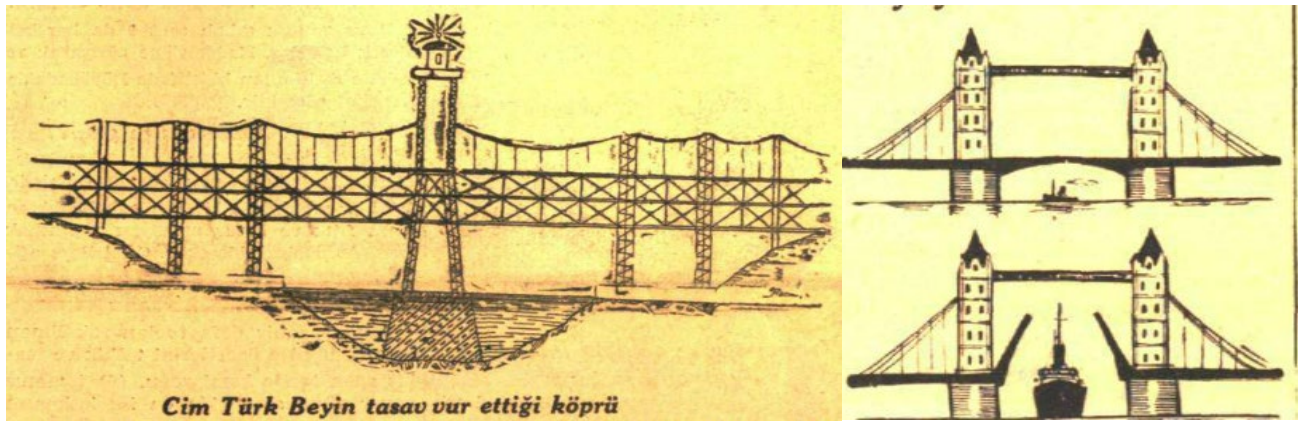
“Standing on the bridge, I enjoy watching you all. Some of you will get mussels from pontoons, some of you a boat, broke the sycamore to go under the bridge ... All of you are on duty for life. Is it only me having pleasure? Who knows one day, I will say a poem, perhaps about you; I will get some money and put some food in my tummy!”

Indeed, the most important bridge over the Golden Horn was a humble bridge which has survived countless misfortunate events. It is a still surviving pontoon bridge being a rare example of its type. Gaston Pigeaud was contracted for the design. When the design he sent from France did not arrive in Constantinople, this was in the news with a heading “wanted”. It concerned the authorities who thought the design might have been stolen by other firms. He had to send the design again. Soon after the opening of the bridge, a storm moved the pavement tiles and the bridge had a “humpback in its very young age”. (Cumhuriyet, 1930; 1937)



1940 Gazi Bridge Top: Photo (www.wow.turkey.com), Bottom: Drawing (Örmecioglu -2010)

This new bridge was very important because it was given the name “Gazi” meaning ‘veteran’ in honour of the nation’s leader, Ataturk. This led the bridge design to face intense scrutiny and to endless debates about whether the bridge should have oriental features to reflect the nation origins or should have a modern appearance to emphasize the new republic. These debates nearly created a revolt between local Authorities during discussions in 1938. Having so much attention and emphasis, in the end, a bridge with no pleasing looks and no dignity was the result. (Örmecioglu, 2010)



Proposals for Gazi Bridge, Left: Two Storey Bridge with Concrete Foundation (Cumhuriyet-1930-06) and Right: Galata Tower Bridge (Cumhuriyet-1933)

The year 1923, the foundation of the republic has opened a new era for everything including bridge building and their meaning in people’s lives. The independence struggle of Anatolia has been won against invaders and also ended the Sultanate. Nation and its people were the Rulers! Engineers have given full dedication and respect to their work. They were highly motivated, fresh and believed in. This also prompted a modern style amongst engineers; they were wearing fedoras and were proud of their work.

Their surnames, picked up by themselves after the “Surname law”, were an indication of their involvement with work. Some examples were: Köprücü (Bridgebuilder), Demirağ (Ironnetwork), Akkaya (Whiterock), Demirci (Ironwork) and Betoncu (Concretemason). Bridge names were also chosen with great care and opening ceremonies were like a public party or at least a very crowded formal ceremony.

I call bridges of this era as “Köpriyet”, a name derived from Köprü (bridge) and Cumhuriyet (Republic).



Bridge during Construction for Sivas-Erzincan Railway Line -1937 (İlk 2013)

The Turkish Republic inherited a diverse culture and knowledge from the Ottomans however the countryside had either been left to its own destiny for years or war had destroyed everything behind it. There was no road network, no material and not many engineers. Moreover with the adoption of a new Latin alphabet, new engineers had to learn their profession with new letters.

The first bridge of this era, constructed in 1928 was a stone bridge most probably clad with concrete for its appearance. Iron was not available, even then the road network did not exist to bring the material to site. It was a single span bridge crossing over Garzan river in Siirt. (Haykır, 2011)

Many and varied bridges were designed and constructed. Most of them were “for the first time bridges of their type”. Concrete arches, Tied-Arches (Bowstring), Bridges with hinges (Gerber) and a few steel bridges were among the types applied. (Nafia, 1933)



Bridgeship :Malabadi ‘Artuqid’ at the back and ‘Köpriyet’ in the front (From: Internet-2018)

Kömürhan Bridge with a 108m span was a real achievement of its time, designed by a Swedish group Nydqvist & Holm AB (NOHAB) and constructed by local firms. Bridge name was determined by a parliament decision and the opening ceremony in 1932 made with a huge celebration. (Nohab, 1937)



Photoshop: 3 Bridges born with the same name “Kömürhan”, (Photo:www.skyscrapercity.com)



Timber preparation for a Bridge near İzmir (Smyrna) Year 1937 (KGM 1970)

This bridge was considered to be a victory and gave hope to people, as it crossed over one of the most formidable rivers, the Euphrates (Fırat). Unfortunately today it is sunken in a Dam Lake.

Railway bridges had a similar history with an elapsed timeline. They needed more technology which was not available locally and also some lines were already given to foreign companies with inherited contracts from Ottoman times.

In fact, it was railway projects and experience established during the execution of them as foreign companies employed local subcontractor workforces that improved the engineering practices in the republic. An important example is the Hejaz railway line project to connect the rail line from Constantinople to the Sacred Lands in the Arabian Peninsula. It was completed in 1908 and had many engineering challenges due to harsh climates, local conditions and geography. (Özyüksel, 2014)

One of these railway bridges, called Boraltan Bridge was used in a movie. The movie called “When the sun will rise?” is based on the true story of Caucasian immigrant refugees evacuated from Europe and destined be delivered to the Soviet authorities towards the end of the Second World War in 1945. Their pleas for permission to settle in Turkey were ignored even though they were doomed to be executed by Stalin’s regime on their return. They crossed the bridge for their execution. This event is known with the name “Boraltan Bridge”. (Kılıç, 1977)



Military School students in front of Railway Bridge, 1891 (courtesy of Engin Özendes)

The actual bridge is not known to me but probably dated to 1930's and exists in this poem by Murat Darga:

“Boraltan is a bridge, passes over Aras – Even if you clean it with Aras water, can't get rid of the black color of your face..”

This movie was filmed in 1977 and was banned from screening in cinemas. Eventually permission was given but one of these showings was the ignition of the Maras Terror which led to the 1980 Military Occupation in Turkey.

Modern day stories about bridges are not as romantic as those of the old times. The famous River Euphrates had laments written for people who lost their lives in the river. For Birecik Bridge whose concrete arch spans the Euphrates River, ground conditions were so poor, the main 57m span had 4 hinges, called a Gerber system. This bridge ended the ferry traffic and long delays. Consequently, during the construction of the bridge, an Engineer has been killed by a ferry owner in 1953. Following his murder engineer, Kadri Cile has been buried at the entrance of the bridge, so his grave is said to be an eternal guard for the bridge. (Cumhuriyet, 1971; Lok 2004)

Another story of an engineer to cross the same river comes as a movie titled simply “Bridge”. There is no information if the film is based on a true story or not but the issues are definitely real. This movie, dated 1975, narrates the life of a boy who lost his mother, who was carried to hospital by boat on the river. He dedicated his life to being an Engineer and building a bridge over the Euphrates. After returning back to his village as an engineer, he started to construct a bridge. This was not welcomed by his stepbrother who earned his living with a ferry transfer across the river. The last scene was a critical argument and the bridge was about to be blown up since the ferry owner had placed dynamite. The ferry owner claimed the bridge as an enemy as it ruined his business and did not show respect for the traditional transportation which had worked fine for many years. The engineer replied saying: it will serve people better and even save their lives. Then he sat down in the middle of the bridge awaiting his death and all the people joined him. The ferry owner had to remove the dynamite from the bridge. (Gören, 1975)



Scene of the Movie “Bridge”- (Gören, 1975)

This movie “Bridge” was to be entered in an international film festival in Karlovy Vary, Czech Republic in 1976. But instead, a movie with the title “Bride” was sent by mistake. *The Bride*, was the story of a family who migrates to Istanbul and their struggle for survival. Bride did not win a prize. The movie “Bridge” was sent to the Tehran film festival instead. (Akad, 1973: Cumhuriyet, 1975)

In Turkey brides have further connections with bridges, there is a tradition that a bride and her entourage should cross a bridge, stand in the middle and throw an apple into the water. This tradition still survives in many places and one famous one is the Cetinkaya Bridge, in Bafra. Cetinkaya Bridge crosses over the Halys River where it reaches to the Black Sea. It is now a Köprüyü bridge dated 1937, 300m long with 6 spans with a tied-arch over the carriageway.



Çetinkaya Bridge over Kızılırmak River, Terme-Samsun (Photo: Internet-2018)

A well known folk song, Köprüden Geçti Gelin, 1937, narrates the story of a bride who was crossing the original wooden bridge at this location. The horses were suddenly frightened by a flying eagle, who had snatched the hairband of the bride and got the other horses worked up as well, so they drove in the river and the bride and her entourage lost their lives.

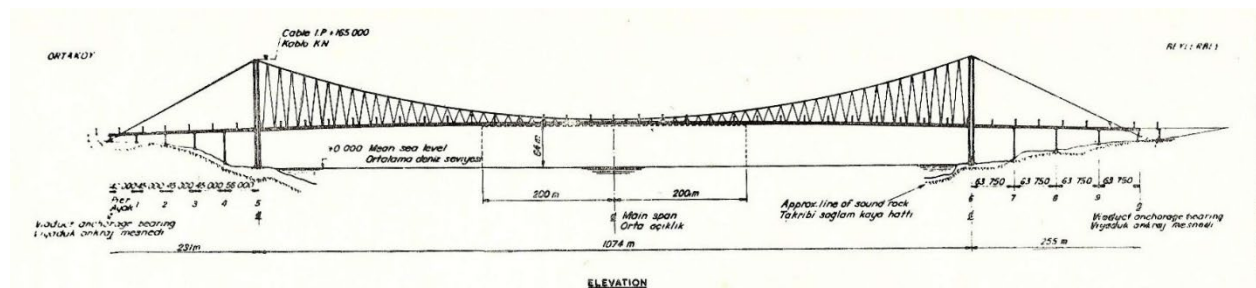
This folk song has been used in many movies, including one filmed around a Seljuk bridge near Aspendos. It starts, “Bride crossed over the bridge, hairband has fallen; you have passed me bride, but I cannot give up on you “. Serik Bridge is constructed over the remains of a Roman Bridge and also uses remnant materials from an aqueduct. (Kessener and Piras 1998; Onal, 1969)



Serik Bridge over the Eurymedon River (Photo: Internet -2018)

The end of the Köpriyet era can be considered to be the Bosphorus Bridge opened in 1973. It was also a project with a long history. Many proposals were made, for example; Carl von Ruppert (1867) with an innovative new design for the bridge, Ferdinand Arnodin with a transporter bridge (1900) and Ulrich Finsterwalder (1958) with a Catenary-cantilever Bridge. The suspension type was selected but it took a long time to secure the contract. (İlter, 1988; The Engineer, 1876; Walther, 1968)

The Bosphorus Bridge used innovation of new aerodynamic steel box section, which was a brave decision when steel truss was becoming a nearly universally typical application. Another new design feature was the inclined hangers, which later in the life of the bridge were discovered to create issues. Testing of this bridge can be considered as a social experiment. Truck drivers were waiting for the long ferry que when the announcement came of the opening of the bridge on the night of 15.10.1973 and they were let on to use the bridge. The trucks were then kept on the bridge for 1.5 hours for each loading condition. (Brown, W.C., Parsons, M.F. and Knox, H.S.G., 1975; Tezcan, 2004)



Bosphorus Bridge between Asia and Europe Continents (Brown at all. 1975)

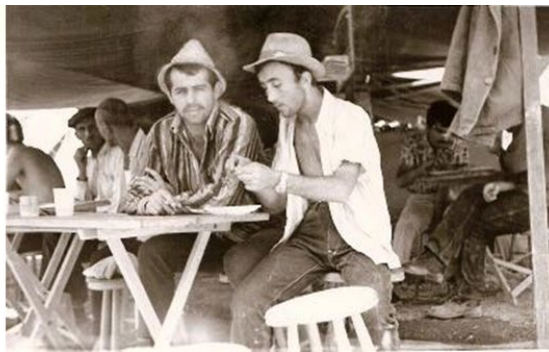
Bosphorus Bridge faced many protests ranging from people living at the bridge approaches to university students. A Theater group was founded by students to start a revolution against imperialism. They acted their play on the streets. Their play about the bridge narrated the story of a village boy who lost his life in a river and his story is connected to Bosphorus Bridge. The decoration was simple a blue scarf was the river and a white sheet was used to resemble the sea. (Üzümkesici, 2016)



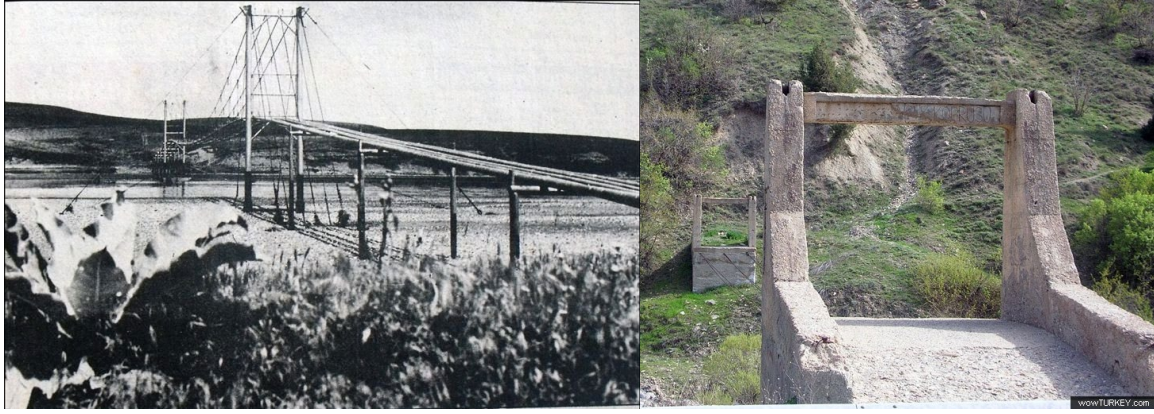
Another protest by a group of young people called “Devrimci”, meaning ‘revolutionist’, started a campaign to construct a bridge over Zap River at the eastern border of the country. Their statement was “Equal wealth and fair distribution of services across the nation”. This campaign was mainly driven by a movie called “Oksüz/Orphan” and a poem called “Anayasa/Constitution”. The campaign was very successful and supported by private companies, universities and local people. The same theatre group set up a play to raise money and special rosettes were sold for funding of the bridge. (Belli, 1968; Olgaç, 1968)

**Opening of Bosphorus Bridge 30 October 1973
(Internet)**

Nearly all material for the subsequent Zap river bridge was donated from the private sector, cables were used from an old bridge carrying pipeline. Groups of volunteer students who travelled from Istanbul camped at the bridge site. The project was guided by a University Teacher and they constructed the bridge themselves. Memories of this are still alive among local people. The bridge is called “Revolution Bridge” and also named for Deniz Gezmis who was the student leader of the revolutionist movement. He has never been to the bridge site and even opposed this naming finding it “populist”. However, his name was a symbol of this movement and he was assassinated by the government together with 2 friends in 1970. (Kabadayı, 2007)

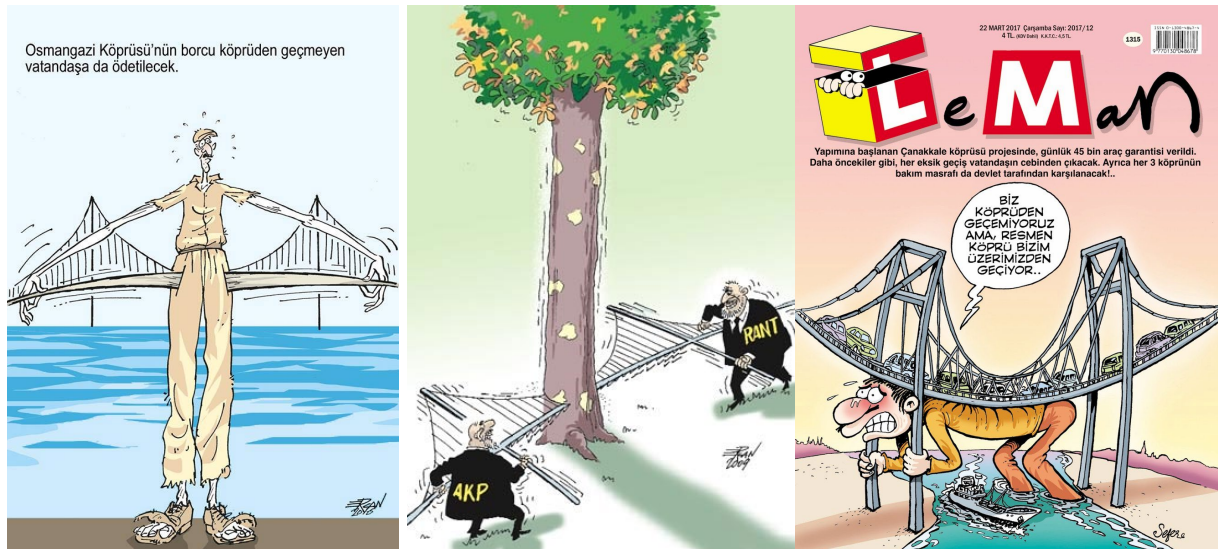


Zap River Project: Logo for theatre Ticket, Students at Construction camp and Truck loaded with Donation for Bridge – (Photos: Internet- <http://kemaloncu.blogcu.com/-Miiliyet> Newspaper)



Left: Pipeline Bridge cables are reused for Zap Bridge – Right: Bridge after its cables were destroyed (Photos: Internet – www.wowturkey.com)

In 1999, this bridge was blown up and remained with its towers as opposing statues waiting to be connected again. The story of the bridge was filmed as a documentary with the name “A Bridge at the Edge of the World” in 2007. This Documentary led to another campaign for the bridge. A concert called “Bridge to Peace” raised enough money to reconstruct the bridge again. Finally, the bridge was opened again in 2010 by 200 students who came from towns all over Turkey.

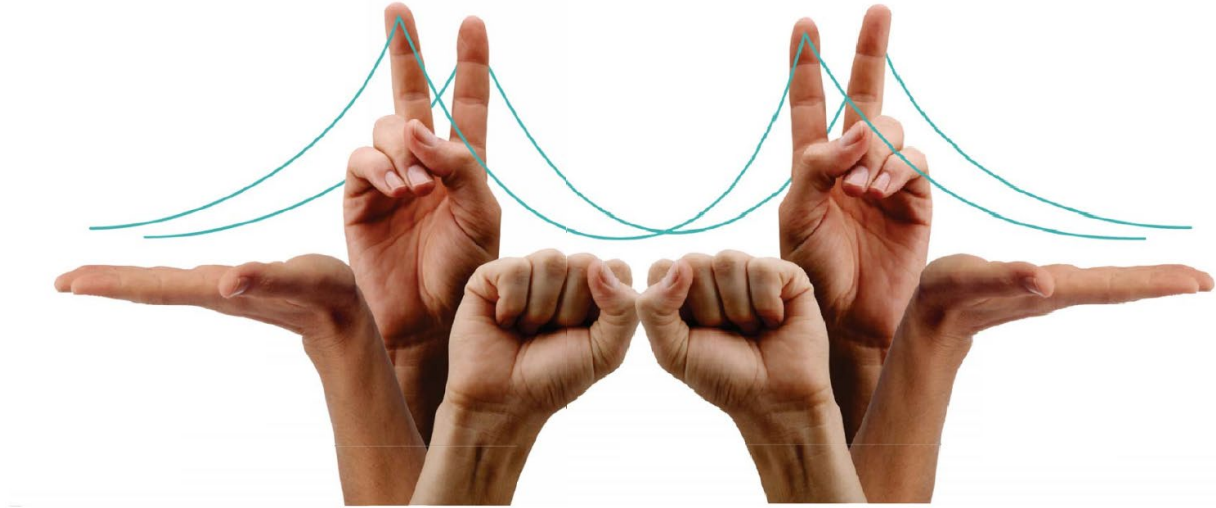


Caricatures from Media in Turkey critising the 3rd Bosphorus suspension bridge

Left: Bridge bill will also be made paid to Citizens who can't pass over it, Middle: Akp vs Rant, Right: We can't cross over it, but, literally it passes over us!

(Left and Middle: <http://e-mizah.blogspot.com>, , Right: <https://www.leman.com.tr>)

Bridge stories in Turkey will never end. “Deli Dumrul” is a mythical character from the epic stories of Oghuz Turks. He had a bridge built across a dry river bed. He collected 33 akchas from anyone who passed over it, he beat and charged 40 akchas anyway even people who didn’t use the bridge. He did this to challenge anyone who thought he was braver than Deli Dumrul. (Ergin, 1997).



Poster for the Concert called “Bridge to Peace” to raise fund for the reconstruction of Zap Bridge

This folk story was recalled by many when an explanation was made by officials: “Everybody, even those who do not cross the bridge, have to pay for the bridge as it is credited with a minimum use guarantee” during the opening ceremony of a 3rd Bosphorus suspension bridge. (Oneido, 2017)

So as the bridges will always witness, serve and carry meaning the stories will never end.

References:

- Akad, L. (1973) Movie: Bride (Gelin) directed and Written by Lütü Akad – Online information: <http://www.imdb.com/title/tt0070099/> – accessed 10th October 2017, Erman Film, Turkey.
- Alagöz, S. (1975) Music Single with Label Polydor for song “Malabadi Köprüsü”, Writer and Director Selçuk Alagöz, 1975, Vinyl.
- Başgelen, N. (1999) Yok Edilen Geçmiş-Yitirilen Gelecek: Cendere Köprüsü, Archeology and Art Mğakeoloji ve Sanat Magazine, available at https://www.arkeolojisanat.com/shop/urun/arkeoloji-ve-sanat-dergisi-sayi-88_11_3141.html
- Belli, S. (1968) Poem: Anayasa (Constitution in Kurdish) – published by İskender Matbaası, 1968, İstanbul.
- Bozkurt, O. (1952) Koca Sinan'ın Köprüleri (Bridges of the Sinan the Great). İstanbul, İ.T.Ü. Architecture Faculty, Ph.D. Thesis.
- Broughton, J. C. H. (1810). Travels in Albania and Other Provinces of Turkey in 1809 & 1810

Brown, W.C., Parsons, M.F. and Knox, H.S.G. (1975) Bosphorus Bridge Part: 1 History of Design. Part21:Construction of Superstructure, Proceedings of the Institution of Civil Engineers, Volume 58 Issue 4, NOVEMBER 1975, pp. 505-567 .

Catalog, (1905), Views of People and Sites in Turkey, The Catalog of the Detroit Publishing Company, available at: <https://www.wdl.org/ar/item/8821/view/1/1/>

Çulpan, C. (1975) Türk Taş Köprüleri (Turkish Masonry Bridges). Türk Tarih Kurumu (Turkish Historical Institution). Ankara

Cumhuriyet (1930) Cumhuriyet Newspaper Achieves – News dated 28 February 1930

Cumhuriyet (1930-06) Cumhuriyet Newspaper Achieves – News dated 30 June 1930

Cumhuriyet (1933) Cumhuriyet Newspaper Achieves – News dated 33 June 1933

Cumhuriyet (1937) Cumhuriyet Newspaper Achieves – News dated 27 November 1937

Cumhuriyet (1971) Cumhuriyet Newspaper Achieves – News dated 6 June 1971

Cumhuriyet (1975) Cumhuriyet Newspaper Achieves – News dated 14 July 1975

Dağlı, Y. and Kahraman, S. A. (2001) Evliya Çelebi Seyahatnamesi –Kitap:4. (Evliya Çelebi Travelogue-Bind 4). Written-Index of Topkapı Palace Library Transcription of Baghdad No:305.

Edwards, L.F. (1959), The Bridge on the Drina by Ivo Andric translated from the Serbo-Croat to English. Original book published in 1945 and translation © George Allen and Unwin Ltd.

Özendeş (2017) Courtesy of Engin Özendeş from her collection-Online photo: <http://www.enginozendes.com> accessed at – accessed 10th October 2017.

Ergin, M. (1997). Dede Korkut Kitabı (Book of Dede Korkut), Türk Tarih Kurumu (Turkish Historical Institution). Ankara.

Evren, B. (1994), Galata Köprüleri Tarihi (History of Galata Bridges). Milliyet Yayınları, İstanbul.

Gabriel, A. (1940). Voyages Archéologiques dans la Turquie Orientale. (1883-1972). Paris: E. de Boccard.

Gies, J. (1963). Bridges and Men, Grosset and Dunlap, New York.

Gilli, E.; Yamaç, A.; Tok, E. (2014) Halys Deviation Tunnel and Cliff Dwellings of Sarıhıdır (Cappadocia Turkey) – Online document:<https://www.researchgate.net> – accessed 10th October 2017

Godley A.D. (2010). Translation of “The Histories” of Herodotus of Halicarnassus translated. Pax Librorum republished after 1920.

Gören, S. (1975) Movie: Bridge (Köprü) directed by Serif Gören and written by Fuat Özlüer and Ahmet Üstel – Online information: <http://www.imdb.com/title/tt0273724/>– accessed 10th October 2017, Akün Film, Turkey.

Griffin J. (1990). Die Ur-sprünge der Historien Herodots’, first published in W. Ax, ed., Memoria Rerum Veterum: Neue Beiträge zur antiken Historiographie und Alten Geschichte . (Stuttgart)

Guinness World Records. (2017). Online Document: <http://www.guinnessworldrecords.com/world-records/oldest-bridge>–accessed 10th October 2017

Haykır, Y. (2011) Atatürk Dönemi Kara ve Demiryolu Çalışmaları (Road and Railway Works during the period of Atatürk). Doctorate Thesis submitted to Fırat University.

Herodian of Antioch (1961) History of the Roman Empire

İlk (2013) STFA from Past to Future. (Geçmişten Geleceğe STFA –) “İLK” and shared with the public.

İlter, F. (1978) Osmanlılara kadar Anadolu Türk köprüleri (Turkish Anatolia bridges until Ottomans). General Directorate of Highways. Ankara.

İlter, İ. (1967) Doomed by Dam. Dismantling of Karamagara Bridge. Middle East Technical University (METU). Faculty of Architecture. Department of Restoration.

İlter, İ. (1988), Boğaz ve Haliç geçişlerinin tarihçesi. (History of Bosphorus and Golden Horn Crossings). General Directorate of Highways, Ankara.

İvestadiyaman (2017) Online Photo: <http://www.investinadiyaman.gov.tr/Cendere-Koprusu--Kahta-fotogaleri-3.html> accessed at 10th October 2017

İşmen, İ. (1972) İnsanlar ve Köprüler (Men and Bridges) Türkiye İş Bankası Kültür Yayınları, İstanbul, Turkey.

Kabadayı, B. (2007) Documentary: Devrimci Gençlik Köprüsü (A Bridge at the Edge of the World) Editor: Burak Dal and Director: Bahriye Kabadayı.

Kantaratlas (2014). Online Blog: <http://kantaratlas.blogspot.qa/2014/12/buyukcekmece-bridge.html> – accessed 10th October 2017

Kantaratlas (2015). Online Blog: <http://kantaratlas.blogspot.qa/2015/09/inikli-bridge.html> – accessed 10th October 2017

KGM (1970) Karayolları Genel Müdürlüğü (General Directorate of Highways). Yearly Calendar. Ankara, Turkey.

Karabekir (2017) Kazım Karabekir Foundation. Online photo : <http://www.kazimkarabekirvakfi.org.tr/resimgalerisi.htm> – accessed 10th October 2017.

Kessener, P. and Piras, S. (1998) The 1998 Campaign of the Aspendos aqueduct research project, Adalya III, 1998, 149–168.

Kılıç, M. (1977) Movie: When the Sun will Rise? (Güneş Ne Zaman Doğacak) directed by Mehmet Kılıç and written by Tufan Güner. – Online information: <http://www.imdb.com/title/tt0183143/>– accessed 10th October 2017. Orhun Filmcilik. Turkey.

Köprüyet (2014). Online blog: <https://kopriyet.blogspot.qa/2015/10/html> accessed 10th October 2017

Köprüden Geçti Gelin (1937) Anonym folk song from Harput region Turkey first complied by Elaziz Community House Art Committee for Turkish Radio and Television Institute, Online

information: <http://www.semsettintasbilek.com/yazi-ve-makalelerim/300-kopruden-gecti-gelin> - accessed 10th October 2017

Laurens, J. (1847) Online photo: https://commons.wikimedia.org/wiki/File:Sinan_Maglova_kemeri.jpg - accessed 10th October 2017.

Lok, M.S. (2004) Assessment of Turkish Bridge Standards and Techniques. A thesis submitted to the Department of Civil and Environmental Engineering. 2004

Nafia (1933) T.C. Nafia Vekaleti, On Senede Türkiye Nafiası 1923 – 1933. (Turkish Republic Public Works, First 10 years) İstanbul Matbaacılık ve Neşriyat, Türk Anonim Şirketi, İstanbul.

Nohab (1937) Nydvist & Holm A.B.; J. Saabye, J.& Lerche,O.; Kampmann, Kierulfe & Saxild' s Construction des Linges de Chemins de Fer- Irmak-Filyos & Fevzipaşa-Diyarbakır, Gotenburg, Copenhagen.

Olgaç, B. (1968) Movie: Öksüz (Orphan) directed and written by Bilge Olgaç – Online information: <http://www.imdb.com/title/tt0346189/>– accessed 10th October 2017, Gaye Film, Turkey.

Önal, S. (1969) Movie: Kalbimin Sahibi (Owner of My Heart) directed and written by Safa Önal – Online information: <http://www.imdb.com/title/tt0436467/>– accessed 10th October 2017, Er Film, Turkey.

Oneido (2017) Online News: <https://onedio.com/haber/osmangazi-koprusu-nden-gecen-de-gecmeyen-de-para-odeyecek-721132> accessed 10th October 2017.

Örmecioglu, H. T. (2010). Technology, Engineering, and Modernity in Turkey: The Case of Road Bridges between 1850 and 1960. Doctorate thesis submitted to Middle East Technical University (METU).

Özyüksel, M. (2014) The Hejaz Railway and the Ottoman Empire: Modernity, industrialisation and Ottoman decline, London: I.B. Tauris, 2014.

Şahin, E.A. (1999) Justinianus'un Bithynia'da Sakarya Nehri Uzerinde İnşa Ettirdigi Köprü ve Kanal Tesisleri (The bridge and Canal Project built by Justinian over Sangarius in Bithynia), online Document: <https://www.academia.edu/3625609/> -accessed 10th October 2017

Şenalp, M. H. (1988) "Sermimaran-ı Hassa Sinan bin Abdulmennan" Lale Dergisi, Sayı:6 (Essay published in Magazine called Lale)

Steinman, D. B. and Watson, S. R. (1957). Bridges and Their Builders, Dover Publications, New York

Tezcan, S. (2004) Bogazici Koprunde halat nicin koptu ? Istanbul Bulten. Issue 71

The Engineer (1876). Gigantic Railway Structures - Carl Von Ruppert. (Illustrated). Proposed Bridge Across the Bosphorus - Carl Von Ruppert, p 230. (Illustrated). Online document: https://www.gracesguide.co.uk/The_Engineer_1867/09/13 - accessed 10th October 2017

Tyrrell, H. G. (1911). History of Bridge Engineering. H. G. Tyrrell, Chicago.

Üzümkesici, B. (2016). Skop Art History Critics Magazine –online Document: <http://www.e-skop.com/skopbulten/koksuz-bir-estetige-karsi-devrim-icin-hareket-tiyatrosu/2931-> accessed 10th October 2017

Walther, R. (1968) Spannbandbrücken. Confrence paper : Vortrag, gehalten an der Studientagung der FGBH über aktuelle Ingenieurprobleme vom 18. Und 19. Okt. 1968 in Zürich. Online available at: www.library.ethz.ch– accessed 10th October 2017

Whitby, M. (1985) Justinian's bridge over the Sangarius and the Date of Procopius' De Aedificiis, Journal of Hellenic Studies.

Wiegand, T. (1904) Reisen in Mysien, 1904



Damage Detection of a Historic Bridge by Operational Modal Analysis

Dilek OKUYUCU

Corresponding Author

Erzurum Technical University/Department of Civil Engineering
Erzurum, Turkey

Ahmet Yasir KANBUR

Erzurum Technical University/Department of Civil Engineering
Erzurum, Turkey

ABSTRACT

This manuscript presents the story of unintentional and unmethodical damage detection of a historic masonry bridge. A research project aimed at the determination of dynamic behaviour parameters of historic bridges by operational modal analysis was studied. The main issue was to evaluate a non-destructive and practical method for material characterisation of historic masonry. As a part of the case studies, in-situ modal parameters of a single span historic masonry arch bridge were studied by operational modal analysis before, during and after its restoration. Experimental mod shapes of the historic bridge were defined to be identical for all restoration phases. However, almost two years after the finalisation of all restoration works, one more operational modal analysis was carried out and it provided some surprising results. First mode shape was experimentally defined to be different than the previous ones. Also, there was no visible sign on the bridge structure that may be a reason for the change of the mode shape. It was a clear sign of separation of the bridge from one of its supporting walls which became quite visible after a few weeks. Hence, the operational modal analysis provided the results which indicated the start of a structural damaging phase of the historic bridge.

Keywords: Historic bridge, operational modal analysis, non-destructive evaluation, damage

1 INTRODUCTION

Historical masonry bridges are among the most important elements of our cultural heritage. East Anatolian province; mainly Erzurum and its surroundings have hosted many civilizations; and a huge number of historic masonry bridges are located within the boundaries of the city. Historic bridge heritage is threatened by many sources like earthquakes, man-made destructions, wrong functionality as being open to vehicle traffics, etc. In Turkey, the responsibility of historic bridges belongs to Turkish General Directorate of Highways. This institution technically works on conservation, restoration and preservation of historic bridges all around the country. During these historic bridge protection works, structural engineering studies like structural evaluation, analysis and health monitoring are generally needed and carried out. Sert, et al. (2015) presents various examples of historic bridge studies realized by Turkish General Directorate of Highways.

By civil engineering perspective, structural evaluation of historic masonry bridges is a difficult task. Lourenco (2002) states some challenging issues which the engineer faces during information collection and condition assessment studies of historic structures. Among them, expensiveness and difficulty of non-homogenous masonry material characterization and unknown

non-visible; but existing damages of a historic structure are underlined by Lourenco (2002). Related literature points out the need for non-destructive and practical methods for material characterisation of historic masonry. Studies like Ozkaya et.al (2015), Ozdogan (2018), Kocaman et al. (2019), Aslay and Okuyucu (2020) focus on the non-destructive determination of mechanical properties of historic masonry by results verification through experimental modal parameters obtained by an operational modal analysis which will be abbreviated as OMA hereafter. Being related to the aforementioned topic, a research project was funded by Erzurum Technical University and carried out to define dynamic behaviour parameters of historic masonry bridges by OMA. Within the scope of ETÜ-BAP 2013-015 project, two historic masonry bridges, *Pehlivanlı (Kireçli) Bridge and Pulur Bridge*, selected by Erzurum 12th Regional Directorate of Highways were studied.

The first phase of the project consisted of several site visits and information gathering about the bridges. In the following stages, masonry material properties were estimated by non-destructive applications, bridge structural analysis models were created and theoretical modal analysis was carried out to calculate theoretical modal behaviour parameters for both historic bridges OMA was performed for experimental estimation of dynamic characteristics. Experimental and theoretical modal behaviour parameters were compared to investigate the success of non-destructive method followed for material characterisation. Considering the theoretical and experimental modal analysis results, structural analysis models were calibrated. properties of historic masonry which were defined by a non-destructive approach. Vehicle load analysis was performed on the calibrated models and dynamic analysis were performed to study the earthquake behaviour of the bridges. It should be underlined that OMA was planned and used as a technical tool to verify the validity of the assigned mechanical properties of the historic masonry.

Both Pulur and Pehlivanlı (Kireçli) bridges were subjected to restoration. Restoration of Pulur Bridge was finished when the project started whereas restoration works of Pehlivanlı (Kireçli) bridge was ongoing. Hence, OMA was carried out for Pulur Bridge only for the post-restoration situation while the process was studied for Pehlivanlı (Kireçli) Bridge during and after the restoration. Besides, Bayraktar (2012) studied experimental modal behaviour of Pehlivanlı (Kireçli) Bridge before its restoration and reported condition assessment details.

The subject of herein manuscript is Pehlivanlı (Kireçli) Bridge. OMA of the bridge was performed before, during and after the restoration. The mod shapes for all three situations corresponded well with some differences in the related periods as expected. After finalisation of the project, almost two years after the restoration one more OMA was carried out for Pehlivanlı (Kireçli) Bridge. The results were surprising. First mode shape was changed. The measurements were renewed and studied to eliminate possible mistakes and errors. The results were the same. In the previous OMA studies, the first mode shape was estimated to be the lateral translational movement of the bridge arch. However, it was the local lateral translational movement of the bridge body at the connection point of the bridge and supporting wall on the side of Kireçli Village for the last experimental analysis. There was no visual sign for separation or damage at the related connection part during the vibration measurements time. Observations continued and only a few weeks after the last OMA; the separation and damage became visible.

This paper provides information about Pehlivanlı (Kireçli) Bridge and its OMA studies which were planned and applied as a verification tool for material characterisation but end up with a damage detection for a historic bridge.

2 MATERIAL: PEHLIVANLI (KIRECLI) BRIDGE

As being one of the most beautiful and magnificent examples of stone bridges in Anatolia; the single-span pointed arch Kireçli (Pehlivanlı) Bridge was constructed at the entrance of Pehlivanlı Town located on the road of Tortum-Uzundere Districts of Erzurum Province. The bridge is spanned over Dumlu River. Kireçli Bridge is known as Pehlivanlı Bridge among local people. There is no inscription or any written information on the bridge. It is not known exactly when and by whom the

bridge was built. However, when the general architecture, arch form, construction style, construction material, technical features of the bridge are taken into consideration and compared with the architectural structures of other stone bridges in Eastern Anatolia (Van, Muş, Bitlis, Ağrı, Erzurum, etc.), it is thought to have been probably built during the Ottoman period, probably in the first half of the XIXth century.

The total slab length of the bridge is approximately 43.47m, the deck width is 5.60m, the height is 12.50m and the arch span is 15.17m. The cut-stone of the bridge was defined to be a very high strength rock; 150 MPa of compressive strength. (Okuyucu et al., 2016) The bridge has been restored by Turkish General Directorate of Highways in 2015. General views of the bridge are presented in Figure 1.



Figure 1: Views of Pehlivanlı (Kireçli) Bridge Before, During and After Restoration (Okuyucu et al. 2016)

3 METHOD: OPERATIONAL MODAL ANALYSIS (OMA)

The method of the study relies on operational modal analysis (OMA) technique. OMA is an experimental, non-destructive and in-situ application which provides the estimation of the modal behaviour parameters of a real structure. It is also called ambient modal analysis since the response of the structure to ambient vibrations are studied to estimate the dynamic characteristics. In other words, OMA does not require to use the response measurements of the structure to the vibrations born from a known source like a shaker. This non-destructive method can be applied when the structure is functional. (Okuyucu, 2021) Considering these advantages, OMA is commonly preferred for historic masonry studies. Foti et al., (2012), Sánchez-Aparicio et al. (2014) and Genç et al.(2019) report to use OMA for theoretical structural model calibration works for various historic structures. OMA is also used for structural health monitoring and damage detection of the historic masonry. Ramos et al. (2010) and Masciotta et al. (2017) publish the details of their studies about the use of OMA for structural health monitoring of historic constructions. Gentile and Saisi, (2011), Conde et al. (2017), Bautista-De Castro et al. (2018) present examples of condition assessment studies of various historic bridges by use of OMA technique.

The application of OMA is rather simple and straightforward. The structure is instrumented with accelerometers at the selected degrees of freedom considering the theoretical mod shapes, response of the structure to the ambient vibrations are measured, the collected data is analysed to obtain spectral density functions and spectral density functions are studied for mod shape, frequency and damping estimation. At the final stage, validation of the mod shapes is studied through a statistical indicator. Modal assurance criteria (MAC) is commonly used for this purpose; as stated by Pastor et al., (2012) MAC values close to zero are accepted as an indicator that the modes are discrete.

In the case of Pehlivanlı (Kireçli) Bridge research, finite element model of the bridge was created and theoretical modal analysis was performed to calculate mode shapes and frequencies. The instrumentation plan was prepared for related degrees of freedom and a total of six points were selected to measure the structural response. Cabled accelerometers and ultra-high sensitive wireless accelerometer sensors were implemented to measure the structural response to ambient vibrations. General instrumentation views of the bridge are presented in Figure 2. It should be underlined that

cabled sensors were used for the last OMA application which was carried out almost two years after the restoration work. The measurement time was kept ~30 minutes for each data set.



Figure 2: General Views from Accelerometer Instrumentation for Pehlivanlı (Kireçli) Bridge

The measured acceleration data was analysed by using Artemis Modal Pro (2017) software. Estimation of the mode shapes and modal frequencies over spectral density functions was primarily done by using frequency domain decomposition (FDD) technique. In the later stages, enhanced frequency domain decomposition (EFDD) analysis technique was also used to estimate damping values as well.

4 RESULTS

Table 1 presents the OMA results of Pehlivanlı (Kireçli Village). Experimental mod shapes were estimated to be the same for all situations; before, during and after restoration as reported by Okuyucu et al. (2016). The first mode was estimated to be the lateral translational movement of the bridge body. However, OMA results obtained ~two years of the restoration provided different mod shapes than the previous ones as stated in Okuyucu (2021) while there was no visible sign which can be linked to the mode shape change. The first mode shape was estimated to be the local lateral translational movement of bridge body at the connection point of the bridge and supporting wall on the side of Kireçli Village for the last OMA.

Table 1 OMA results of Pehlivanlı (Kireçli) Bridge

Mod Nu.	Mod Shape Explanation	Frequency (Hz) (Okuyucu et al., 2016)			Mod Shape Explanation	Frequency (Hz) (Okuyucu, 2021)
		Before Restoration	During Restoration	Soon After Restoration		~Two Years After Restoration
1	Lateral translational movement	5.28	5.44	7.42	Local lateral translational movement of bridge body at the connection point of the bridge and supporting wall on the side of Kireçli Village	7.51
2	Lateral torsional movement	7.35	7.62	15.70	Lateral torsional movement	10.87
3	Vertical translational movement	10.09	10.55	17.95	Vertical translational movement with participation of the connection point of the bridge and supporting wall on the side of Kireçli Village	15.72
4	Vertical torsional movement	13.23	14.81	19.46	Vertical torsional movement with participation of the connection point of the bridge and supporting wall on the side of Kireçli Village	19.98

Schematic explanation of first mode shapes of the historic bridge soon and ~two years after the restoration is presented in Figure 3. The first mode shape estimated by the last OMA could be an indicator of a separation or damage at the connection point of the bridge and supporting wall on the side of Kireçli Village. However, there was no visual sign to support this diagnosis.

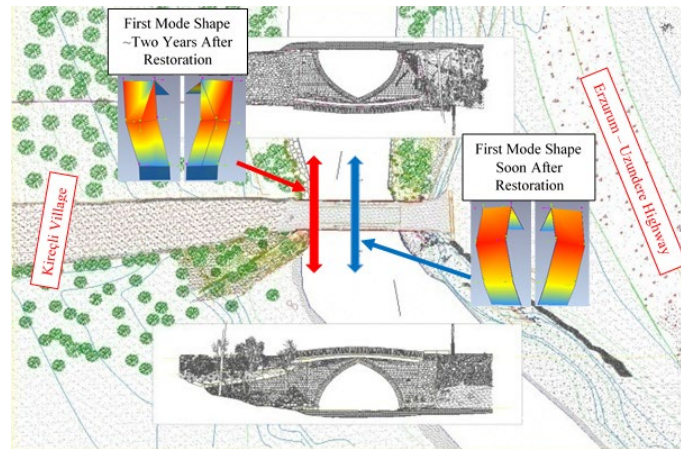


Figure 3: Schematic View of First Mode Shapes of Pehlivanlı (Kireçli) Bridge Soon and ~Two Years After the Restoration

The observation of the historic bridge was continued by the help of the villagers. Only a few weeks after the last OMA application, another site visit was done and the pictures presented in Figure 4 were taken. A major vertical collapse on the supporting wall of the bridge by the Kireçli Village side had occurred together with wide cracks (~30mm width) which were observed at the bridge and supporting wall connection.



Figure 4: Damage Views from Pehlivanlı (Kireçli) Bridge on Kireçli Village Side

5 CONCLUSION

This paper presents information about an unintentional damage detection of historic Pehlivanlı (Kireçli) Bridge by OMA application while the damage was not visible. As the main conclusion of the study, OMA application may be used as a non-destructive method for condition assessment of historic bridges. More OMA application studies on different historic bridges are of great importance and needed to validate the efficiency of OMA method for damage detection of historic bridges.

ACKNOWLEDGEMENT

This study has been funded by Erzurum Technical University as a part of the research project ETÜ-BAP:2013-015. Authors present sincere thanks to Erzurum 12th Regional Directorate of Highways for the official permission to evaluate historical Pehlivanlı (Kireçli) Bridge. Special acknowledgements are felt for Ms Zeynep AKGÜL, Mr Esat Mahmut PARTAL for their help and encouragements. Mrs Halide SERT was a pioneer technical person to underline the need for structural investigation of historic bridges before restoration. Authors feel deep sadness for her pass away and dedicate this paper for her.

REFERENCES

- Artemis Modal Pro, (2017, Operational Modal Analysis Software, Erzurum Technical University, Erzurum, Turkey.
- Aslay, S., E., Okuyucu D., (2020), Technical evaluation of abscissa damage of Erzincan Değirmenliköy church, Journal of the Faculty of Engineering and Architecture of Gazi University, 35(1), pp. 387-402. (in Turkish)
- Bautista-De Castro, Á., Sánchez-Aparicio, L., J., Ramos, L., F., Sena-Cruz González, J., Aguilera, D., (2018), Integrating geomatic approaches, OMA, advanced numerical and updating methods to evaluate the current safety conditions of the historical Bôco Bridge, Construction and Building Materials, 158, pp.961-984.
- Bayraktar, A., (2012), Technical Evaluation and Condition Assessment of Historical Erzurum Pehlivanlı (Kireçli) Bridge, Technical Report, Karadeniz Technical University, Trabzon, Turkey. (in Turkish)
- Conde, B., Ramos, L., F., Oliveira, D., V., Riveiro, B., Solla, M., (2017), Structural assessment of masonry arch bridges by the combination of non-destructive testing techniques and three-dimensional numerical modelling Application to Vilanova bridge, Engineering Structures, 148, pp.621-638.
- Foti, D., Diaferio, M., Gianoccaro, N., I., Mongelli, M., (2012), Ambient vibration testing, dynamic identification and model updating of a historic tower, NDT&E International, 47, pp. 88-95.
- Genç, A., F., Ergün, M., Günaydın, M., Altunişik, A., C., Ateş, Ş., Okur, F., Y., Mosallam, A., S., (2019), Dynamic analyses of experimentally-updated FE model of historical masonry clock towers using site-specific seismic characteristics and scaling parameters according to the 2018 Turkey building earthquake code, Engineering Failure Analysis, 105, pp. 402-426.
- Gentile, C., Saisi, A., (2011), Ambient vibration testing and condition assessment of the Paderno iron arch bridge (1889), Construction and Building Materials, 25(9), pp.3709-3720.
- Kocaman, I., Okuyucu, D., Kazaz, I., (2019), Determination of historical building material properties with dynamic parameters: the case of Lala Paşa Mosque, Teknik Dergi, 30(3), pp. 9125-9146. (in Turkish)
- Lourenco, P. B., (2002), Computations on historic masonry structures, Progress in Structural Engineering and Materials, 4(3), pp. 301-319.

Masciotta, M., G., Ramos, L., F., Lourenço, P., B., (2017), The importance of structural monitoring as a diagnosis and control tool in the restoration process of heritage structures: A case study in Portugal, *Journal of Cultural Heritage*, 27, pp.36-47.

Okuyucu, D., Kazaz, I., Çodur, M., Y., (2016), Determination of historical bridge seismic behaviour parameters using operational modal analysis method, *Scientific Research Project: 2013/015*, Project Coordination Office, Erzurum Technical University, Erzurum, Turkey. (in Turkish)

Okuyucu, D., (2021), Application of Operational Modal Analysis Method for Historic Masonry Structures, Chapter in Book, *Handbook of Cultural Heritage Analysis*, Editor-in-Chief: Sebastiano D'Amico, Springer Nature's Major Reference Works. (accepted)

Ozdoğan, D., B., (2018), Investigation of the use of Schmidt hammer method for definition of material properties of historical masonry structures: application of Erzurum Kadana Mosque, MSc Thesis, Erzurum Technical University. (in Turkish)

Ozkaya, G. G., Kazaz, I., Okuyucu, D., (2015), Kemerli Yığma Köprü Sismik Davranışının Sonlu Eleman Yöntemiyle İncelenmesi, *Proceedings of Symposium On Strengthening and Preserving Historical Buildings and Cultural Heritage-5*, Vol. 1, Turkish Chamber of Civil Engineers, Erzurum, pp. 43-58. (in Turkish)

Pastor, M., Binda, M., Harcarik, T., (2012), Modal assurance criterion, In *MMaMS 2012-Procedia Engineering*, 48, pp. 543–548.

Ramos, L., F., Marques, L., Lourenço, P., B., De Roeck, G., Campos-Costa, A., Roque, J. (2010), Monitoring historical masonry structures with OMA: Two case studies, *Mechanical Systems and Signal Processing*, 24(5), pp. 1291-1305.

Sánchez-Aparicio, L., J., Riveiro, B., González-Aguilera, D., Ramos, L., F., (2014), The combination of geomatic approaches and OMA to improve the calibration of finite element models: A case of study in Saint Torcato Church (Guimarães, Portugal), *Construction and Building Materials*, 70, pp. 118-129.

Sert, H., Partal, E. M., Nas, M., Yılmaz, S., Demirci, H., Avşın, A., Turan, G. S., (2015), Tarihi Köprülerin Restorasyonları Kapsamında Yürütülen Yapısal Analiz Çalışmaları ve Sonuçları, *Proceedings of Symposium On Strengthening and Preserving Historical Buildings and Cultural Heritage-5*, Vol. 2, Turkish Chamber of Civil Engineers, Erzurum, pp. 75-82. (in Turkish)

Artificial Intelligence



AI On The Management Of Existing Bridges

José Matos

ISISE, University of Minho
Guimarães, Portugal

Carlos Santos

ISISE, University of Minho
Guimarães, Portugal

Mário Coelho

ISISE, University of Minho
Guimarães, Portugal

ABSTRACT

The present paper presents a brief discussion on the current practice regarding bridge management. The main goal of this discussion is the attempt of finding some trends in the research and development of existing bridge management systems (BMS). To achieve this, it is firstly important to analyse the entire process of bridge management, understand which parts of the process are being properly addressed by current BMS and which parts are not account for nowadays. The next step consists in providing some guidance on how to improve BMS considering the parts not being well covered. Likewise, some orientation is required to deal with the parts not yet being accounted for in existing BMS. To this end, insights and tools already used in other fields of knowledge can be considered, adapted and adopted in future BMS. In this regard, artificial intelligence algorithms appear as a sound candidate.

Keywords: BMS, Asset Management, AI, BrIM.

1 INTRODUCTION

Mobility is nowadays taken for granted all over the world. Contrarily to what happened a few centuries ago, today's human life is highly dependent on the capacity of moving people and goods between places increasingly more distant one from another. In the particular case of terrestrial mobility, transportation systems composed by roadways and railways play a crucial role in assuring the desired mobility.

From the various assets that compose the referred transportation systems, bridges are one of the most important due to their relevance for the entire system. In fact, while the amount of bridges in each network is normally very limited, when compared with the extension of other longitudinal elements (e.g. pavement/rail track), they can behave as bottlenecks of the network in case of functionality loss, thus assuming a considerable importance.

This importance is highly recognized, and since beginning of 1970's several proposals have been presented worldwide on how to manage bridge stocks – the so called Bridge Management Systems (BMS). Following sections presents an overview of current BMS.

Bridges, due to their inevitable exposure to natural environment, deteriorate with time. This deterioration can be slower or faster, depending on many factors such as quality of design and/or construction. Also, adequacy of design to real loads (e.g. traffic load tends to increase beyond what was considered in design). Finally, natural and man-made hazards are also a source of concern regarding bridges performance throughout their lifetime. In particular, regarding natural hazards it has been seen lately that they are happening more frequently and with higher impacts due to climate-change effect [1].

On the other hand, many bridges are approaching the end of their design lifetime. This increases the criticality level of bridges regarding the mobility of people and goods that they need to ensure.

2 BRIDGE MANAGEMENT SYSTEMS

Bridge management systems (BMS) were originally proposed as simple inventory databases [2]. Since then, other modules have been added and, nowadays, the current BMS are constituted by at least three major modules, namely, Inventory Module, Performance Model and Maintenance Optimization Module [3]. In the following, each of these is further presented.

The content of following sections resulted from the review on more than 40 BMS [4]. This is still an ongoing work, thus the observations written in what follows are the first preliminary observations that can be extracted from that review.

2.1 Inventory Module

The basilar module of BMS is, as already mentioned, the inventory one. Despite the evolution suffered by BMS, the data related with the bridge stock being managed is still required to be stored and used [5]. The major difference from the original inventory modules to the current ones, lies in the bigger amount of data stored but, most importantly, in the type of data stored. In fact, as new modules became included in BMS, the type of data required to feed them was also required to get its own space in the inventory database. Hence, this inventory module gained a wider amplitude and nowadays includes also data not directly related with the bridges.

2.2 Performance Module

Soon bridge managers understood that, while having a systematic data collection of the bridge stock was very important, the real advantage would come from the use of the stored data. That was the trigger for the appearance of what can be designated a performance module. This module is dedicated to the hard task of predicting bridges' performance in time. To that purpose, deterioration models, associated with the most relevant deterioration mechanisms found in bridges, begun being applied in the context of bridge management.

Five main types of deterioration models can be found in the literature [6], namely:

- Physical models: this type of models considers the mechanical behavior of the bridge components, as well as the deterioration mechanism undergoing and influencing the performance evolution. Some examples of physical models include carbonation-induced corrosion, chloride-induced corrosion, alkali-aggregate reaction and freeze/thaw attack, among other;
- Deterministic models: like physical models, deterministic models are based on a set of analytical expressions. However, deterministic category includes models that are deduced essentially in a mathematical fashion. This category includes multiple linear regression, polynomial regressions and ordinal logistic regressions, and similar regression-based models;
- Stochastic models: in this category can be found all those models that include uncertainty, regardless to its source, in the prediction process. Majority of bridge management systems available worldwide use predictive models of this category. Particularly, Markov models (including pure, semi and hidden versions) are the most widely used;

- Artificial intelligence (AI) models: this category has been increasingly used in the last years, benefiting from the widespread of AI algorithms and tools. These models aim at exploring the large amounts of data available from multiple monitoring sources existing nowadays, which is not possible using previous models. Models based in artificial neural networks, fuzzy logic and case-based reasoning, are just few examples of what can be found recently in the literature.
- Graph theory-based models: besides the four categories mentioned before, there can be also found some other prediction models. These, even though used with promising results in many cases, do not fall within a single category thus are grouped in this last and generic category. Bayesian networks and Petri nets are two examples of such kind of prediction models.

2.3 Maintenance Optimization Module

Performance module was a big step forward in the existing BMS. However, considering the final goal of BMS, which should be supporting the bridge managers to take decisions regarding their stock maintenance, this was not enough. Hence, next big module implemented, that most advanced BMS worldwide include, was the maintenance optimization module.

This module aims at providing a schedule of maintenance interventions for a provided time horizon. It is supported on the performance predictions produced by performance module. Those are now combined with new information related with the maintenance interventions. This information includes, at least, a description of each possible maintenance intervention, the frequency in which it can/should be applied, the effect it produces in the current performance, as well as the associated costs. This is one example of the new type of data, not directly associated with the bridge itself, that nowadays inventory module store.

Up to this point, the present module behaves just as a maintenance module. The term optimization only appears when this process of maintenance schedule is provided with some kind of optimization. And this is one major difference between existing BMS, i.e. the type of optimization strategy implemented. To this purpose, optimization can be single-objective or multiple-objective, depending on the number of optimization goals considered. The most common adopted goals refer to overall performance (either cumulative, average or worst, among other possibilities), the overall maintenance costs and/or other specific goals such as performance/cost for specific critical bridges in the stock. On the other hand, it is usual to set some boundary conditions in this optimization process, either in terms of performance or costs limitations.

3 AI ON THE MANAGEMENT OF BRIDGES

Following the overview on bridge management systems, presented in previous section, in the next paragraphs some of the most relevant uses of artificial intelligence (AI) are highlighted. For a matter of clarity, these AI uses are introduced in the same order that BMS modules were discussed before: inventory, performance and maintenance optimization modules.

3.1 Inventory Module

Inventory module in many BMS still consists on simple tables where bridge data is stored. This is not adequate as the stocks increase. Thus, first improvement mandatory for those BMS that do not already have that implemented, is to move to better database technologies. Relational databases are the most widely used technology to this purpose. However, as the databases increase, both in terms of number of bridges but most importantly, in terms of the amount of data being collected per bridge, new technologies should be considered in the next years. This aspect is further discussed.

On the other hand, even the data already existing in the inventory module, is not being fully used. In fact, majority of BMS seldom explore other data besides bridge condition state rate. However, it would be very relevant to take advantage of all other data available in the inventory

module. This would allow identifying behavioural tendencies, which would then be important in the definition of bridges' clusters, thus improving the results obtained by performance module [7,8].

3.2 Performance Module

As referred in section 2.2, one of the types of performance models already being used consists on artificial intelligence algorithms. Several examples can be found in the literature of the use of such models.

Ariza et al. [9] is one of several examples that could be shown. In particular, in that work a comparison was made between AI performance prediction models and the most commonly used stochastic models. It was clearly shown the superior behaviour of AI models when compared to stochastic ones. However, it was also highlighted that more data is employed in AI models. In that work, from the 116 data types available in the bridges' database, only 8 were used in the final model.

This aspect, further emphasizes the importance of developing new models that further explore the available databases. It is a waste of time and resources to collect large sets of data if, at the end of the day, only small parts of it are used.

3.3 Maintenance Optimization Module

At a first glance, from all the three modules in classical BMS, this would be the module in which AI algorithms might seem to fit better. This is somehow right. In fact, majority of optimization algorithms implemented in optimization modules belong to the family of AI algorithms.

One example of maintenance optimization module was presented by Denysiuk et al. [10]. To this purpose, a multi-objective optimization algorithm was implemented. This algorithm aimed at defining the best maintenance actions' schedule, which simultaneously minimized the deterioration of the bridge and the total costs of the maintenance actions during the analysis period.

4 FUTURE BRIDGE MANAGEMENT SYSTEMS

The future of bridge management systems is highly associated with the future of the sector to which it belongs. Nowadays, a transition to digitalization is taking place in the Architecture, Engineering and Construction (AEC) sector. The most visible aspect of this transition is related with the Building Information Modelling (BIM) working philosophy, even though this digitalization transition goes far behind it, and concepts such as virtual reality or augmented reality are no longer just buzz words in the sector [11].

In the context of the present work, what is relevant to emphasize is that next generation of BMS are already being developed considering their capability to be used in a BIM context [12]. To this purpose, the most direct impact in the classical BMS presented in previous sections, is associated with inventory module. In fact, the data associated to each bridge available in the inventory will now be replaced by bridge digital models, usually designated BrIM (Bridge Information Models). Hence, all the functionalities that are nowadays included in existing BMS, will need to be adapted to this new context. On the other hand, new functionalities are expected to be added in the next generation of BMS, taking advantage of the digital environment in which the entire bridge management process will take place.

Analysing what can be this digital BMS and some of the features it might have, several aspects are easily found, in which AI tools will be essential.

Firstly, the problem of creating the BrIM itself. While this can be done by hand from scratch, using any of the several BIM software available, that is not feasible for large stocks of bridges. The process being attempted, consists on the use of laser scanners to obtain the cloud of points which represent the external surfaces of the bridge components. Then, this cloud of points is imported to the BIM software and structural elements are created using the cloud of points as reference. The idea is

to inscribe the structural elements inside the cloud of points, so that the external surface of the elements lies over the cloud of points. This process is time-consuming and new algorithms are required to allow element detection, directly from the cloud points. In this regard, artificial intelligence algorithms would be certainly valuable in the near future, even though work in this topic is already undergoing [13].

Secondly, assuming BrIM models are already in place, one can look at the use of data contained in those models. At this stage, two main issues might arise, one related with the number of parameters (or the number of data types involved) and another one related with the amount of data (total amount of memory required to store data) involved.

One solution to the first aspect might be related with the use of different database technologies. Recently NoSQL was proposed as alternative to traditionally used relational databases [14]. Likewise, one solution to second aspect might be found in the adoption of big data technologies [15]. In both situations, it is not difficult to foresee the appearance of other alternatives based on the use of AI in the near future. In fact, there are very good AI algorithms that can be applied in these contexts.

Thirdly, now that BrIM and tools to use the data stored are in place, one might think on how to update the existing models as new data becomes available. This might be the case of updating the BrIM with data obtained in new inspections or data obtained from some intervention made on the bridge. To address this issues, several research works are undergoing presently worldwide. In particular, works related with updating BrIM with damage detected in bridges' inspection are already being conducted [16,17].

5 CONCLUSION

The common practice in bridges management is nowadays assisted by the use of Bridge Management Systems (BMS). An overview on the evolution of such systems was presented, and the most relevant features were detailed in the present work. It was then highlighted some successful application of Artificial Intelligence (AI) algorithms in the context of existing BMS.

Considering the future developments associated with BMS, it is now clear that Bridge Information Modelling (BrIM) is the direction in which all BMS should evolve in the next years. BrIM should be a reality in the near future, thus a more efficient management of bridges is expected to occur. Also in this regard, AI tools are expected to play an important role. Several examples of aspects that will benefit from the use of AI were left herein.

A fully integrated approach, supported by AI tools, should be the next step in bridge management systems' evolution after BrIM become standard. In that longer future, when the technology allows us to, a complete Digital Twin model of the whole network will be possible. While today it might seem an ambitious goal, it is almost an inevitable one and all signs point in that direction [18].

REFERENCES

- [1] P.J. Ward, V. Blauhut, N. Bloemendaal, E.J. Daniell, C.M. De Ruiter, J.M. Duncan, R. Emberson, F.S. Jenkins, D. Kirschbaum, M. Kunz, S. Mohr, S. Muis, A.G. Riddell, A. Schäfer, T. Stanley, I.E.T. Veldkamp, W.C. Hessel, Review article: Natural hazard risk assessments at the global scale, *Nat. Hazards Earth Syst. Sci.* 20 (2020) 1069–1096. <https://doi.org/10.5194/nhess-20-1069-2020>.
- [2] K.D. Flaig, R.J. Lark, The development of UK bridge management systems, *Proc. Inst. Civ. Eng. Transp.* 141 (2000) 99–106. <https://doi.org/10.1680/tran.2000.141.2.99>.
- [3] Z. Mirzaei, B. Adey, L. Klatter, P. Thompson, Overview of existing Bridge Management Systems, Report by the IABMAS Bridge Management Committee, 2014.
- [4] C. Santos, M. Coelho, J. Matos, Bridge management systems review (working paper), (2020).
- [5] C. Hanley, V. Pakrashi, Reliability analysis of a bridge network in Ireland, in: *Proc. Inst. Civ. Eng. Bridg. Eng.*,

Thomas Telford Services Ltd, 2016: pp. 3–12. <https://doi.org/10.1680/jbren.13.00026>.

- [6] M. Santamaria, J. Fernandes, J. Matos, Overview on performance predictive models – Application to bridge management systems, in: IABSE Symp. Guimaraes 2019 Towar. a Resilient Built Environ. Risk Asset Manag., 2019.
- [7] C. Santos, S. Fernandes, M. Coelho, J. Matos, The impact of clustering in the performance prediction of transportation infrastructures, in: IPW2020, 18th Int. Probabilistic Work., 2021.
- [8] X. Wang, W. Dou, S.-E. Chen, W. Ribarsky, R. Chang, An Interactive Visual Analytics System for Bridge Management, *Comput. Graph. Forum.* 29 (2010) 1033–1042. <https://doi.org/10.1111/j.1467-8659.2009.01708.x>.
- [9] M. Santamaria Ariza, I. Zambon, H. S. Sousa, J.A. Campos e Matos, A. Strauss, Comparison of forecasting models to predict concrete bridge decks performance, *Struct. Concr.* (2020) suco.201900434. <https://doi.org/10.1002/suco.201900434>.
- [10] R. Denysiuk, J. Fernandes, J.C. Matos, L.C. Neves, U. Berardinelli, A computational framework for infrastructure asset maintenance scheduling, *Struct. Eng. Int.* 26 (2016) 94–102. <https://doi.org/10.2749/101686616X14555428759046>.
- [11] J.M. Davila Delgado, L. Oyedele, P. Demian, T. Beach, A research agenda for augmented and virtual reality in architecture, engineering and construction, *Adv. Eng. Informatics.* 45 (2020) 101122. <https://doi.org/10.1016/j.aei.2020.101122>.
- [12] D. Isailović, M. Petronijević, R. Hajdin, The future of BIM and Bridge Management Systems, in: IABSE Symp. Guimaraes 2019 Towar. a Resilient Built Environ. Risk Asset Manag., 2019.
- [13] F. Xue, W. Lu, K. Chen, C.J. Webster, BIM reconstruction from 3D point clouds: A semantic registration approach based on multimodal optimization and architectural design knowledge, *Adv. Eng. Informatics.* 42 (2019) 100965. <https://doi.org/10.1016/j.aei.2019.100965>.
- [14] S. Jeong, R. Hou, J.P. Lynch, H. Sohn, K.H. Law, An information modeling framework for bridge monitoring, *Adv. Eng. Softw.* 114 (2017) 11–31. <https://doi.org/10.1016/j.advengsoft.2017.05.009>.
- [15] S. Jeong, R. Hou, J.P. Lynch, H. Sohn, K.H. Law, A big data management and analytics framework for bridge monitoring, in: *Struct. Heal. Monit. 2017 Real-Time Mater. State Aware. Data-Driven Saf. Assur. - Proc. 11th Int. Work. Struct. Heal. Monit. IWSHM 2017*, DEStech Publications, 2017: pp. 155–162. <https://doi.org/10.12783/shm2017/13862>.
- [16] D. Isailović, V. Stojanovic, M. Trapp, R. Richter, R. Hajdin, J. Döllner, Bridge damage: Detection, IFC-based semantic enrichment and visualization, *Autom. Constr.* 112 (2020) 103088. <https://doi.org/10.1016/j.autcon.2020.103088>.
- [17] R. Sacks, A. Kedar, A. Borrmann, L. Ma, I. Brilakis, P. Hühwohl, S. Daum, U. Kattel, R. Yosef, T. Liebich, B.E. Barutcu, S. Muhic, SeeBridge as next generation bridge inspection: Overview, Information Delivery Manual and Model View Definition, *Autom. Constr.* 90 (2018) 134–145. <https://doi.org/10.1016/j.autcon.2018.02.033>.
- [18] Q. Lu, X. Xie, J. Heaton, A.K. Parlikad, J. Schooling, From BIM towards digital twin: Strategy and future development for smart asset management, in: *Stud. Comput. Intell.*, Springer Verlag, 2020: pp. 392–404. https://doi.org/10.1007/978-3-030-27477-1_30.



Review and Assessment of Technical and Legal Challenges in Drone-Driven Structural Health Monitoring of Bridges

Alireza Adibfar

Ph.D. Candidate, M.E. Rinker SR. School of Construction Management, University of Florida
Gainesville, Florida, United States

Mohamad Razkenari

Assistant Professor, College of Environmental Science and Forestry
Syracuse, New York, United States

Aaron Costin

Assistant Professor, M.E. Rinker SR. School of Construction Management, University of Florida
Gainesville, Florida, United States

ABSTRACT

Using robotics and drones is a novel method for safe, precise, and reliable monitoring of bridges. In recent years, there has been a substantial push for automating operational tasks in the infrastructure monitoring sector through robotic technology. Drones can reduce cost, time, and labor for tasks such as bridge monitoring while accelerating speed and precision. Despite all the benefits, there are major concerns about using drones, specifically inside the cities and metropolitan areas. Engineering and technical issues, privacy concerns, safety concerns, liabilities, and audio-visual disturbance for the public are concerns that hindered the full adoption and application of drones. This paper reviews the commercial applications of drones and evaluates challenges to using drones for infrastructure and bridge monitoring. The impacts of these concerns are discussed, and the areas that require attention and could be addressed by future research are highlighted.

Keywords: Bridge, Robotics, Drone, Structural Health Monitoring (SHM), Challenge.

1 INTRODUCTION

Bridges are essential nodes to maintain the traffic flow through the road transportation network. In order to ensure the reliability and safety of bridges, all the bridges need to be thoroughly inspected biannually in the United States (Costin et al. 2018). All the inspection data are being stored in the National Bridge Inventory (NBI), which is an online platform and is accessible through the Federal Highway Administration (FHWA) website (FHWA 2020a). Federal Highway Administration (FHWA) and American Association of State Highway and Transportation Officials (AASHTO) are responsible for developing road transportation standards. FHWA has developed the National Bridge Inspection Standards (NBIS) (FHWA 2020b). National Highway Institute (NHI) is the entity who is responsible for the development of manuals and training materials for bridge inspection in the United States and trains the inspectors through various courses (NHI 2020).

There are different methods for bridge inspection and Structural health monitoring (SHM). United States Department of Transportation (U.S. DOT) has enumerated five types of bridge inspection that includes initial inspection, routine inspection, in-depth inspection, damage inspection, and special inspection. Special inspections are being done over suspected or identified deficiency.

The inspections are mostly based on visual inspection and expert judgment and may include destructive/non-destructive tests (U.S. DOT 2020).

The regular inspection procedure is to send an inspection crew to climb up a bridge to inspect it. In this method, a team of inspectors and engineers would be equipped with all the required technical and safety equipment to explore and inspect a bridge. The manual inspection is hard, burdensome, unsafe, and prone to error. Moreover, during the inclement weather condition, it is impossible to send the crew over a bridge due to safety concerns. This method also falls short in quick response to disaster management scenarios such as hurricanes while the conditions have not been stabilized yet.

The other method is to use machinery, equipment, and vehicles to facilitate the inspection process. The team uses heavy equipment with an extendable arm (Boom lift) to get close to the body of the bridge and inspect it. This way, the inspection crew can monitor the bridge without the need for climbing it. But this method still has some shortcomings. This method is expensive, slow, could hardly be used for bridges with wide decks, and could not be used in inclement weather conditions.

Lack of sufficient experienced inspectors and human resources is a major obstacle to the bridge inspection process. Moreover, the high number of bridges in some states such as Texas and California, and the high ratio of deficient bridges in other states such as Rhode Island turns the allocation of financial resources into a complex puzzle (Adibfar and Costin 2018). From the theoretical side, these complexities require high-level problem-solving methods such as multiple criteria decision-making (MCDM) techniques and artificial intelligence to improve the robustness of methods and reliability of results (Jozaghi et al. 2018). From the technical side, there is a need to boost technology utilization and increase the effectiveness of inspections and reduce the human role in the process (Adibfar and Costin 2019).

Emerging technologies assist the construction industry and minimize the human role while optimizing their presence in the system (Hosseini et al. 2017). Intelligent Transportation Systems (ITS) and specifically Weigh in Motion (WIM) systems are one of the pioneer technologies in reducing the need for human-based control of commercial vehicles' weight in managing roads. They could significantly reduce costs and improve the effectiveness of operations (Adibfar and Costin 2019). This approach is becoming universal as other innovative approaches such as Cyber Physical Systems (CPS) are also focusing on human and technology integration to minimize the need for humans' presence while increasing their effectiveness in the system (Tehrani et al. 2019).

Using robotics and drones is another novel method for safe, precise, and reliable monitoring of bridges. In recent years, there has been a significant push for automating operational tasks in the infrastructure monitoring sector through robotics. California Department of Transportation (Caltrans) was one of the first states that funded a project to develop bridge inspection studies in 2008 (Tamoiczek et al. 2019). Minnesota Department of Transportation has funded a project to improve bridge inspection quality through Unmanned Aerial Vehicles (UAV) (Tamoiczek et al. 2019). Florida Department of Transportation funded projects to evaluate drone utilization efficiency for structural health monitoring bridges (Otero et al. 2015; Bridge 2018). According to the latest report from AASHTO, Department of Transportation in 49 out of 50 states have adopted drone application for different purposes. This has led to an increasing need for a skilled workforce to manage the drone operation (AASHTO 2019). Overall, more personnel will be working with drones and the number of drone-driven projects is on the rise.

The first use of pilotless planes goes back to the first world war. The U.S. Army started to produce UAVs in 1918 to help in the process of war. The first non-military use of drones happened in 2006. Government agencies started to use drones for disaster management, surveillance of the country borders, and wildfire fighting (Stamp 2013). Some corporations started to use drones for inspection of pipelines and some others used them for spraying pesticides on agricultural farms (AASHTO 2019). After Federal Aviation Administration (FAA) was convinced that commercial drones are safe to be operated for commercial and personal uses, they issued the first drone permit in 2006. It has been predicted that by 2020 there will be more than 250,000 drones flying around the world for commercial uses. Also, the market size has been estimated to be around \$100 billion between 2016-2020 (Wells and Lovelace 2018).

Drones have been proven to be cost, time, and labor effective and can accelerate the speed and precision of bridge monitoring. Despite all the benefits of drones, there are major concerns for their utilization, specifically inside the cities and metropolitan areas. Engineering and technical issues, privacy concerns, safety concerns, liabilities, and their audio-visual disturbance for the public are some of the concerns that hindered their full adoption and application. This paper briefly reviews the commercial application of drones and elaborates on some of the biggest challenges for the development of drone utilization for infrastructure and bridge monitoring. The importance and impact of each concern are evaluated, and the areas with require attention and could be addressed by more research.

2 METHODOLOGY

This research is primarily based on reviewing the available literature for finding out the most crucial obstacles toward the utilization of drones in bridge inspection. Authors reviewed 8 journal papers, 2 conference papers, and 4 websites to extract information. Besides the academic journals, authors reviewed 15 technical reports in which seven of them were including the information about recent bridge inspection projects using drones funded by the U.S. government or State Departments were discussed (Table 1). The challenges identified in those studies are discussed at the end of the research to highlight and conclude the findings. Research gaps and potentials will be discussed to help researchers find solutions for the current challenges and pave the way toward increasing drones' utilization in bridge inspections and their other utilizations in the Architecture, Engineering, and Construction industry.

Table 1 – Bridge inspection projects using drone

Project Name	Sponsoring Organization	Source
Development of a Pilot Program to Integrate UAS Technology to Bridge and Rail Inspections	Massachusetts Department of Transportation	Plotnikov et al. 2019
Unmanned Aircraft Systems Impact on Operational Efficiency and Connectivity	South Carolina Department of Transportation	Burgett et al. 2019
Improving the Quality of Bridge Inspections Using Unmanned Aircraft Systems (UAS)	Minnesota Department of Transportation	Wells et al. 2018
Bridge Inspecting with Unmanned Aerial Vehicles, R&D	U.S. Department of Transportation	Darby 2018
Evaluating the Use of Drones for Timber Bridge Inspection	U.S. Department of Agriculture	Seo et al. 2018
Implementation of Unmanned Aerial Vehicles (UAVs) for Assessment of Transportation Infrastructure	Michigan Department of Transportation	Brooks et al. 2018
Eyes in the sky: bridge inspections with Unmanned aerial vehicles	Oregon Department of Transportation	Gillins et al. 2018

3 TECHNICAL CHALLENGES

Drones need just one person to operate them remotely, can fly over and under bridges without any safety issues, and can continuously work for several hours. They could be equipped with different cameras and sensors such as thermal sensors, laser scanners, and other sensors to capture precise information from bridges. The recorded data could be stored and reviewed several times by different people. Altogether, it has been proven that the use of drones could bring significant savings in cost and time and also increased the safety and accuracy of the process (Bridge 2018). While drones are proven technologies for their assistance and precision, technical challenges have hindered their application to become prevalent yet. Some of these technical challenges have been reviewed in this section.

3.1 DESIGN AND ENGINEERING

There are engineering challenges that influence the design and engineering of the shape of drones. These include weight, wingspan, wing loading, range, maximum altitude, speed, endurance, and production cost. Currently, engineers are trying to reduce the size of drones, increase their endurance and range, and decrease their energy consumption (Stamp 2013). Developing drones that can satisfy current needs, have higher data capturing capabilities and precision, and still be economically reasonable are engineering challenges. Energy consumption and providing a power source that can address the required energy for drones' long operations is another challenge in designing the systems. The weight of drone and its mounted sensors, trip distance and optimization of the route are three main concerns for optimizing energy consumption in drone operations (Hassanalian and Abdelkefi 2017). Design Copyright infringement (Adibfar et al. 2020a, Adibfar et al. 2020b) and protection of innovations in drone's performance and efficiency is another important issue in design challenges.

3.2 SAFETY

As mentioned previously, the drone industry is moving toward commercialization. It means the drones need to have more flight frequencies to be more beneficial, economical, and operationally advantageous. With the increase in the number of drone permits in urban areas, safety concern increases. Safety could be called the main concern for the development of drones. Pilots and fly crew are being constantly trained to handle the failure cases and can safely land the planes in any emergency. But for drones, if the system fails to work properly, there is no other auxiliary controlling media that can help in safe landing of the drone.

As the air safety regulatory agency in the United States, the Federal Aviation Administration (FAA) chose a restrictive approach about drones to maintain air safety while increasing the knowledge about drones. The first permit for commercial use of drones was granted in 2013. Another part of the law was passed in 2016, which broadened the use of commercial drones weighing less than 55 pounds, but the safety concerns still persist. Safety challenges and their consequences will be furtherly discussed in legal challenges section (OECD/ITF 2018).

3.3 CYBERSECURITY

Cybersecurity risks are the other big challenge for drones. Drones are now being designed to have an easy and quick setup process. Thus, their hacking is a simple process for hackers. There are some sensitive data about the drone itself, including the drone's user, mission, flight path, and other private information that needs to be protected. Hackers are interested in taking control of drones as well as accessing their captured data. Sometimes the data need to be captured from a bridge that is near a high importance or a military facility, where security is the priority, and any leak of captured data is unjustifiable. Furthermore, in a worse case, their setup could be altered for a collision scenario. Protecting the drone from being hacked is a big challenge for their developers (OECD/ITF 2018; Vincent and Gartenberg 2019).

3.4 OPERATOR

Drones are being controlled by human operators. The operator's knowledge and experience is an important factor in successful operation of drones and capture of the required data. As the operator may be inexperienced, or operate the drone in unstable environmental conditions such as windy weather, there should be systems developed to control abnormal operational activities, or prevent the drone from crashing into bridges or other objects during the operation. The unauthorized flight and landing of the drones by the operator is another challenge. The drone operator can fly around a house,

hotel, or a business tower and stare at a window, or land on roof, or yard to collect data and videos. The spying attacks are another category of concern for developers of drones. The drone can approach a critical infrastructure or can enter the wireless network zone and start listening if it has been hacked(OECD/ITF 2018).

3.5 AUDIO-VISUAL POLLUTION

Aviation noise is another major challenge in development of drones. Like for the airports, frequent flight of drones causes a noise that may be harmful for psychophysical wellbeing. The noise can cause distractions, sleep disturbance, and be a serious problem for mental health and even cause cardiovascular diseases. Drone engineers have been testing changes in the drone rotors to decrease their noise level, but the rotors' noise remained a significant concern and challenge. Visual impacts are also another problem for development of drones. The increase in the number of drones may influence the perception of cities and their landscaping. Therefore, designers are trying to reduce the size of drones to partially overcome this challenge (Vincent and Gartengerg 2019).

4 LEGAL CHALLENGES

Technical challenges are a function of technology and could be resolved through the advancement of technologies during the time. Legal challenges on the other hand are more crucial as finding a conclusive and legitimate resolution toward the problems is not a function of time and technology, but a function of knowledge, experience, and time. Legal challenges have been discussed in this section.

4.1 JURISDICTION AND STANDARDIZATION

Drones activities are different from airplane activities, and their activities are also harder to anticipate and justify. Thus, their regulations need to be constantly updated. Air traffic management is one of the challenges for development of drones. SKY ATM research joint (SESAR JU) has started to develop the "Roadmap for the safe integration of drones into all classes of airspace" (Wells and Lovelace 2018).

Most of the jurisdictions tried to address the challenges under three categories. The first category is administrative rule that applies to license and training, registration of aircrafts and their insurance. The second category is working on the operational limitations, including their maximum weight, the restrictions about the flight altitudes, and vertical and horizontal landings. The third category works on airspace management rules that included flight authorization, defining the restricted flying zones, and the maximum altitude that the drones can fly in (Wells and Lovelace 2018).

4.2 LIABILITY AND INSURANCE

Following safety concerns, liability issues are another challenge for drone developers. In case of failure in drone's operation, if the drone hits something and makes damage, the liability could be ambiguous as it may be manufacturer, operator, or software provider's fault. This problem will have a higher magnitude when the drone hits another drone or an aircraft. Insurance policies are still ambiguous about drones, and it could become a complicated problem as the drones may not be so expensive, but the damage they can make could be enormous.

The drone can crash on anything or anyone causing secondary accidents that could be more severe than the drone's failure and crash. In other possible scenarios, flying a drone over a crowded highway bridge can distract drivers and lead to accidents with other vehicles or pedestrians that will have significant damages and even lead to people's death. Insurance companies are still unsure about dealing with these scenarios and cannot guarantee the full response to these cases (OECD/ITF 2018).

4.3 PRIVACY PROBLEMS

This section has been initially discussed in operator challenges. Privacy issues are critical challenges for the development of drones. The law requires that any photography from people happen with their knowledge and consent, and any unauthorized capturing could be sued. Drones can fly high and captured huge number of photos and videos without any permission. Flying drones above bridges near residential neighborhoods can arise arguments by the neighbors as they are distressed by drones' interference with their privacy and disturbance. Flying drones near bridges located in the metropolitan areas and near interchanges that are close to towers and high rises can also disturb the residents and start an argument.

To address privacy concerns, 27 European jurisdictions have established the European Commission and passed E.U. Directive 2016/680: The General data protection regulations (GDPR). Some other countries, such as China, are not much disturbed with privacy challenges and already have some regulation in effect. China has developed a “social credit system” that controls people’s financial behavior. They also monitor people's behavior with 170 million surveillance cameras across China, and the use of drones will be appended to that system (OECD/ITF 2018).

4.4 SOCIAL IMPACT

Policy makers are facing another problem with the impact of drones on social impacts and real estate values. Frequent flight of drones may have a negative impact on the comfortability of the available real estates in the area and decrease their value. Also, there are other concerns about accountability and liability, workforce impacts, social equity, environmental integrity and visual amenity and pollution, and the impact on infrastructure.

5 DISCUSSION

Despite all the challenges, drones are proven to be effective in improving bridge inspection process. There are many projects funded by state departments to develop guidelines and instructions for using drones for bridge inspection process improvement. The recommendations to improve drone applications for bridge inspection are in three categories of pre-inspection planning, drone operation, and post-operation analysis.

Pre-planning drone operation for bridge inspection must include detailed mission objectives and all the potential safety concerns. Drones cannot replace hands-on inspection procedures and under bridge inspection but make documentation more convenient and reduce the inspectors' safety hazard. The planning must specify the scope of work for the drone. Besides this, collected images must be high-quality and viable for further analysis. The image quality may vary depending on field conditions, weather, bridge types, bridge locations, and bridge configurations vary widely. The inspectors are responsible for verifying image quality manually, based on their qualifications and experience. It would be possible to use cloud-based automated image verification using simultaneous mapping algorithms.

While operating drones require FAA certifications in most states, the inspection organizations have a limited number of licensed drone pilots within their agencies. Therefore, drone operations and fleet management are most often handled by external third parties. During the drone operation, a certified operator must control the drone. Some software packages can be used for pre-planning drone flights. If the details inspection plan is developed, the pilot can use those tools to pre-plan drones flight while continuously monitoring its situation. Collision-tolerant drones must be used for automated inspection in confined space inspections and the inspection of multi-beam bridges. The benefit of this approach is reducing the safety challenges and increasing the precision. As the operator’s full awareness and health during the operation are so important, the use of wearable sensors

and development of IoT-based leading indicators methodologies (Costin et al. 2019) for detecting any abnormal body activities can help to prevent accidents and problems.

One of the most important challenges repeatedly mentioned in the projects is the difficulty in flying under bridges where GPS signals are blocked. To address this challenge, drone pilots can pre-plan the path under and to the sides of the bridge, where GPS signals can be established. Taller bridges allow for a more aggressive angle improving the field of view.

Since bridge inspection using drones carries some real risks of losing the aircraft and expensive instruments, it is suggested to use low-cost drones with lower manoeuvrability and image quality. This would increase the risk of crashes but reduce the cost to replace the units.

The data collected from drones need to be processed using computer vision algorithms. These algorithms are complex and mostly only in the development phase. Their practical implementation requires buying cloud capabilities to manage data storage and run the computationally expensive algorithms in cloud computing platforms. While the technology has developed to provide results with a high accuracy level, data analysis requires experts to develop these algorithms and interpret the results. There is a need to develop software packages to provide end-to-end solutions for data collection, data analysis, and creating inspection reports.

The overburden of regulation that comes with drone-based inspection restrain the work and complicate the inspection process. FAA is facilitating the adoption and reduce restrictions. For example, they developed B4UFLY Mobile Application to address some of the drone flight challenges. The application, called Low Altitude Authorization and Notification Capability, allows drone integration into the airspace. The drone pilot would request controlled airspace before launching the drone (below 400 feet) and be aware of any restricted area. The application also records where and when drones are operating, and this data would be visible to Air Traffic Professionals.

6 CONCLUSION

This study reviewed the commercial applications of drones and performed case studies of drone applications for bridge inspection in the U.S. The biggest technical and legal challenges to using drones for infrastructure and bridge monitoring were recognized, and the impacts of these concerns were discussed. The pre-inspection, operational, and post-inspection approaches were suggested to mitigate these challenges.

REFERENCES

- [1] AASHTO (2019). "AASHTO UAS/Drone Survey of All 50 State DOTs- Mission Control," AASHTO, Park City, UTAH.
- [2] Adibfar, A. and Costin A. (2018). " Next generation of transportation infrastructure management: Fusion of Intelligent Transportation Systems (ITS) and Bridge Information Modeling (BrIM)", 43-50, *Advances in Informatics and Computing in Civil and Construction Engineering*", Springer, Cham. https://doi.org/10.1007/978-3-030-00220-6_6
- [3] Adibfar, A. and Costin A. (2019). " Evaluation of IFC for the Augmentation of Intelligent Transportation Systems (ITS) into Bridge Information Models (BrIM)", *Proceedings of ASCE International Conference on Computing in Civil Engineering 2019*, Atlanta, Georgia, 177-184. <https://doi.org/10.1061/9780784482421.023>.
- [4] Adibfar A., Costin, A., and Issa, RRA. (2020a). "Design copyright in architecture, engineering, and construction industry: Review of history, pitfalls, and lessons learned", *Journal of Legal Affairs and Dispute Resolution in Engineering and Construction*, 12(3), ASCE, 04520032.
- [5] Adibfar A., Costin, A., and Issa, RRA. (2020b). "Review of Copyright challenges in AECO industry and prospective developments for Building Information Modeling (BIM)", *Proceedings of Construction Research Congress (CRC)*, March 18-20, Tempe, Arizona.
- [6] Bridge, J. (2018). "Small Unmanned Aerial Vehicles (SUAV) for Structural Inspection (Project #: BDV31-977-55)," Florida Department of Transportation, Tallahassee.

- [7] Brooks, C., Dobson, R., Banach, D., Oommen, T., Zhang, K., Mukherjee, A., Havens, T., Ahlborn, T., Escobar-Wolf, R., Bhat, C., Zhao, S., Lyu, Q., and Marion, N. (2018). Implementation of Unmanned Aerial Vehicles (UAVs) for Assessment of Transportation Infrastructure. < <https://tinyurl.com/y4lrd49q> > (March 14, 2020).
- [8] Burgett, J. M., Bausman, D. C., and Commert, G. (2019). Unmanned Aircraft Systems Impact on Operational Efficiency and Connectivity. < <https://tinyurl.com/yyjyqt9> > (March 14, 2020).
- [9] Costin, A., Adibfar, A., Hu, H., and Chen, S. (2018). "Building Information Modeling(BIM) for transportation infrastructure - Literature review, applications, challenges, and recommendations," Automation in Construction, 94, pp. 257-281.
- [10] Costin, A., Wehle, A.J., and Adibfar, A. (2019). "Leading Indicators—A Conceptual IoT-Based Framework to Produce Active Leading Indicators for Construction Safety", Safety, 5(4), 86.
- [11] Darby, P. (2018). Bridge Inspecting with Unmanned Aerial Vehicles, R&D. < <https://tinyurl.com/y2qz8ldg> > (March 22, 2020)
- [12] Federal Highway Administration (FHWA) (2020a). " National Bridge Inventory", < <https://www.fhwa.dot.gov/bridge/nbi.cfm> > (October 27, 2020).
- [13] Federal Highway Administration (FHWA) (2020b). " National Bridge Inspection Standards", <<https://www.fhwa.dot.gov/bridge/nbis.cfm>> (October 27, 2020).
- [14] Gillins, D. T., Parrish, C., Gillins, M. N., and Simpson, C. (2018). *Eyes in the sky: bridge inspections with Unmanned aerial vehicles*. < https://www.oregon.gov/ODOT/Programs/ResearchDocuments/SPR787_Eyes_in_the_Sky.pdf >
- [15] Hassanalian, M. and Abdelkefi A. (2017). "Classifications, applications, and design challenges of drones : a review" Progres in Aerospace Sciences, 91, pp. 99-131, 2017.
- [16] Hosseini, M., Banihashemi, S., Zaeri, F., and Adibfar, A. (2017). "Advanced ICT methodologies (AIM) in the construction industry", Encyclopedia of Information Science and Technology, Fourth Edition - Chapter 47, IGI Global, 539-550.
- [17] Jozaghi, A., Alizadeh, B., Hatami, M., Flood, I., Khorrami, M., Khodaei, N. and Tousi, E. (2018). " A Comparative Study of the AHP and TOPSIS Techniques for Dam Site Selection Using GIS: A Case Study of Sistan and Baluchestan Province, Iran", Geoscience, 8(12), 494. <https://doi.org/10.3390/geosciences8120494>.
- [18] Martinez, K. (2019). "The History Of Drones (Drone History Timeline From 1849 To 2019)," <<https://www.dronethusiast.com/history-of-drones/>> (October 20, 2020).
- [19] National Highway Institute (NHI) (2020). "Safety Inspection of In-Service Bridges for Professional Engineers", < <https://tinyurl.com/y3akykzw> > (October 27, 2020).
- [20] OECD/ITF, (2018) "(Un) Certain Skies? Drones in the world of tomorrow" International Transportation Forum < https://www.itf-oecd.org/sites/default/files/docs/uncertain-skies-drones_0.pdf > (October 15, 2020).
- [21] Otero, L., Gagliardo, N., Dalli, D., Huang, W. and Cosentino, P. (2015). "Proof of Concept for Using Unmanned Aerial Vehicles for High Mast Pole and Bridge Inspection," Florida Department of Transportation, Tallahassee.
- [22] Plotnikov, M., Ni, D., and Price D. (2019). The Application of Unmanned Aerial Systems in Surface Transportation - Volume II-A: Development of a Pilot Program to Integrate UAS Technology to Bridge and Rail Inspections. < <https://www.mass.gov/lists/unmanned-aerial-systems-in-surface-transportation-final-report> > (March 14, 2020).
- [23] Seo, J., Wacker, J. P., and Duque, L. (2018). *Evaluating the Use of Drones for Timber Bridge Inspection*. < https://www.fpl.fs.fed.us/documnts/fplgtr/fpl_gtr258.pdf > (October 27, 2020).
- [24] Stamp, J. (2013). "Unmanned Drones Have Been Around Since World War I," Smithsonian, < <https://tinyurl.com/y23nymxl> > (March 14, 2020).
- [25] Sifton, J. (2012) "A Brief History of Drones," < <https://www.thenation.com/article/brief-history-drones/> > (October 27, 2020).
- [26] Tomiczek, A., Whitley, T., Bridge, J. and Ifju, P. (2019). "Bridge inspection with small unmanned aircraft systems: Case studies," Journal of bridge engineering, 24(4), [https://doi.org/10.1061/\(ASCE\)BE.1943-5592.0001376](https://doi.org/10.1061/(ASCE)BE.1943-5592.0001376).
- [27] U.S. Department of Transportation (U.S. DOT) (2020). "Highway Bridge Inspections", <<https://tinyurl.com/y6aj7q6u>> (October 27, 2020).
- [28] Vincent, J. and Gartenberg, C. (2019). "Here's Amazon's new transforming Prime Air delivery drone," The Verge, < <https://tinyurl.com/y3kdy4r5> > (March 14, 2020).
- [29] Wells, J. and Lovelace, B. (2018) "Improving the Quality of Bridge Inspections Using Unmanned Aircraft Systems (UAS)," Minnesota Department of Transportation Research Services & Library, St. Paul, Minnesota.



Bridge Inspection and AI (IBridge 2020)

Mustafa Can Yücel, Ph.D.

Bridgewiz Engineering R&D
Ankara, Turkey

ABSTRACT

Regular inspection of bridges is very important to maintain a healthy bridge inventory and minimize repair costs by utilizing the principles of preventative maintenance. Due to these reasons, countries across the globe spend a considerable amount of their yearly maintenance budgets on inspections which are carried by field teams of experts and auxiliary personnel. One of the major components of the total maintenance cost is forming these inspection teams with enough experience and manpower to be able to inspect all the bridges that require attention in the given limited time frame. This challenge puts additional strain on inspectors, which when combined with the inherent flaws of human inspection, causes non-standard inspection routines and non-uniform inspection results. Artificial Intelligence (AI) is a relatively old area of study when reviewed with software engineering mind due to the fact that many astonishing discoveries are no more than ten years old whereas AI studies go back several decades. However, the recent improvements in hardware capabilities made carrying AI-capable devices in hand, and the newly constructed AI models and algorithms increased the accuracy and training-time of machine learning applications vastly. These achievements made AI-powered semi-automatic hand-held inspection applications possible, however, there are still fairly limited studies in this domain. This paper aims to address several of the handicaps of conventional inspection schemes, give the reader an idea of what the AI can accomplish, and finally how it can improve several of the issues raised about the consistency of inspections within a team and among multiple teams.

Keywords: bridge inspection, artificial intelligence

1 INTRODUCTION

Bridge inspection is one of the most important aspects of bridge maintenance, therefore many countries (both developing and developed) work hard to improve the practices in terms of accuracy and ease of use. This has roots in the fact that preventative (or sometimes referred to as preventive) maintenance is almost always the most efficient way, both in terms of time and money, to maintain a bridge (or any other asset in this regard) in an operative state.

In the current paradigm, the two commonly utilized types of inspections are after-disaster and regular ones. There is a third and quite specialized type of inspection which is called “structural health monitoring”, which aims to monitor the vital parameters of the bridge continuously so that any issue on the components should be detected as soon as it manifests itself as an abrupt change in the supervised parameters. This approach can be regarded as an automated regular instrumented inspection performed in very short intervals. Although the principals of artificial intelligence can be used to distinguish the patterns in the collected data that may shed a light on the potential problems

of a bridge, this topic is not the main focus of this paper; in this study, the fundamental aim is to give insight on the improvements that AI can deliver for the site inspections performed by field teams.

In conventional regular (sometimes referred to as cursory or eye) inspection applications, the inspection team goes to the site of the bridge with an agenda that includes the components to be audited. These teams usually consist of one or more experienced engineers who have a major influence on the decisions of the state of individual components as well as the overall state of the bridge. The team goes over every item in their checklist and assign a grade for them. The grading schemes differ significantly from one region to another both in terms of scale and direction. In some countries, the grades are scaled between 1 and 3 where 1 is the worst and 3 is the best whereas in others the range is from 1 to 100 where 100 is the worst. Each component also has a different weight on the combined grade result; it is obvious that defects in non-structural components such as railing do not pose a threat as great as deficiencies in central pier foundations. Once all the components are graded, the overall status of the bridge is determined by the weighted average of the marks of individual components, and further decisions such as ranking the urgency of maintenance within a bridge stock is done over these bridge grades.

If these periodic inspections are performed properly, any problem that may lead to a catastrophic result may be discovered in a stage where repair is significantly easier. For example, if deteriorations on a beam supporting the deck of a bridge are discovered in the early spalling stages, it is undoubtedly easier to repair when this condition is realized after the reinforcements are corroded beyond repair and beam-replacement is required (Figure 1).

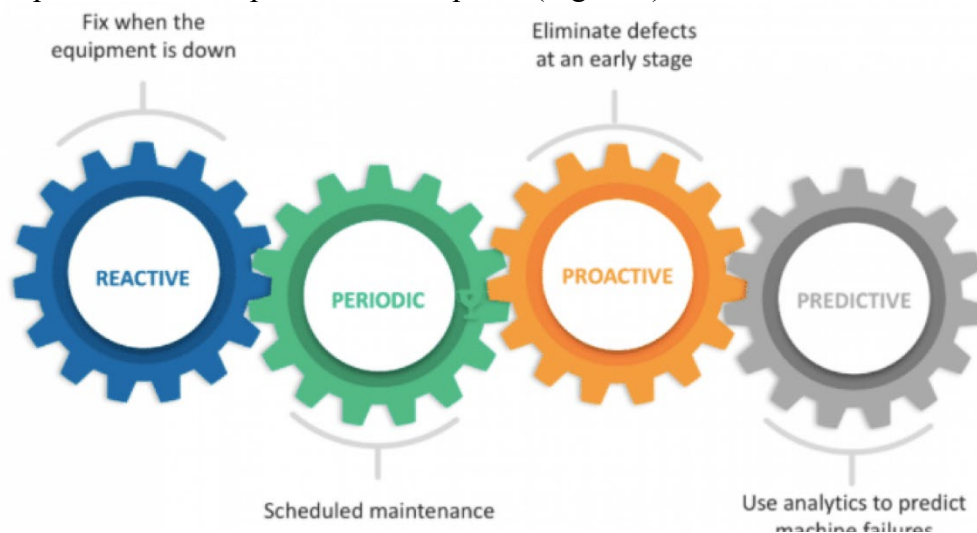


Figure 1: Reactive and Proactive Maintenance Schemes

2 COMMON PROBLEMS IN BRIDGE INSPECTION PRACTICES

For the inspection paradigm to work as intended, the inspection results should be accurate and the inspection processes should be completed efficiently so that they can be completed in time with minimal expenditures. The inspection chain (procedure) explained above has one important weak link; it is as good as the inspector. This case poses several issues; first training a capable inspector requires time as he needs to be familiar with different cases by being exposed to them, and second human judgment can be affected by a variety of external factors. Moreover, since the grading of components is done by personal experience, different inspectors with varying ideas on severity levels for a defect will assign different scores to the same scene. This divergence will cause issues when the decision-makers are trying to rank different bridges for the urgency of maintenance repairs. For example, due to the lesser experience of an inspector, a bridge might be assigned a worse grade than it is because that condition is the worst the inspector has seen in his professional life, however in reality there exist much worse cases.

2.1 Problems Due to Grading System Scale

As mentioned before, different countries have distinct grading schemes that vary significantly from one another, each approach having its strengths and weaknesses.

2.1.1 Low Number of Divisions

When the overall scale of grading is divided into few steps, (1-3 for example), the main advantage gained is that the comparison between different ranks is quite simple. A person who is reading an inspection report will easily realize that a component with a grade of 2 is in a significantly worse condition than one with a grade of 3 (assuming 1 is the best). This results in an easier assessment for the interpreters that work on the already-written inspection reports. Moreover, since the borders of grades are very distinct, different inspectors will grade similar marks since there are much fewer to choose from the beginning.

However, this approach results in naturally broad areas between grades where there is no distinction of status. For example, two components graded as 2 out of 3 are the same on paper, however, one might be closer to the good end whereas the other to the bad. The reviewer of the report will have no idea of the exact case without further information.

2.1.2 High Number of Divisions

When the overall scale of grading is divided into many steps (1-100 for example), the main advantage gained is that the exact status of a component can be expressed better by the field inspector. Out of two components with similar degradation levels, the better one can be graded as 70 and the worse one can be graded as 60. These grades will be more coherent for a single inspector.

However, this approach results in blurred differences between close grades, especially if these grades are assigned by different inspectors. An interpreter working on two reports may struggle to differentiate the status of two components that are graded as 60 and 65, for example. Even though grades are similar, the divergent experience levels of inspectors might mean reasonably different deterioration levels.

2.2 Problems Due to Human Experience

As stated above, an inspector grades an element by comparing it to the best and worst exhibits that he has been exposed in his professional life. Since it is not possible to train inspectors with identical experience levels, there will always be differences between grades given by different field teams. The grading system may augment this difference based on its scale, as explained in the previous section.

2.3 Problems Due to Human Subjectivity

The effect of human subjectivity in inspections can be presented in two different types; subjectivity among others and within the self.

The subjectivity among others stems from the facts explained in the previous sections; the variance of experience levels. Simply summarized, the team who has seen worse cases will give higher grades than the team that has worked on much better cases.

The subjectivity within self can be explained as the difference of grades that the same person assigns at different points in time. As humans, our judgment is affected by many factors that can be physical or emotional in nature. Simply put, an inspector that has emotional distress will most likely assign worse grades to the same components compared to the case when is in a better mood. It is also a common occurrence for humans to rush finishing a task when they are hungry, tired, or trying to finish their over-assigned schedule.

2.4 Problems Due to Speed and Efficiency

Many countries have a high number of bridges that need to be maintained and usually, a smaller number of teams to accomplish this, since raising proper teams requires budget and time. This conundrum results in busy schedules for inspectors which may result in inaccurate grades as well as the inability to process all the bridges in a stock.

Additionally, human inspectors may require to refer to references and textbooks to infer a better judgment for a case. This is an approach that increases the accuracy of the inspections for the cost of time and efficiency. If the inspectors are not highly experienced, the occurrence of these cases increases in number, causing inspections to take much longer time and delays.

3 AI & MACHINE LEARNING

Machine learning is the study of computer algorithms that improve automatically through experience, and most of the time it is seen as a subset of artificial intelligence, which is intelligence demonstrated by machines, unlike the natural intelligence displayed by humans and animals [1] (Figure 2).

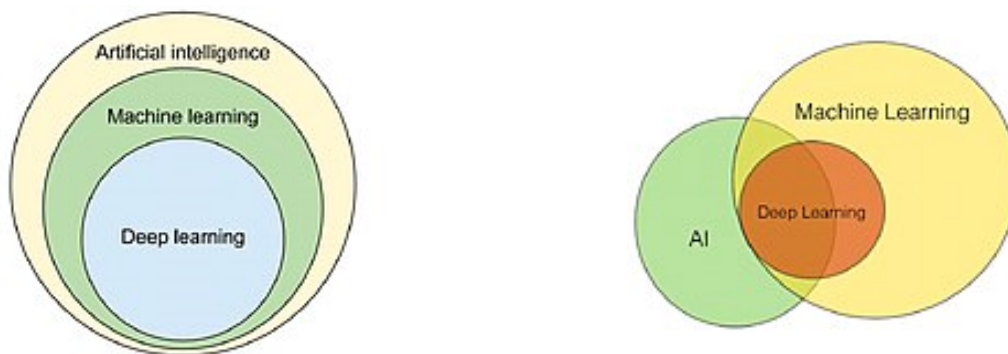


Figure 2 AI and Machine Learning

Machine learning involves computers discovering how they can perform tasks without being explicitly programmed to do so [2]. It involves computers learning from data provided so that they carry out certain tasks. For simple tasks assigned to computers, it is possible to program algorithms telling the machine how to execute all steps required to solve the problem at hand; on the computer's part, no learning is needed. For more advanced tasks, it can be challenging for a human to manually create the needed algorithms. In practice, it can turn out to be more effective to help the machine develop its own algorithm, rather than having human programmers specify every needed step [3], [4].

There are very different types of machine learning models and training algorithms, which are outside of the scope of this paper. The most commonly used training practices in engineering practices are supervised and unsupervised models.

3.1 Common Learning Algorithms

3.1.1 Supervised Learning

Supervised learning algorithms build a mathematical model of a set of data that contains both the inputs and the desired outputs. The data is known as training data and consists of a set of training examples. Each training example has one or more inputs and the desired output, also known as a supervisory signal. In the mathematical model, each training example is represented by an array or vector, sometimes called a feature vector, and the training data is represented by a matrix. Through iterative optimization of an objective function, supervised learning algorithms learn a function that can be used to predict the output associated with new inputs [5]. An optimal function will allow the algorithm to correctly determine the output for inputs that were not a part of the training data. An

algorithm that improves the accuracy of its outputs or predictions over time is said to have learned to perform that task.

3.1.2 Unsupervised Learning

Unsupervised learning algorithms take a set of data that contains only inputs, and find structure in the data, like grouping or clustering of data points. The algorithms, therefore, learn from test data that has not been labelled, classified or categorized [6]. Instead of responding to feedback, unsupervised learning algorithms identify commonalities in the data and react based on the presence or absence of such commonalities in each new piece of data.

3.2 Machine Learning Models

Even though there are a variety of different models, the most commonly used model in image processing and classification is convolutional neural networks.

3.2.1 Convolutional Neural Networks

In deep learning, a convolutional neural network (CNN) is a class of deep neural networks, most commonly applied to analysing visual imagery. They are also known as shift invariant or space invariant artificial neural networks (SIANN), based on their shared-weights architecture and translation invariance characteristics. They have applications in image and video recognition, recommender systems, image classification, medical image analysis, natural language processing, brain-computer interfaces, and financial time series. The mathematics and computational science behind CNNs are beyond the scope of this paper.

4 INCORPORATING AI IN VISUAL INSPECTIONS

The nature of CNNs makes them a very valuable asset in the determination of the existence of a pattern or property in an image. Due to their intrinsic capabilities, the distortion or orientation changes of the pattern rarely affect the success of a CNN provided that an adequate amount of training data is supplied. This results in the fact that any deformation, deterioration, or change that can manifest itself in a photograph can be identified with sufficient training. These issues are listed but not limited to:

- Cracks
- Excessive deformations
- Efflorescence
- Alkali-silica reactions
- Any types of colouring and chemical reactions that result in colour change
- Scouring

4.1 Advantages of Using AI in Visual Inspections

4.1.1 Reducing Subjectivity

As explained in previous sections, human subjectivity in self and among colleagues is possibly the weakest link of the inspection procedure. An AI-powered inspection system can negate this problem completely; if the same machine learning model trained with the same data is used in a bridge stock for inspection, the results will be completely uniform and consistent; i.e., a component will be graded the same mark independent of time of the day, physical conditions, how long the inspection process is going for...etc. This uniformity will help the decision-makers to evaluate the

conditions of different bridges since they are confident that the grades are compliant with each other in the bridge stock inventory.

4.1.2 Increasing Speed and Efficiency

The machine learning models can work continuously and very fast. Considering how powerful contemporary hand-held devices (even mobile phones) are, the processing of a single or several frames by a CNN takes milliseconds to seconds based on the image size. This results in an increased speed in inspections since it only takes around a minute to take a multitude of photos of a component and get a result from the AI inspection model.

Moreover, this process eliminates the occurrences of consulting to records and references since AI completely works on the experience collected as a training set.

4.1.3 Decreased Necessity for Experience

Since the AI makes its decision based on the collective experience used during the training phase, the experience source for an inspection is shifted from the inspector to the AI. It is vital for the inspector using the AI to have a certain level of experience to decide if the AI results are reasonable, but he will be able to utilize the combined experience of the training data set as a tool. Therefore, instead of having a few highly experienced specialists, a higher amount of moderately experienced inspectors will be sufficient.

4.1.4 Extracting Minuscule Details

5 Humans, by nature, tend to focus their attention on items with larger traces. An inspector can overlook a minor trace of corrosion in a component when there are other larger though unrelated items that exist. Additionally, when site teams are rushed to complete as many inspections as they can in a limited inadequate time, it is unavoidable to miss several tiny details that may be the culprit of more important conditions. The AI models do not expose this kind of behaviours; they perform exactly how they are trained and their success is determined by their training phase, not how large or small the condition is.

6 SHORTCOMINGS OF IMPLEMENTING AI IN INSPECTIONS

6.1 Gathering Adequate Training Set

The most important factor determining the accuracy of an ML model is the training phase. To acquire high levels of successful labeling for a specific condition, the training set should include a vast collection of that condition in varying features (size, color, shape, different lighting...etc.). This data collection and manual labeling process are usually cumbersome and sometimes costly; if there are not enough images of a specific defect, teams should be formed to go to different sites and gather photos.

Determining adequate training set size is a debate among academics, but usually, any data set that has less than around 1000 images is deemed as “small”. For different identification purposes, it is not uncommon to use tens or even a hundred thousand images in the training phase. For evaluation and testing, usually, 10%-25% of the training set is customary.

It should be noted that even though new ML algorithms allow to train of a model with very few training data, the accuracy of the results is always correlated with the size of the input set.

6.2 Specialization in Development

AI and ML practices highly depend on mathematical processes; they are one of the most advanced implementations of regression and statistical analysis combined with several other domains of mathematics. Their software implementations require highly optimized parallelized codes and approaches with the inclusion of advanced vector extensions and other native CPU and GPU access functions in order to be able to perform a high volume of operations in a reasonable time frame. These applications are far from simple programming tasks and require specialized knowledge.

An alternative approach is using the already available frameworks of AI (such as TensorFlow, Keras...etc.). These libraries wrap and abstract the low levels of machine learning procedures so that users can utilize high-level functions for their usage with little prior knowledge of the underlying mathematics and software. For simpler cases this approach works well; a layman programmer with basic Python (or C++) knowledge can train a set and use the trained model in another environment. However, if there are specialized needs that cannot be met with the already available abstractions, the source of these frameworks should be edited, which is not a rudimentary task. It may take quite a large budget to create a new framework or edit an existing one on a larger scale.

6.3 Initial Time and Money Investment

Due to the items explained in the previous two sections, creating an application for implementing AI in visual inspections may require a higher initial budget and longer mobilization time frame. This has roots in the fact that an adequate training set should be constructed (by collecting existing data and field studies for new data), AI models should be created and trained (if necessary, an extension of existing libraries should be conducted by specialists), and the required system of software should be constructed (client and server sides if necessary).

Even though these items possibly result in an increased initial budget, it can be seen that they will pay what is invested in the long run with the increased efficiency and decreased additional expenses for field inspections.

7 EXAMPLE APPLICATIONS

Bridgewiz Engineering is working on an Android application that will be used to identify different types of damage exposed on bridge components (Figure 3).



Figure 3 Bridgewiz Android Application

